

3
2006

LIBRARY
Michigan State
University

This is to certify that the
thesis entitled

**SOURCES OF CHLORIDE TO SURFACE WATERS IN THE
MUSKEGON RIVER WATERSHED**

presented by


Nathaniel Paul Saladin

has been accepted towards fulfillment
of the requirements for the

M.S. degree in Environmental Geosciences



Major Professor's Signature



Date

PLACE IN RETURN BOX to remove this checkout from your record.
TO AVOID FINES return on or before date due.
MAY BE RECALLED with earlier due date if requested.

DATE DUE	DATE DUE	DATE DUE

**SOURCES OF CHLORIDE TO SURFACE WATERS IN
THE MUSKEGON RIVER WATERSHED**

By

Nathaniel Paul Saladin

A THESIS

**Submitted to
Michigan State University
in partial fulfillment of the requirements
for the degree of**

MASTER OF SCIENCE

Department of Geological Sciences

2005

ABSTRACT

SOURCES OF CHLORIDE TO SURFACE WATERS IN THE MUSKEGON RIVER WATERSHED

By

Nathaniel P. Saladin

The freshwater resources of the lower peninsula of Michigan overlie concentrated aqueous solutions (brine) of the Michigan Basin. The interaction of these fluids has been discovered and there is a question as to the extent of the interaction. Therefore, the geochemistry of surface waters (streams, lakes and wetlands) in the Muskegon River Watershed were studied to determine the source(s) for Cl. A portion of this watershed is in the Michigan Lowlands and it is possible (based on observations of processes occurring in the Saginaw Lowlands) that a source for the Cl is the upwelling of saline ground water. This study used geochemical indicators (e.g., Na/Cl ratios) and graphical and GIS analyses to examine the likelihood for this and other possible sources for Cl. The results indicate four sources for Cl; halite, formation brine, septic/wasted, and natural (atmosphere and water-rock reaction). Halite and brine appear to be the most dominate sources, with road salting, road brining, and activities associated with oil and gas production as important pathways. The impact of upwelling saline water on surface water chemistry is limited in extent and not an important pathway for Cl as it has been shown for the Saginaw Lowlands.

Copyright by
Nathaniel Paul Saladin
2005

ACKNOWLEDGEMENTS

I thank Dr. David Long, my advisor, for his patience and guidance throughout this project. I also thank my committee members (Dr. Grahame Larson and Dr. David Hyndman) for providing their comments on this thesis. I thank the office staff (Jackie, Kathy, Loretta, and Michelle) for keeping an eye on impending deadlines and direction through the University paperwork. I would like to acknowledge the help of the graduate students in the Department of Geological Sciences for technical help as well as encouragement. I am also grateful to the zoology graduate students who collected the lake and wetland samples that were used within this thesis. Similarly, I also thank the graduate and undergraduate students who helped to collect the stream samples that were needed for this project. I am in debt to Diane Baclawski (Department of Geological Sciences Librarian) and Norm Granneman (USGS, Lansing) for their help in finding geological information on Michigan. I thank the members of the Graduate Intervarsity Fellowship at Michigan State University and Bretton Woods Covenant Church of Lansing for their encouragement. I finally would like to thank the members of my family for their support and encouragement.

TABLE OF CONTENTS

LIST OF TABLES.	vii
LIST OF FIGURES.	viii
CHAPTER 1: INTRODUCTION	
Scope and Purpose.	1
Related Studies.	4
Hypothesis and Approach.	11
Study Site.	11
CHAPTER 2: METHODS	
Field Data and Sample Collection.	20
Supplementary Data.	26
Sample Analysis.	29
Data Analysis.	30
CHAPTER 3: GEOCHEMICAL MODELING OF SURFACE WATERS AND GROUND WATERS	
Introduction.	33
Calcite SI.	35
Dolomite SI.	43
Gypsum SI.	50
Quartz SI.	58
Summary.	66
CHAPTER 4: CHEMICAL GRAPHICAL DATA	
Introduction.	71
Na/Cl (M) Histograms and Ratios.	71
Na/Cl (M) ratios for bedrock aquifers and MRW watershed	81
Na/Cl ratios for SBW Drift and SBW streams	83
Logarithmic Na (M) vs. Cl (M) Charts.	95
Calcium vs. Magnesium.	107
Summary.	119
CHAPTER 5: PIPER DIAGRAMS	
Introduction.	123
Piper Diagrams.	126
Summary.	140
CHAPTER 6: GEOGRAPHIC INFORMATION SYSTEMS	
Introduction.	145
Oil and Gas Wells.	146

Quaternary Geology of Watersheds.	150
Road Salt.	156
Treated Sewage Septic Systems.	160
Summary.	165
CHAPTER 7: SUMMARY AND CONCLUSIONS	
Summary.	168
Conclusions.	175
Bibliography:	177

LIST OF TABLES

Table 1. Table of the Log K_{sp} values for minerals whose saturation indices were geochemically modeled. Modified from Long et al. (Unpublished).	35
Table 2. Table of the average Na/Cl (M) of different formation waters in the Michigan basin Data. From Wilson (1989).	77
Table 3. Table showing the percentage of samples that plot within different ranges of Na/Cl (M) values for ground water samples from the Pennsylvanian bedrock aquifer. Data are from the ground water data set (Dannemiller and Baltusis, 1990; Wahrer, 1993; Meissner, 1993).	80
Table 4. Table showing the percentage of samples that plot within different ranges of Na/Cl (M) values for ground water samples from the Mississippian bedrock aquifer. Data are from the ground water data set (Dannemiller and Baltusis, 1990; Wahrer, 1993; Meissner, 1993).	81
Table 5. Table showing the percentage of samples that plot within different ranges of Na/Cl (M) values for ground water samples within the MRW drift. Data are from the ground water data set (Dannemiller and Baltusis, 1990; Wahrer, 1993; Meissner, 1993).	85
Table 6. Table showing the percentage of samples that plot within different ranges of Na/Cl (M) values for stream water samples in the MRW.	86
Table 7. Table showing the percentage of samples that plot within different ranges of Na/Cl (M) values for lake water samples in the MRW.	87
Table 8. Table showing the percentage of samples that plot within different ranges of Na/Cl (M) values for wetland water samples in the MRW.	88
Table 9. Table showing the percentage of samples that plot within different ranges of Na/Cl (M) values for Drift water samples in the SBW. Data are from the ground water data set (Dannemiller and Baltusis, 1990; Wahrer, 1993; Meissner, 1993).	93
Table 10. Table showing the percentage of samples that plot within different ranges of Na/Cl (M) values for stream samples in the SBW. Data are from Kolak (2000).	95

LIST OF FIGURES

- Figure 1.** Map of the locations of the Muskegon Lowlands (ML), the Saginaw Lowland Area (SLA), Muskegon River Watershed (MRW), Saginaw Bay Watershed (SBW), Muskegon County, and the Regional Aquifer-System Analysis (RASA) boundary. Base Map from the Michigan Geographic Data Library, (2005). 3
- Figure 2.** The arrows show the simulated groundwater flow directions within the Marshall aquifer (Mandle and Westjohn, 1989). Images in this thesis are presented in color. 6
- Figure 3.** The map shows the concentration of dissolved chloride in the RASA region in Michigan (Wahrer et al., 1996). 10
- Figure 4.** Map of the Muskegon River Watershed with respect to the glacial provinces in the lower peninsula of Michigan. (Modified from Westjohn, 1994) Images in this thesis are presented in color. 14
- Figure 5.** Map of the Muskegon River Watershed and the bedrock underneath the watershed. Base Map from Michigan Geographic Data Library, (2005). Images in this thesis are presented in color. 17
- Figure 6.** Graph showing the relationship between Unit (the designation used in this thesis to divide up the different ground water regions) and the stratigraphy. Modified from Meissner, (1993); (Modified from Mandle and Westjohn, (1989); stratigraphic column modified from Michigan Geological Survey, 1964, Graph 1). 18
- Figure 7.** Map showing the stream sample locations within the Muskegon River Watershed. Base Map from Michigan Geographic Data Library, (2005). 23
- Figure 8.** Map showing the lake sample locations in the Muskegon River Watershed. Base Map from Michigan Geographic Data Library, (2005). 24
- Figure 9.** Map showing the wetlands in the Muskegon River Watershed. All samples used were either within the Muskegon River Watershed or 12km or less distance from the edge of the watershed. Base Map from Michigan Geographic Data Library, (2005). 25

Figure 10. Map showing the sample locations that were used to determine the chemistry of the drift ground water for the Muskegon River Watershed. All samples used were either within the Muskegon River Watershed or 12km or less distance from the edge of the watershed. Data are from the ground water data set (Dannemiller and Baltusis, 1990; Wahrer, 1993; Meissner, 1993). Base Map from Michigan Geographic Data Library, (2005).	28
Figure 11. Calcite saturation indices from the Mississippian. Modified from Long et al. (Unpublished).	38
Figure 12. Calcite saturation indices for the Pennsylvanian. Modified from Meissner (1993).	39
Figure 13. Calcite saturation indices for the glacial drift. Data from ground water data set (Dannemiller and Baltusis, 1990; Wahrer, 1993; Meissner, 1993).	40
Figure 14. Ground water within the Muskegon River Watershed Drift. The data were selected from the ground water data set (Dannemiller and Baltusis, 1990; Wahrer, 1993; Meissner, 1993).	40
Figure 15. Calcite saturation indices for streams within the Muskegon River Watershed.	41
Figure 16. Calcite saturation indices for lakes within the Muskegon River Watershed.	41
Figure 17. Calcite saturation indices for wetlands within the Muskegon River Watershed.	42
Figure 18. Dolomite frequency histogram of saturation indices in the Mississippian. Modified from Long et al. (Unpublished).	45
Figure 19. Dolomite frequency histogram for the Pennsylvanian. Histogram modified from Meissner (1993).	46
Figure 20. Dolomite frequency histogram for saturation indices for water in the glacial drift. Data from ground water data set (Dannemiller and Baltusis, 1990; Wahrer, 1993; Meissner, 1993).	47
Figure 21. Dolomite frequency histogram of saturation indices of drift samples within the Muskegon River Watershed. The data were selected from the ground water data set (Dannemiller and Baltusis, 1990; Wahrer, 1993; Meissner, 1993).	47
Figure 22. Dolomite frequency histogram for the streams in the Muskegon River Watershed.	48

Figure 23. Dolomite frequency histogram of saturation indices for the lakes in the Muskegon River Watershed.	48
Figure 24. Dolomite frequency histogram of saturation indices for the wetlands within the Muskegon River Watershed.	49
Figure 25. Gypsum frequency histogram for the Mississippian. Modified from Long et al. (Unpublished).	53
Figure 26. Gypsum frequency histogram for the Pennsylvanian. (Modified from Meissner, 1993).	54
Figure 27. Gypsum frequency histogram for water in the glacial drift. Data from ground water data set (Dannemiller and Baltusis, 1990; Wahrer, 1993; Meissner, 1993). .	55
Figure 28. Gypsum frequency histogram of saturation indices for drift within the Muskegon River Watershed. The data were selected from the ground water data set (Dannemiller and Baltusis, 1990; Wahrer 1993; Meissner, 1993).	55
Figure 29. Gypsum frequency histogram for streams in the Muskegon River Watershed.	56
Figure 30. Gypsum frequency histogram for lakes in the Muskegon River Watershed. . .	56
Figure 31. Gypsum frequency histogram of wetlands in the Muskegon River Watershed.	57
Figure 32. Quartz frequency histogram for samples within the Mississippian. Modified from Long (Unpublished).	61
Figure 33. Quartz frequency histogram for the Pennsylvanian. Modified from Meissner (1993).	62
Figure 34. Quartz frequency histogram for regional glacial drift. Data from ground water data set (Dannemiller and Baltusis, 1990; Wahrer, 1993; Meissner, 1993). .	63
Figure 35. Quartz saturation indices frequency histogram for the glacial drift within the buffered region of the Muskegon River Watershed. The data were selected from the ground water data set (Dannemiller and Baltusis, 1990; Wahrer, 1993; Meissner, 1993).	63
Figure 36. Quartz saturation indices histogram for streams in the Muskegon River Watershed.	64

Figure 37. Quartz saturation indices histogram for lakes in the Muskegon River Watershed.	64
Figure 38. Quartz saturation indices histogram for wetlands in the buffered region of the Muskegon River Watershed.	65
Figure 39. Graph of Na/Cl (M) vs Cl ppm for streams within the Muskegon River Watershed. Sewage sites downstream of the Muskegon County Wastewater Disposal System are surrounded by a box. Septic System Effluent Data from Robertson et al. (1991).	78
Figure 40. The Na/Cl ratio for groundwater within the Pennsylvanian bedrock aquifer. Data are from the ground water data set (Dannemiller and Baltusis, 1990; Wahrer, 1993; Meissner, 1993).	79
Figure 41. The Na/Cl ratio for groundwater within the Pennsylvanian with a ratio of 3.8 or less. Data are from the ground water data set (Dannemiller and Baltusis, 1990; Wahrer, 1993; Meissner, 1993).	79
Figure 42. Na/Cl ratio for groundwater within the Mississippian Data are from the ground water data set (Dannemiller and Baltusis, 1990; Wahrer, 1993; Meissner, 1993).	80
Figure 43. Na/Cl ratio for groundwater within the Mississippian with a ratio less then 3.8. Data are from the ground water data set (Dannemiller and Baltusis, 1990; Wahrer, 1993; Meissner, 1993).	81
Figure 44. Frequency histogram of Na/Cl ratios for ground water wells within the Muskegon River Watershed Drift. Data are from the ground water data set (Dannemiller and Baltusis, 1990; Wahrer, 1993; Meissner, 1993) and includes drift data within 12 km of the watershed.	84
Figure 45 Frequency histogram of Na/Cl ratios for ground water wells within the Muskegon River Watershed Drift that have ratios below 3.8. Data are from the ground water data set (Dannemiller and Baltusis, 1990; Wahrer, 1993; Meissner, 1993).	84
Figure 46. Na/Cl (M) ratios for stream water within the Muskegon River Watershed. .	85
Figure 47. Na/Cl (M) ratios for stream water within the Muskegon River Watershed with Na/Cl less than 3.8..	86
Figure 48. Na/Cl (M) ratios for lake water within the Muskegon River Watershed. . .	87

Figure 49. Na/Cl (M) ratios for wetland water within the Muskegon River Watershed.	88
Figure 50. Na/Cl (M) ratios of groundwater in the Saginaw Bay Watershed. Data are from the ground water data set (Dannemiller and Baltusis, 1990; Wahrer, 1993; Meissner, 1993)..	92
Figure 51 Na/Cl (M) ratios of groundwater in the Saginaw Bay Watershed with Na/Cl (M) ratios less then 3.8. Data are from the ground water data set (Dannemiller and Baltusis, 1990; Wahrer, 1993; Meissner, 1993).	93
Figure 52. Cl/Na (M) ratios for streams in the Saginaw Bay Watershed. Data are from (Kolak, 2000)..	94
Figure 53. Cl/Na (M) ratios for streams in the Saginaw Bay Watershed with Na/Cl ratios less then 3.8. Data are from (Kolak, 2000).	94
Figure 54. Graph showing the relationship between the log molar concentrations of Na and Cl in the Pennsylvanian, Mississippian, seawater evaporation curve (McCaffery et al., 1987), and the envelope on the graph where the water from the glacial drift plot. Ground water data are from the ground water data set (Dannemiller and Baltusis, 1990; Wahrer, 1993; Meissner, 1993).	100
Figure 55. Graph showing the relationship between the log molar concentrations of Na and Cl in the Muskegon River Watershed Drift, Pennsylvanian bedrock, seawater evaporation curve (McCaffery et al., 1987), and the envelope on the graph where the glacial drift plot. Ground water data are from the ground water data set (Dannemiller and Baltusis, 1990; Wahrer, 1993; Meissner, 1993).	101
Figure 56. Graph showing the relationship between the log molar concentrations of Na and Cl in the Muskegon River Watershed streams, Muskegon River Watershed drift, halite dissolution line, and the seawater evaporation curve (McCaffery et al., 1987). Ground water data are from the ground water data set (Dannemiller and Baltusis, 1990; Wahrer, 1993; Meissner, 1993).	102
Figure 57. Graph showing the relationship between the log molar concentrations of Na and Cl in the Muskegon River Watershed lakes, regional drift, Muskegon River Watershed drift, Pennsylvanian bedrock, halite dissolution line, seawater evaporation curve (McCaffery et al., 1987), and the envelope on the graph where the glacial drift plot. The Muskegon River Watershed Drift data includes data up to 12km outside of the Muskegon River Watershed boundary. Ground water data are from the ground water data set (Dannemiller and Baltusis, 1990; Wahrer, 1993; Meissner, 1993).	103

Figure 58. Graph showing the relationship between the log molar concentrations of Na and Cl in the Muskegon River Watershed wetlands, Muskegon River Watershed drift, dissolution of halite, seawater evaporation curve (McCaffery et al., 1987), and the envelope on the graph where the glacial drift plot. Ground water data are from ground water data set (Dannemiller and Baltusis, 1990; Wahrer, 1993; Meissner, 1993).	104
Figure 59. Graph showing the relationship between the Saginaw Bay Watershed drift, regional drift, Muskegon River Watershed drift, halite dissolution, seawater evaporation curve (McCaffery et al., 1987), and the envelopes on the graph where the MRW and SBW drift plot. Ground water data are from the ground water data set (Dannemiller and Baltusis, 1990; Wahrer, 1993; Meissner, 1993).	105
Figure 60. Graph of Ca (M) vs. Mg (M) for ground water samples within the Mississippian bedrock. Data are from ground water data set (Dannemiller and Baltusis, 1990; Wahrer, 1993; Meissner, 1993).	111
Figure 61. Graph of Ca (M) vs. Mg (M) for ground water samples within the Mississippian bedrock with Ca(M) concentrations less than .005. Data are from ground water data set (Dannemiller and Baltusis, 1990; Wahrer, 1993; Meissner, 1993).	112
Figure 62 Graph of Ca (M) vs. Mg (M) for ground water samples within the Pennsylvanian bedrock. Data are from the ground water data set (Dannemiller and Baltusis, 1990; Wahrer, 1993; Meissner, 1993)..	112
Figure 63. Graph of Ca (M) vs. Mg (M) for the Pennsylvanian with Ca (M) concentrations lower than .00032 (M). Data are from the ground water data set (Dannemiller and Baltusis, 1990; Wahrer, 1993; Meissner, 1993).	113
Figure 64. Graph of Ca (M) vs. Mg (M) for ground water samples within the glacial drift. Data are from the ground water data set (Dannemiller and Baltusis, 1990; Wahrer, 1993; Meissner, 1993).	113
Figure 65. Graph of Ca (M) vs. Mg (M) for ground water samples within the regional drift with Ca concentrations below 0.005 (M). Data are from the ground water data set (Dannemiller and Baltusis, 1990; Wahrer, 1993; Meissner, 1993).	114
Figure 66. Graph of Ca (M) vs. Mg (M) for the Muskegon River Watershed buffered Drift. Data are from ground water data set (Dannemiller and Baltusis, 1990; Wahrer, 1993; Meissner, 1993).	114
Figure 67. Graph of Ca (M) vs. Mg (M) for streams within the Muskegon River Watershed.	115

Figure 68. Graph of Ca (M) vs. Mg (M) for lakes within the Muskegon River Watershed..	115
Figure 69 Graph of Ca (M) vs. Mg (M) for wetlands within the Muskegon River Watershed..	116
Figure 70. Piper diagram showing the different hydrochemical facies (Piper, 1944; Drever, 1997)..	125
Figure 71. Piper diagram of the ground water in the Pennsylvanian bedrock. Data are from ground water data set (Dannemiller and Baltusis, 1990; Wahrer, 1993; Meissner, 1993)..	128
Figure 72. Piper diagram of the ground water in the Mississippian bedrock. Data from the ground water data set (Dannemiller and Baltusis, 1990; Wahrer, 1993; Meissner, 1993)..	129
Figure 73 Piper diagram of the ground water in the glacial Drift. Data are from the ground water data set (Dannemiller and Baltusis, 1990; Wahrer, 1993; Meissner, 1993)..	130
Figure 74 Piper diagram of ground water samples within the buffered region of the Muskegon River Watershed Drift. Data are from the ground water data set (Dannemiller and Baltusis, 1990; Wahrer, 1993; Meissner, 1993)..	132
Figure 75 Piper diagram of ground water samples within the glacial drift of the Saginaw Bay Watershed. Data are from the ground water data set (Dannemiller and Baltusis, 1990; Wahrer, 1993; Meissner, 1993)..	133
Figure 76. Ternary Diagram for base flow river data from the Saginaw Bay Watershed. The data were modified (i.e. lake data removed) from the RIV3 data set from Kolak (2000)..	136
Figure 77. Piper diagram of the stream water within the Muskegon River Watershed. The data points in which sewage were expected to influence the stream water were circled..	137
Figure 78. Piper diagram of lake water within the Muskegon River Watershed..	138
Figure 79. Piper diagram of wetland water within the Muskegon River Watershed..	139

- Figure 80.** Map of the Lower portion of the Muskegon River Watershed. Locations of wells that may have produced brine were taken from the Department of Environmental Quality (2005) website. Locations of samples with Na/Cl (M) ratios less than .8 are shown in brown. The concentration of Cl at the sample location is represented as the length of the brown column. Base Map from the Michigan Geographic Data Library (2005) website. Images in this thesis are presented in color.148
- Figure 81.** Map of the Upper portion of the Muskegon River Watershed. Locations of wells that may have produced brine were taken from the Department of Environmental Quality (2005) website. Locations of samples with Na/Cl (M) ratios less than .8 are shown in brown. The concentration of Cl at the sample location is represented as the length of the brown column. Base Map from the Michigan Geographic Data Library (2005) website. Image in this thesis are presented in color.149
- Figure 82.** Map of the Quaternary Geology (for quaternary geology legend see figure 85) of the Saginaw Bay Watershed. Base Map from the Michigan Geographic Data Library (2005) website. Images in this thesis are presented in color.152
- Figure 83.** Map of the Quaternary geology (for quaternary geology legend see figure 85) of the lower half of the Muskegon River Watershed. Locations of samples with Na/Cl (M) ratios less than 0.8 are shown in brown. The concentration of Cl at the sample location is represented as the length of the brown column. Base Map from the Michigan Geographic Data Library (2005) website. Images in this thesis are presented in color.153
- Figure 84.** Map of the Quaternary geology (for quaternary geology legend see figure 85) of the Upper portion of the Muskegon River Watershed. Locations of samples with Na/Cl (M) ratios less than .8 are shown in brown. The concentration of Cl at the sample location is represented as the length of the brown column. Base Map from the Michigan Geographic Data Library (2005) website. Images presented in this thesis are presented in color.154
- Figure 85.** The legend shows the different colors and patterns used to show distinct types of quaternary surface geology in the Muskegon River Watershed. This legend is to be used with Figures 82-84. Images in this thesis are presented in color.155
- Figure 86.** Map of the lower portion of the Muskegon River Watershed. Shows the locations of surface water sites that have a Na/Cl molar ratio between 0.8 and 1.2. The concentration of Cl is represented by the length of the bar. Base Map from the Michigan Geographic Data Library (2005) website. Images in this thesis are presented in color.158

- Figure 87.** Map of the upper portion of the Muskegon River Watershed. Shows the locations of surface water sites that have a Na/Cl molar ratio between 0.8 and 1.2. The concentration of Cl is represented by the length of the bar. Base Map from the Michigan Geographic Data Library (2005) website. Images in this thesis are presented in color. 159
- Figure 88.** Map of surface water samples in the lower portion of the MRW with Na/Cl (M) ratios above 1.2. Map shows the concentration of Cl by the length of the columns. Base Map from the Michigan Geographic Data Library (2005) website. Images in this thesis are presented in color.162
- Figure 89.** Map of surface water samples in the upper portion of the MRW with Na/Cl (M) ratios above 1.2. Map shows the concentration of Cl by the length of the columns. Base Map from the Michigan Geographic Data Library (2005) website. Images in this thesis are presented in color.163
- Figure 90.** Map of surface water samples near the city of Muskegon with Na/Cl (M) ratios above 1.2. Map shows the concentration of Cl by the length of the columns. Base Map from the Michigan Geographic Data Library (2005) website. Images in this thesis are presented in color.164

Chapter 1

Scope and Purpose

The Great Lakes of North America comprise one-fifth of the world's fresh surface water (GLIN, 2005). However a portion of the Great Lakes watershed overlies the Michigan Basin, a geologic structure that contains some of the most concentrated aqueous subsurface fluids (formation waters) on Earth (Case, 1945). For example, total dissolved solids of formation waters in the deeper central portion of the basin are greater than 400,000 mg/L (Case, 1945). It is possible there is the potential for mixing of the saline and freshwater.

A series of studies (Long et al., 1988; Wahrer et al, 1996; Mandle and Westjohn, 1989) have shown that such mixing is occurring in the Saginaw Lowland area (SLA) of Michigan (Figure 1). Characteristics of near-surface ground water in the SLA include high Cl concentrations and very light stable isotopes of oxygen and hydrogen in water molecules. Data from ground water in and near the Michigan Lowland area (ML) (Figure 1) of Michigan show some ground water with elevated Cl concentrations and light stable isotopes of oxygen and hydrogen (Long, 2005). Thus, it is possible that hydrogeochemical processes identified in the SLA could be occurring in the ML.

This study of the biogeochemistry of surface waters in the Muskegon River Watershed (MRW) (Figure 1) provides a database that allows for the investigation of hydrogeochemical processes within the ML. Since there are no natural sources for Cl in

near surface sediments in the ML, the concentration of Cl should be less than 10 ppm, if the ground water is from recent precipitation (Wahrer et al., 1996). If ground water (maximum of 10 ppm Cl) and rainwater (average 0.10 mg/L Cl (NADP, 2002)) are the major inputs to surface waters in the MRW then the surface waters should have a Cl concentration of less than 10 ppm. Elevated Cl concentrations have been identified in surface waters and ground waters of the MRW. Therefore, this thesis will examine the hypothesis that the cause of the elevated Cl concentrations is from the interaction of deeper saline ground water with near surface ground water and surface waters (rivers, lakes, wetlands). Alternatively the elevated Cl concentrations could be the result of human activities within the watershed (e.g., road salting, oil and gas production, septic leakage). These hypotheses will be explored using graphical and geochemical modeling analyses and comparisons to results from the SLA.

The research in this thesis (Ground Water Surface Water Interactions in the Muskegon River Watershed) is part of a larger study, the Great Lakes Fisheries Trust Muskegon River Initiative. The overall goal of the Great Lakes Fisheries Trust Muskegon River Initiative is to study the effect of anthropogenic influences on organisms and their habitat within the Muskegon River Watershed. Preliminary results from the work of Lindeman et al. (2002) also related to the goals and objectives of the Great Lakes Fisheries Trust Muskegon River Initiative, show that anthropogenic influences such as land use have an effect on surface water chemistry.

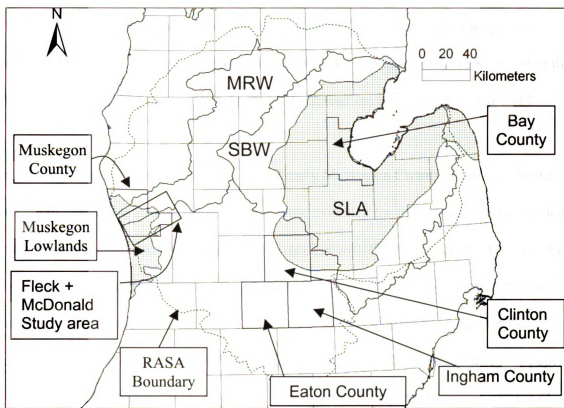


Figure 1. Map of the locations of the Michigan Lowlands (ML), the Saginaw Lowland Area (SLA), Muskegon River Watershed (MRW), Saginaw Bay Watershed (SBW), Muskegon County, and the RASA boundary. Base Map from Michigan Geographic Data Library, (2005).

Related Studies

The presence of saline water in the SLA (Figure 1) has been known for a long time.

Douglass Houghton documented the presence of saline springs within the SLA, along the Tittabawassee and Salt rivers (Houghton, 1928), sometime between 1837 and 1844.

In certain portions of the MRW, more specifically Muskegon County (Figure 1), which is located in the Michigan Lowlands, there is some evidence for the potentiometric surface of the bedrock aquifer to be high enough to interfere with the drift aquifer. A well drilled into a sandstone aquifer approximately 4 miles from the mouth of the Muskegon River flowed at 20 gallons per minute (USGS Well 431540086145601) showing that the potentiometric surface in the underlying bedrock was higher than ground level. A paper by Fleck and McDonald (1978) included a description of the potentiometric surface of the Marshall Aquifer in a region that overlapped with the southwestern most portion of the MRW (Figure 1). Fleck and McDonald (1978) determined that the potentiometric surface of the Marshall Aquifer in the eastern most portion of their study region to be 30m lower than the water table, and determined that this is the recharge zone of the Marshall aquifer. However, at the shore of Lake Michigan, the western most portion of the Fleck and McDonald study region, the Marshall Aquifer has a potentiometric surface 3 meters above that of lake level where it has the potential to discharge into the overlying aquifer or into Lake Michigan. The Michigan Lowlands is not the only place in the Lower Peninsula of Michigan that has hydrologic conditions that would be conducive to upwelling from bedrock layers below.

Long et al. (1988) stated that the source of dissolved solids to the SLA could be the natural upward advection and diffusion of ions from formation waters below (Long et al., 1988). It was established that the potentiometric surface of the bedrock aquifer in some areas of the east central portion of the Lower Peninsula was higher than the overlying drift aquifer in other areas (Long et al., 1988). This difference indicates that there is a potential for upward flow from the bedrock into the drift aquifer (Long et al., 1988). Advective flow is the result of topographic-controlled flow within the SLA. However, other factors such as the presence of clay (Long et al., 1988) can have an effect on the ability for these saline waters to enter into the near surface aquifer, decreasing the effectiveness of advective flow and favoring diffusive flow.

Meissner (1993) found three different water types in the Pennsylvanian aquifers; meteoric water, glacial meteoric water, and Parma-Bayport brine. Meissner (1993) found that all of these water masses were mixing near the Saginaw Bay in the Pennsylvanian aquifers.

Ground water models of the RASA study region (Figure 1) showed that there is an upward component to the ground water movement in the bedrock aquifer (Figure 2) beneath both the Saginaw Bay area as well as the Michigan Lowlands (ML) (Mandle and Westjohn, 1989). The upwelling region also includes the southern most portion of the Muskegon River Watershed.

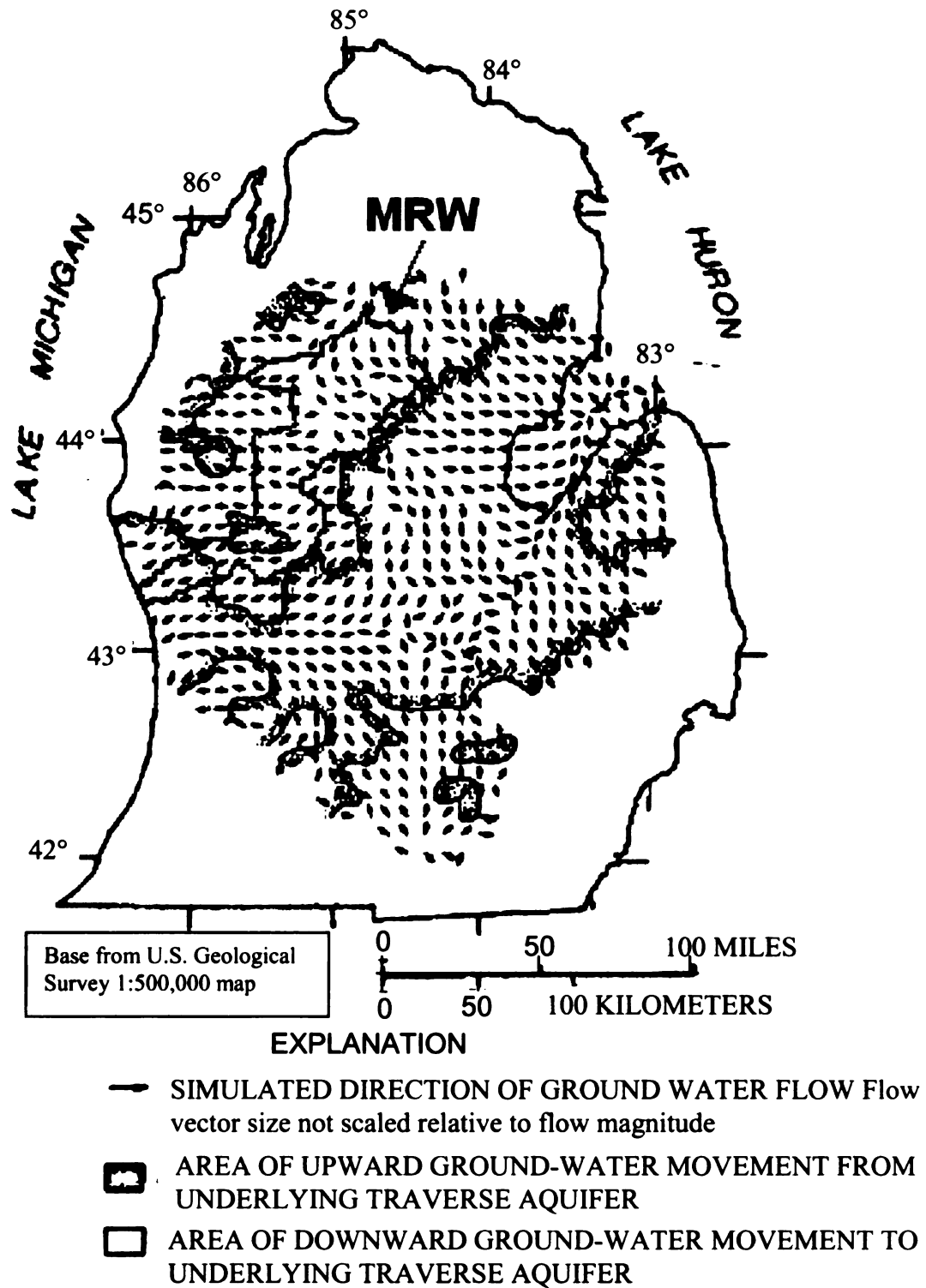


Figure 2. The arrows show the simulated groundwater flow directions within the Marshall aquifer (Modified from Mandle and Westjohn, 1989). Images in this thesis are presented in color.

Wahrer (1993) concluded that the two major processes controlling the chemistry of water for the regional drift in the RASA study region were water-rock interactions and the mixing of fresher water with more concentrated fluids from underlying aquifers. The later process was occurring in the Saginaw Bay area. The geochemical data used by Wahrer (1993) revealed that the bedrock aquifers underlying the glacial drift have similar chemistries as those in the drift. However, the aquifers contained progressively more concentrated solutions with depth. Wahrer (1993) found that the drift aquifer in the Saginaw Lowland area contained water that had a high level of dissolved solids and light $\delta^{18}\text{O}$ values. Wahrer (1993) also noted that the Quaternary geology of the Saginaw Lowland was composed of impermeable sediments. A map of the distribution of Cl in the glaciofluvial aquifer in the RASA region (Figure 3) shows that the waters with the highest concentration of Cl are in or near the Saginaw Bay (Wahrer et al., 1996).

The Regional Aquifer-Systems Analysis Project (RASA) was started by the United States Geological Survey to gather the information needed to understand the regional ground water flow and establish a database of various geological, hydrological, and geochemical data to help assess ground water resources. One of the regions studied in the RASA project was the central portion of the Lower Peninsula of Michigan (Westjohn and Weaver, 1998).

A paper for the Regional Aquifer-System Analysis (RASA) program by Westjohn and Weaver (1996) listed geologic controls that control the presence of freshwater in the RASA region. A direct contact between a sandstone aquifer and permeable glacial units,

would allow for the mixing of waters between these two different hydrologic units. The presence of lodgment tills may impede the upward migration of saline waters from sandstone layers below. Vertical hydrologic barriers within the sandstone aquifers and between the different sandstone bedrock units could slow the movement of waters between and within the bedrock units. The presence of the low permeability Jurassic Red Beds may be able to prevent the upward discharge of saline water or the downward movement of freshwater into the bedrock.

Kolak (2000) took stream samples and core samples in the Saginaw Bay Watershed (SBW) (Figure 1); the SBW includes the SLA (Saginaw Lowland Area) , and suspected that there was some release of Cl to rivers through the discharge of ground water to streams. However, methods used to determine the source of Cl in a watershed, such as Cl/Br ratios, were confounded by sources of Br to a watershed such as the degradation of organic matter, pesticides and possible leakage from oil and gas production (Kolak, 2000).

Preliminary results from the work of Lindeman et al. (2002), also related to the goals and objectives of the Great Lakes Fisheries Trust Muskegon River Initiative, show that anthropogenic influences such as land use have an effect on surface water chemistry. Lindeman et al. (2002) hypothesized that each different type of land use (e.g., urban, agriculture, and forested) had its own unique biogeochemical effect on the ecosystem and therefore each land use type would have its own unique suite of biogeochemical parameters. Lindeman et al. (2002) uses two different watersheds in determining the

biogeochemical fingerprint of the different land uses, those watersheds are the Muskegon River Watershed and the Traverse Bay Watershed. The preliminary analysis from Lindeman's work has revealed that Ca and Mg are associated with agricultural type land use and Na and Cl is associated with urban type land use. Lindeman (2002) noticed a correlation between concentrations of Na (M) and Cl (M) in surface waters and urban land use.

It has been shown that the Bay County area (Long et al., 1988) and the Michigan Lowlands (Fleck and McDonald, 1978) have hydrogeologic conditions that would allow waters within the bedrock to migrate into the near surface aquifer. The abnormally high levels of dissolved solids found in the Bay County area have been attributed to the upward migration of saline waters from bedrock layers below (Long et al., 1988). Much of the MRW does not overlie impermeable bedrock units like the Jurassic Red Beds that would prevent the discharge of saline water to the glacial drift aquifer. It is suspected that the source of Cl to the streams in the Saginaw Bay Watershed can be at least in part due to the upward migration of saline water into the shallow aquifer, and those streams are being fed by this saline water (Kolak, 2000). The MRW has some abnormally high Cl concentrations in the surface waters and drift water. The lower portion of the MRW overlies the Michigan Lowlands and therefore overlies an area known to have the hydraulic potential to drive water in the bedrock into the shallow aquifer. Therefore the possibility that the source of dissolved solids to the MRW is upward migrating saline waters from bedrock layers below needs to be explored.

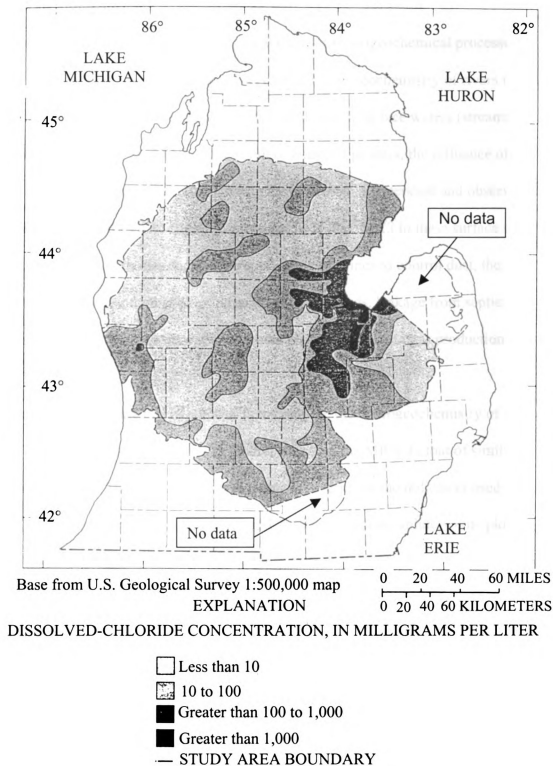


Figure 3. The map shows the concentration of dissolved chloride in the RASA region in Michigan (Modified from Wahrer et al., 1996).

Hypothesis and Approach

Based on the results of the RASA study, knowledge of hydrogeochemical processes occurring in the SLA, and preliminary observations of the geochemistry of rivers in the MRW, the working hypothesis is that a portion of the Cl in surface waters (streams, wetlands, and lakes) of the MRW is the result of a natural process, the influence of upward migrating saline water. Considering the land uses in watershed and observations of Lindeman et al. (2002), an alternative hypothesis is that the Cl in these surface waters is a result of human activities such as the application of brines to control dust, the application of halite (and other chloride salts) to de-ice roads, leakage from septic systems, discharges from waste water treatment plants, and oil and gas production.

The approach to examine this hypothesis is to compare the hydrogeochemistry of surface (rivers, wetland, and lakes) waters and ground waters of the MRW to that of similar waters in the SLA. The comparisons will be made in terms of the indicators used to identify hydrogeochemical processes in the SLA. These include, solute-solute plots, Piper plots, and geochemical modeling.

Study Site

The MRW is located in the west central part of the Lower Peninsula of Michigan (Figure 1). The headwaters are Houghton and Higgins Lake in the north. The river flows southwest into Muskegon Lake before eventually emptying into Lake Michigan. The watershed covers approximately 7,052 square kilometers and is about 352 kilometers

long. The watershed includes portions of Wexford, Missaukee, Osceola, Clare, Mecosta, Montcalm, Roscommon, Newaygo, and Muskegon counties (Stout, 2005).

The Muskegon River Watershed overlies a portion of two different glacial provinces as mapped by Westjohn et al. (1994). Almost all of the watersheds except for the southern most portions overlie deposits that are glaciofluvial and coarse textured till. The small southern portion of the watershed overlies glacial drift that is mostly moraines and outwash sediments (Figure 4).

A more specific study of the Quaternary and bedrock geology was done by Fleck and McDonald in 1978. The region studied by Fleck and McDonald (1978) included the southern most portion of the MRW, this region is shown on Figure 1. The western portion of the region is located within the Michigan Lowlands (ML). According to Fleck and McDonald (1978) this region is composed of sediments that range from tight clay to fine gravel. The upper 6 to 24 meters of the glacial sediments are composed of well-sorted sand, with fine gravel and silt interlayered within. Beneath this layer is a relatively impermeable confining layer.

The confining layer is of varying thickness and separates the bedrock layer from the upper aquifer. The confining layer is composed of silt, clay and shale. The confining layer is approximately 245m thick near Newaygo and is only 24m thick at Lake Michigan near Muskegon.

Beneath the glacial drift is bedrock. The MRW overlies various bedrock units.

Figure 5 shows that the MRW overlies the Jurassic Red Beds, the Saginaw aquifer, the Saginaw confining unit, the Parma-Bayport aquifer, the Michigan confining unit, and the Marshall aquifer. Figure 6 shows the relationships between the stratigraphic units and the hydrogeologic units of the different bedrock units in the RASA study region (the RASA study region includes the MRW.) It also shows the way in which the bedrock units in this thesis will be grouped and that is shown under the column labeled Unit.

The uppermost rock unit is the Jurassic confining unit. This rock unit is composed primarily of red clay, mudstone, siltstone, and sandstone. It also contains some gray-green shale and gypsum beds (Westjohn et al., 1994). The red beds contain both saline and brine waters, the top of the Red Beds correlate with the base of the freshwater zone. Most rocks within this unit have poor permeability (Westjohn and Weaver, 1998). The Jurassic red beds are spotty in presence but still cover a large portion of the central part of the Michigan Basin (Figure 6).

The Saginaw aquifer, which includes both the Grand River Formation and the Saginaw Formation, lies directly underneath the Jurassic red beds. The Saginaw aquifer consists of sandstone, siltstone, shale, coal, and limestone. It is used extensively in Clinton, Ingham, and Eaton (Figure 1) counties for drinking water (Westjohn and Weaver, 1998). The Saginaw aquifer contains both saline and freshwater.

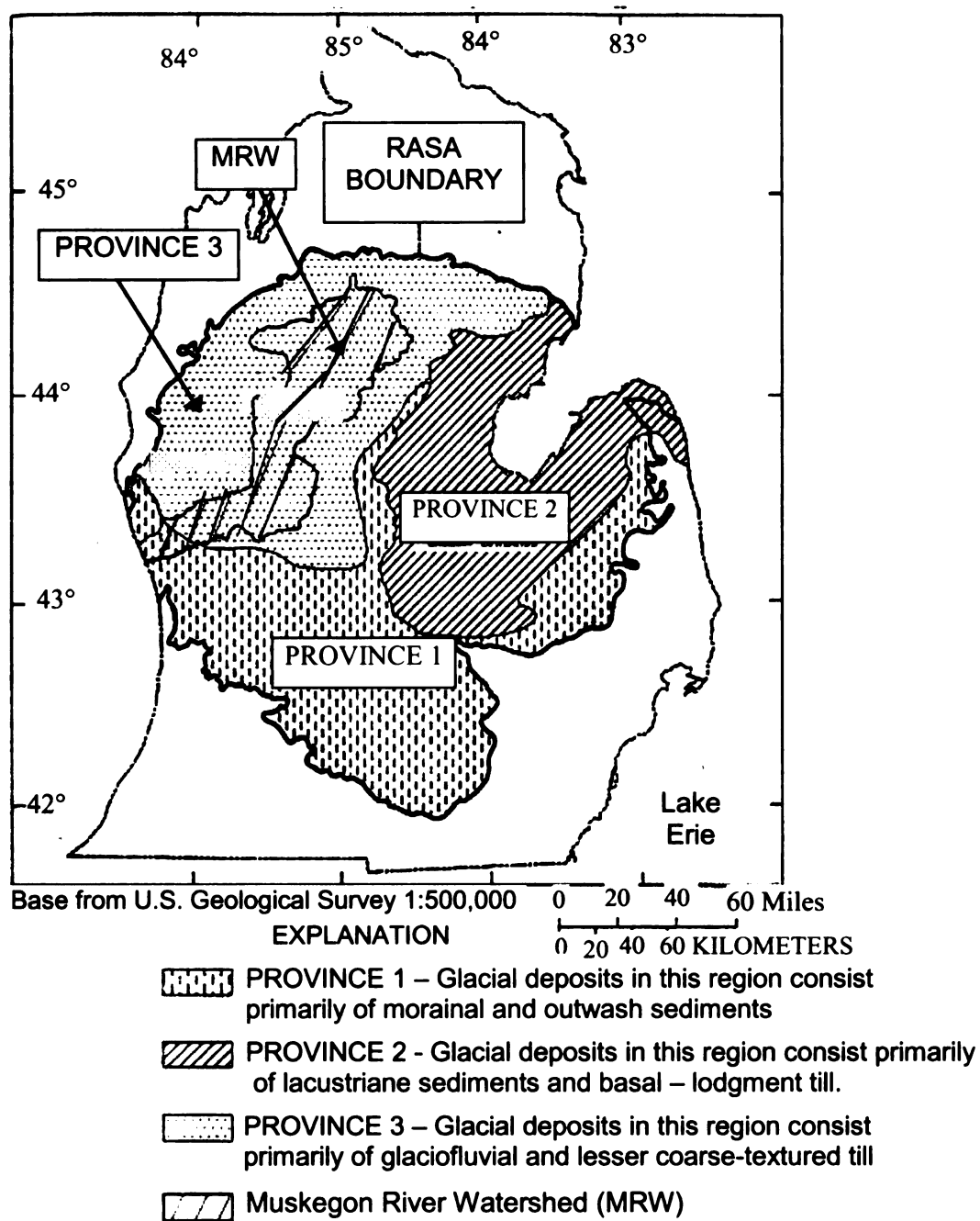


Figure 4 Map of the MRW with respect to the glacial provinces in the lower peninsula of Michigan (Modified from Westjohn, 1994). Images in this thesis are presented in color.

The Saginaw confining unit lies underneath the Saginaw aquifer. It is primarily composed of shale but also contains some thin beds of sandstone, coal, siltstone, and limestone. The sandstone and siltstone lenses tend to be less than 4.6m thick and only run for a few miles but they do contain some saline and brine waters (Westjohn and Weaver, 1998).

The Parma-Bayport aquifer lies below the Saginaw confining unit. The Parma-Bayport aquifer is usually 100 to 150 feet thick and is composed of sandstone and carbonates. It contains both fresh and saline waters (Westjohn and Weaver, 1998).

The Michigan Confining unit underlies the Parma-Bayport aquifer and is primarily composed of shale, carbonate, evaporites, and some thin laterally discontinuous siltstone and sandstone beds. This confining unit does not contain a significant portion of water (Westjohn and Weaver, 1998).

The Marshall aquifer lies below the Michigan confining unit and is composed chiefly of sandstone. It also contains some siltstone and shale that are interfingered with the sandstone. The Marshall aquifer is the lowest aquifer that is in contact with the glacial material that underlies Muskegon River Watershed. The Marshall aquifer contains both freshwater and brines (Westjohn and Weaver, 1998).

The Parma Sandstone is the stratigraphically deepest portion of the Pennsylvanian. The Bayport Limestone is the stratigraphically highest portion of the Mississippian.

Although, the Bayport Limestone and the Parma Sandstone are not part of the same bedrock unit in this thesis; they are hydraulically connected and are sometimes grouped together as the Parma-Bayport aquifer (Westjohn, 1998). The Saginaw confining unit lies between the Parma Sandstone and the Saginaw Formation. It has been suggested by Meissner (1993), that the Parma-Bayport aquifer within the Saginaw Lowland area or Saginaw Bay watershed is the source of dissolved solids to the overlying Grand River Saginaw aquifer as well as to the drift.

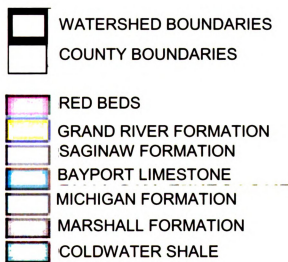
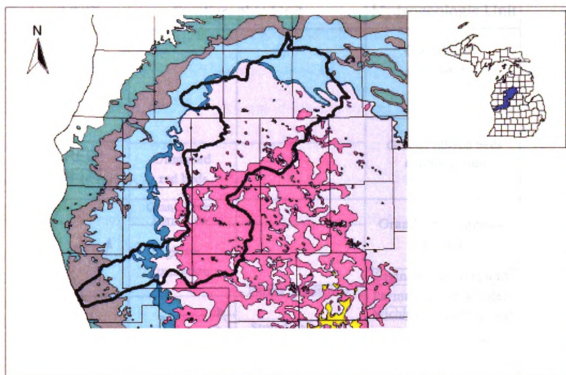


Figure 5. Map of the Muskegon River Watershed and the bedrock underneath the watershed. Base Map from Michigan Geographic Data Library, (2005). Images in this thesis are presented in color.

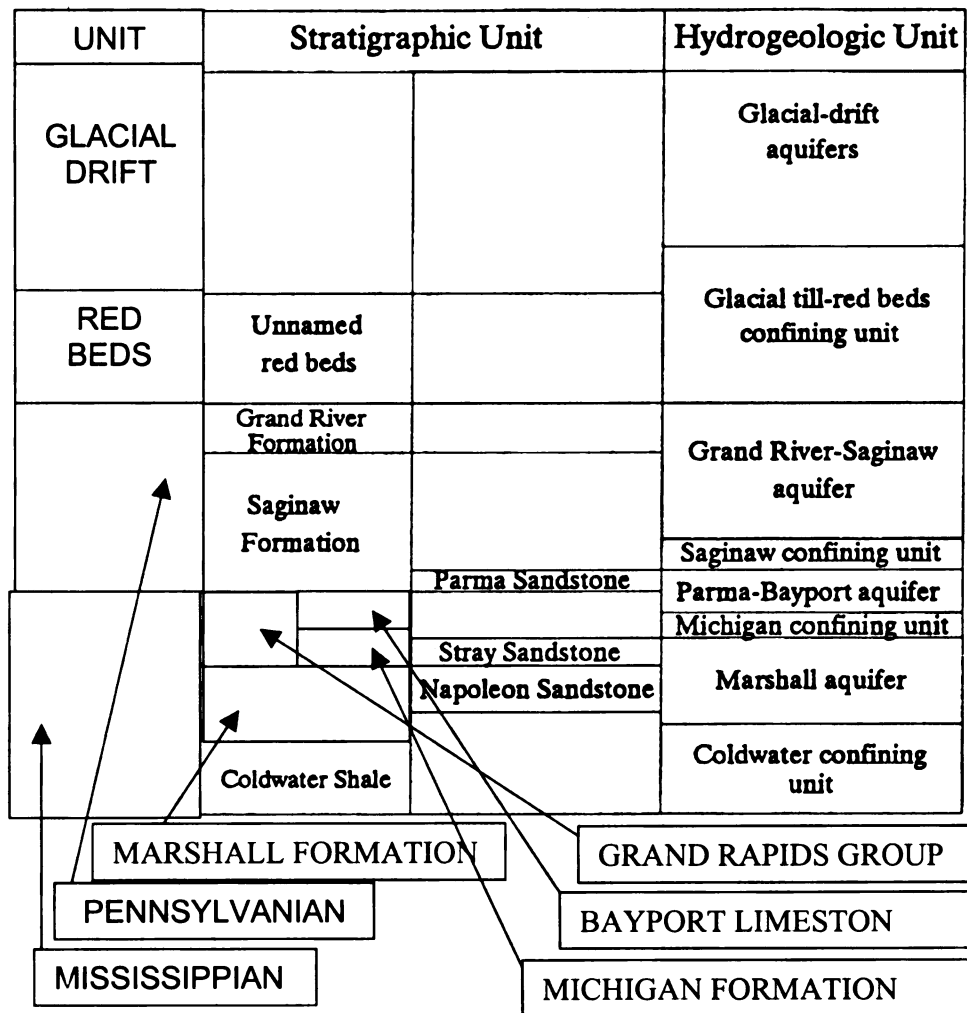


Figure 6. Graph showing the relationship between Unit (the designation used in this thesis to divide up the different ground water regions) and the stratigraphy. Modified from Meissner, (1993); (Modified from Mandle and Westjohn, (1989); stratigraphic column modified from Michigan Geological Survey, 1964, Graph 1).

If the streams and lakes above a region with an upward advective flow out of the bedrock, into the drift aquifer, are recharged by ground water then the formation waters could influence the overlying surface water chemistry. The presence of low permeability sediments can increase the salinity of ground water in an area that already has advective flow of saline waters into it. The low permeability sediments can decrease the amount meteoric water infiltrating into the ground water (Long et al., 1988) and therefore prevent saline water already in the aquifer from being diluted by fresher meteoric water.

Alternatively, the occurrence of excess Cl in the watershed could be from the application of halite to roads. Salt and brines are applied throughout the watershed. The application of road salt to roads is done extensively in the winter in order to melt and prevent the formation of ice. As a result Cl and Na levels in streams should be elevated above natural background levels especially during the spring snowmelt. Brines are applied to dirt roads in order to help prevent and minimize road dust. Brines can enter into lakes and streams when applied on bridges or over culverts. Brines can also enter into streams and lakes as run-off from brined roads

Chapter 2

Methods

Field Data and Sample Collection

Water samples were taken from streams, lakes and wetlands in the Muskegon River Watershed. In order to make stream sampling efficient, sample locations of streams were picked preferentially at places where roads crossed streams. The stream samples were taken from the thalweg of the stream, sampling upstream to avoid the possible influence of bridges, roads and culverts on stream chemistry. Streams were sampled at base flow so that the effect of runoff would be minimal, a time when ground water should be the largest contributor to the stream. The lake samples were taken over the deepest portion of the lake. The sampler used takes an integrated sample of the epilimnion. The wetland samples are taken at open water within the wetland.

Stream water was collected with a sampler that consisted of a plastic weight attached to the bottom of a J-shaped piece of Plexiglas. The bend in the Plexiglas is just wide enough to fit a 250 ml bottle. Once the bottle had been inserted into the sampler it was made secure with rubber bands. A length of rope was attached to the sampler so the sampler could be tossed or lowered into the stream.

The lake water samples were taken from the epilimnion. If the epilimnion was greater than 3m deep, an integrated tube was used for taking the water sample. The integrated tube allowed water in for the entire depth of the water column. The sample is poured out

of the tube into a bucket where it was mixed, and then the sample was taken from the bucket. If the epilimnion was less than 3 m deep then a Van Dorn sampler was used to take sub samples from the bottom, middle, and top of the epilimnion. Those 3 sub samples were then poured into a bucket and mixed. The samples captured for chemical analysis were taken from the mixed samples (Lougheed, 2005).

The wetland samples were taken at a location that was relatively free of vegetation. The wetland samples were collected by submerging an open sample bottle (Lougheed, 2005).

All the samples were filtered through a 0.45 μ m disposable Millipore® filter. The 60ml cation samples were filtered then acidified with 400 μ l of trace metal grade nitric acid.

The Cl and F samples were filtered but no preservative was added. The 30ml SO₄ samples were filtered then preserved with 250 μ l of formaldehyde. Samples for dissolved organic carbon, approximately 35ml, were filtered then preserved with the addition of 1ml of 2 normal sulfuric acid. All of the samples mentioned above were placed on ice after filtration and preservation. The anions were filtered and then flash frozen on dry ice.

Measurements taken in the field included; water temperature, dissolved oxygen concentration, redox potential, specific conductance, pH, alkalinity, longitude, and latitude. The chemical and physical measurements were taken via a YSI multiparameter probe after allowing 20 or more minutes for equilibration. Alkalinities were determined

using the Gran titration method (Stumm and Morgan, 1996) on site or within 24 hrs of sample collection.

A total of 260 stream samples (Figure 7) were taken during: July, August and November of 2001, July and August of 2002, and August of 2003. Stream sampling trips were done synoptically. A total of 158 lake samples (Figure 8) were taken during September 2001, May, August, June, and September 2002, and April and May of 2003. A total of 83 wetland samples (Figure 9) were taken during July and August of 2001, June and July of 2002, and July and September of 2003. Wetland and lake data were not taken synoptically but instead periodically throughout the spring, summer, and fall.

All of the stream and lake samples, collected as part of the MRW project, were taken within the watershed. However, wetland samples were taken within as well as outside of the watershed. Due to the limited number of wetland samples taken within the watershed, samples within 12 km of the outside boarder of the MRW watershed were included in the dataset to represent the chemistry of the watershed in this thesis. The 12 km boundary was set as a function of Quaternary geology, since one of the factors in controlling the chemistry of the ground waters in the Michigan basin may be Quaternary geology (Long et al., 1988). Coarse glacial deposits dominantly underlie the MRW; the coarse sediments extend to at least 12 km from the border in any point along the MRW. Beyond the 12 km buffer range the geology especially in the eastern portion changes to more fine-grained materials.

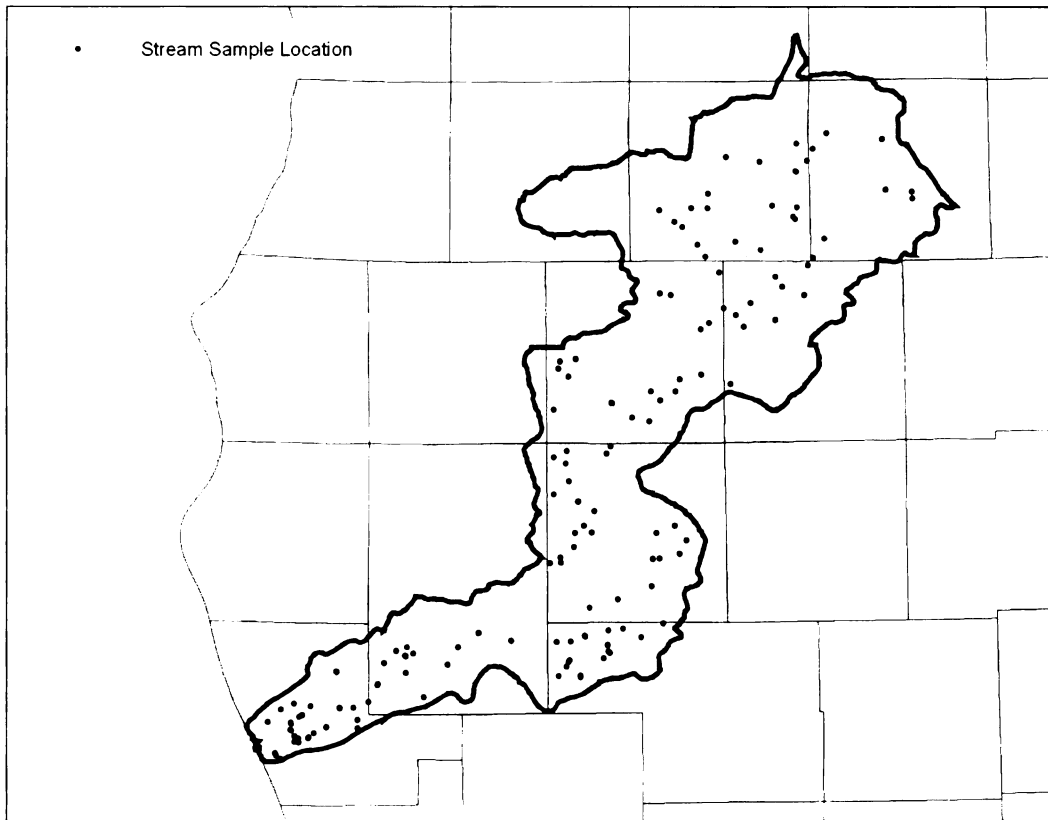


Figure 7. Map showing the stream sample locations within the Muskegon River Watershed. Base Map from Michigan Geographic Data Library, (2005).

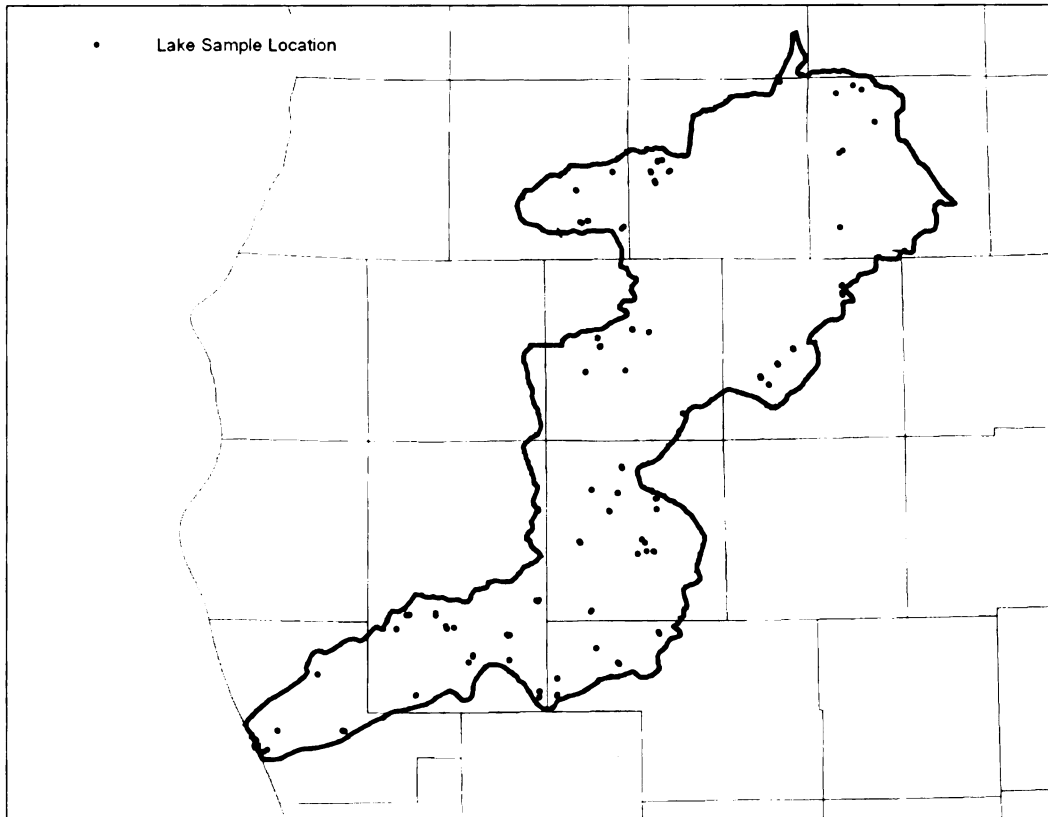


Figure 8. Map showing the lake sample locations in the Muskegon River Watershed. Base Map from Michigan Geographic Data Library, (2005).

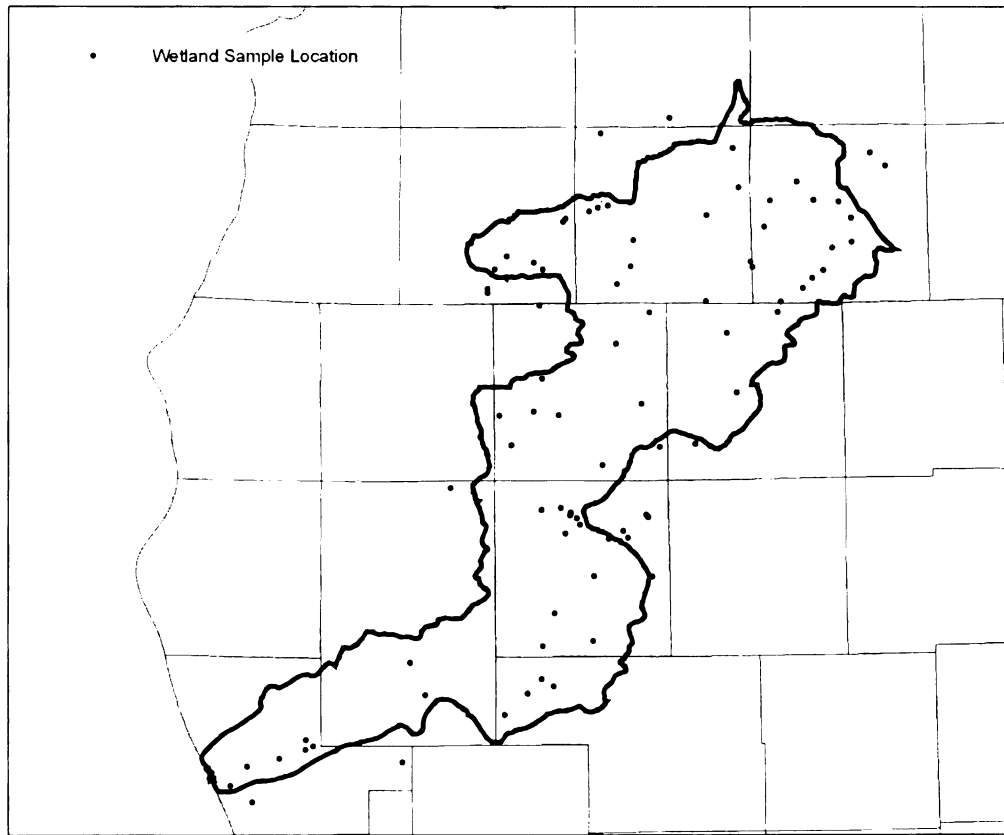


Figure 9. Map showing the wetland sample locations in the Muskegon River Watershed. All samples used were either within the Muskegon River Watershed or 12km or less distance from the edge of the watershed. Base Map from Michigan Geographic Data Library, (2005).

Supplementary Data

The data set used in this thesis to characterize ground water in the glacial drift and bedrock is a compilation of several different data sets. One of those data sets is the RASA data set. The RASA data set was compiled by Dannemiller and Baltusis (1990) and comprises a significant number of the samples in the data set. Several other sources for data include the Department of Natural Resources (Wood, 1969), USGS WATSTORE 1974-1987 database, Long et al. (1988) database, and the Department of Health (Mark Breithart, 1992) database. The data set as a whole will be called the ground water data set. The ground water data set will have three subsets representing the three different ground water domains explored in this thesis (i.e., the glacial drift, the Mississippian bedrock unit, and the Pennsylvanian bedrock unit). The Mississippian includes samples from the Marshall, Bayport, Michigan, and Coldwater Stratigraphic units. The Pennsylvanian unit includes samples from the Grand River Formation, the Saginaw Formation, and the Parma Sandstone. The glacial drift and Pennsylvanian bedrock water data include location, depth, temperature, pH, ROE, latitude, and longitude. It also includes concentrations of Al, As, B, Br, Ca, Cl, F, Fe, Li, Mg, Mn, O₂, K, SiO₂, Na, Sr, SO₄, S, Zn, N, NH₄, DOC, Ba, Fe (II), ²H, ¹⁸O, and ¹³C. Ground water data from the Mississippian were more limited. This data set included alkalinity, Br, Ca, Cl, Mg, K, Na, Sr, SO₄, and O₂. The RASA data are from several different data sources. Most of the data comes from a study done by Dannemiller and Baltusis (1990) and appended by Wahrer (1993) and Meissner (1993).

The glacial drift data set will be used as a whole to represent the waters within the drift within the RASA boundary (Figure 1). The SBW Drift data set is all of the ground water drift data that plot within the SBW (Figure 1). The MRW Drift data set all of the ground water drift data that plot within the MRW.

Drift data within the MRW watershed (Figure 10) was relatively sparse; however, many data points lie close to the watershed but do not lie within it. All drift points within the MRW watershed along with points within 12km of the watershed boundary were combined and used to represent the MRW watershed. This subset of data will be termed the MRW Drift. The 12 km boundary was used for the same reasons as those used for the wetland data set.

The National Atmospheric Deposition Program (NADP) was started in 1978 to collect precipitation data with the purpose of monitoring short and long-term changes in its chemistry. It uses state and federal agencies along with private organizations to accomplish this goal. The NADP has two stations (Figure 1) near but not within the MRW, Kellogg Biological Station at Gull Lake and one at Wellston Michigan, these two stations provide the most current and geographically closest precipitation data to the study site and therefore will be used for precipitation data for the MRW.

Kolak (2000) collected base flow river measurements from the Saginaw Bay Watershed. Kolak (2000) named one of the base flow datasets he collected RIV3. The RIV3 data set contains Cl, Na, Br, Ca, Mg, K, SiO₂, temperature, alkalinity, SO₄, pH, longitude and

latitude data. This data set will be used to represent the Saginaw Bay watershed streams and will be called SBW streams.

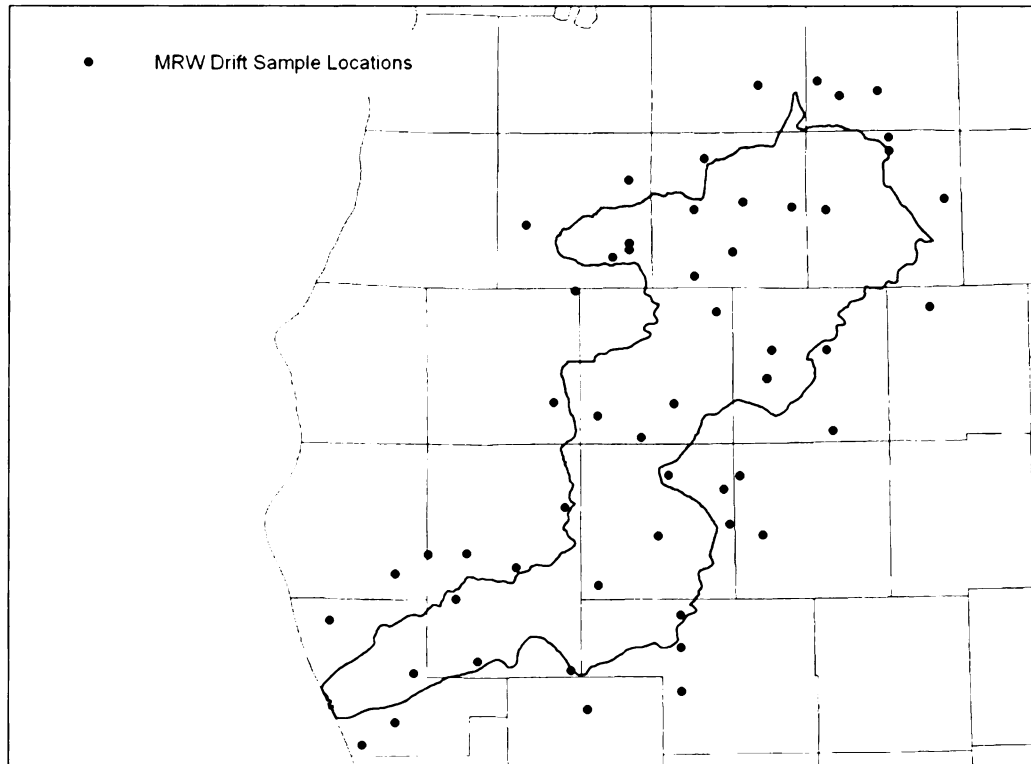


Figure 10. Map showing the sample locations that were used to determine the chemistry of the drift ground water for the Muskegon River Watershed. All samples used were either within the Muskegon River Watershed or 12km or less distance from the edge of the watershed. Data are from the glacial drift data set (Dannemiller and Baltusis, 1990; Wahrer, 1993; Meissner, 1993). Base Map from Michigan Geographic Data Library, (2005).

Sample Analysis

Calcium, potassium, magnesium, and sodium were analyzed via a Perkin Elmer® 5100 PC atomic absorption spectrophotometer (AAS) using an acetylene air flame. Calcium and magnesium were analyzed by atomic absorption. Half of a milliliter of a lanthanum chloride solution was added to each 5 mL sample to reduce interferences. The lanthanum chloride solution was made by adding 29.0 grams of La_2O_3 to a small amount of E-pure filtered water in a 500 mL volumetric flask. Then 250 mL of concentrated trace metal grade hydrochloric acid was slowly added to the slurry. Finally, the solution was diluted to 500 mL with E-pure filtered water.

Sodium and potassium were analyzed by atomic emission. Sodium was analyzed with the addition of a 100 μL of a 1.28 M potassium chloride solution, added to reduce interferences, to each 5 mL sample. This solution was made by dissolving 9.53 g of potassium chloride in E-pure filtered water then diluting up to 100 mL with the E-pure. Potassium was analyzed with the addition of a 100 μL of 2.17 M sodium chloride solution, added to reduce interferences, to each 5 mL sample. This solution was made by dissolving 12.71 grams of sodium chloride in E-pure filtered water then diluting up to 100 ml with E-pure filtered water.

Fluoride analysis was done by specific ion electrode. Fluoride was analyzed with the addition of 1 mL of Fisher Scientific® total ionic strength adjusting buffer (TISAB) to each 10 mL sample.

Chloride, Suphate, and Nitrate were analyzed by capillary electrophoresis (Hewlett Packard® 3DCE).

Data Analyses

Elemental ratios in the water can be compared to theoretical values from the dissolution of minerals, combined with knowledge of minerals available for dissolution in the watershed; the evolution of the water can be determined. Piper diagrams can be used to show the chemical character of water samples and to graphically show the mixing of different chemically distinct waters (Piper, 1944).

Dissolution indices from geochemical modeling programs such as PHREEQC (Parkhurst, 1995) can give insight into what minerals are controlling the water chemistry. Before geochemical data can be used in modeling programs, its accuracy must be checked. Charge balance can be used to check the accuracy of the geochemical data (Hem, 1985). Charge balance is calculated by subtracting the amount of cations (in milliequivalents/Liter) from the amount of anions (in milliequivalents/Liter). In the ideal case, the equivalents of cations should equal the equivalents of anions. However, this is rarely the case, and as a result, a certain amount of error needs to be allowed for a substantial amount of data to be available for use in data analysis. The maximum amount of charge imbalance allowed for samples to be used in the calculation of saturation indices and for use in Piper diagrams is +/- 15%.

The SBW streams did not contain enough anion data to make a Piper diagram. As a result a ternary diagram containing the same cations represented in a cation triangle of a Piper diagram was made for this data set. Another effect of having sparse anion data is that charge imbalance could not be calculated for this data set.

The parameters needed for basic geochemical modeling are temperature, pH, Ca, Mg, Na, K, HCO_3 , Cl, SiO_2 , SO_4 , NO_3 , and alkalinity.

The graphing of one dissolved ion vs. another dissolved ion can also be helpful in determining the origin and evolution of water in a watershed. Graphing Ca (M) vs. Mg (M) can give insight into the geochemical processes such as precipitation of calcium carbonate in lakes. Graphing the logarithmic molar concentration of Na vs. the logarithmic molar concentration of Cl will allow the different hydrologic domains to be compared to one another and conclusions can be drawn from their similarities. Graphing Na/Cl (M) histograms allows for the comparisons of dominant Na/Cl (M) ratios to expected Na/Cl (M) ratios from known sources of Cl to the watershed. Expected sources of Cl to the MRW are road salt, sewage treatment plants, and brines. The data used in the histograms, logarithmic graphs, and ion vs. ion graphs were not checked for charge balance.

Geographical Information Systems (GIS) were used to create maps that can give insight into spatial relationships between surface water chemistry and Quaternary geology or

bedrock geology. Maps showing the location of stream samples along with their respective chemistries have been created to show these relationships.

Chapter 3

Geochemical Modeling of Surface Waters and Ground Waters

Introduction

Geochemical modeling used in this thesis takes the concentrations of the major ions in water and determines how saturated that water is with respect to minerals naturally found in the Earth. The program that accomplishes this is Aquachem (AquaChem, 1998), which uses the PHREEQC (Parkhurst, 1995) code to determine how saturated the water is with respect to the minerals in its database. The saturation indices can be used to determine if it is favorable for a water to dissolve or precipitate a certain mineral. By comparing the saturation indices between different hydrologic domains (i.e., bedrock water, drift water, lakes, streams, wetlands) we can gain insight into what minerals are precipitating and therefore insight into how water changes from one domain to the next. Saturation indices (SI) are determined by dividing the ion activity product (IAP) by the equilibrium constant (K_{sp}) and then taking the log of that number (Equation 1).

Equation 1 $SI = \log(IAP / K_{sp})$

The IAP and the K_{sp} use the same equation but in different ways (Equation 2). In order to demonstrate how this equation works an example has been set-up. If the chemical equation is written as Equation 2,

Equation 2
$$nN + mM = rR + sS$$

then the equilibrium expression or ion activity product expression would be shown in Equation 3 (Drever, 1997).

Equation 3
$$IAP = \frac{a_R^r a_S^s}{a_N^n a_M^m}$$

When the reaction is at equilibrium, Equation 3 will equal the K_{eq} ; as a result, the saturation index is equal to zero. When the IAP is greater than the K_{eq} the saturation index is greater than zero, and the solution is supersaturated with respect to this mineral. If the IAP is less than the K_{eq} the saturation index will be less than zero, and as a result, the mineral will be undersaturated (Langmuir, 1997). A water will be considered to be near equilibrium with respect to that mineral if data plots within +/- 5% of the log of the K_{sp} (Long et al., 1988). The values for the K_{sp} that were used to determine this were the same as those found in a Long et al. (Unpublished) paper and are listed in Table 1 along with the reference used in that paper. The range designated to be near equilibrium will be represented on each histogram as the area between two parallel lines running from top to bottom on each graph. The differences in the saturation indices of different ground water domains will be explored in an attempt to understand what processes are occurring between these domains.

Mineral Name	Log K_{sp}	Reference
Calcite	-8.48	Plummer and Busenberg (1982)
Dolomite	-16.54	Nordstrom et al. (1990)
Gypsum	-4.58	Nordstrom et al. (1990)
Quartz	-3.98	Nordstrom et al. (1990)

Table 1. Table of the Log K_{sp} values for minerals whose saturation indices were geochemically modeled. Modified from Long et al. (Unpublished).

The saturation indices of surface waters in the MRW will be compared to the saturation indices in the drift water to see how the water changes as it moves from the ground water environment to the surface water environment. The surface water domains that will be compared to ground water are wetlands, lakes, and streams. The surface water domains will also be compared against themselves to see how they differ.

Calcite SI

Figure 11 shows the saturation indices (SI) for the water in the Mississippian bedrock unit. The samples in the Mississippian are, according to Long et al. (Unpublished), considered to be near equilibrium with respect to calcite.

Figure 12 shows the saturation indices for water in the Pennsylvanian bedrock. Meissner (1993) stated that the Grand River Saginaw Aquifer, located within the Pennsylvanian bedrock, was near equilibrium with an average calcite saturation index of +0.054. The

figure has been modified from the original with vertical bars showing the range that will be considered near equilibrium with respect to calcite. The bulk of the samples are located between these bars. Most of the samples in the Pennsylvanian bedrock will therefore be considered to be near equilibrium with respect to calcite.

Figure 13 shows the saturation indices for the glacial drift water data. The majority of the SI data from this drift aquifer ranges between -0.5 and +1. The median SI value from this aquifer is +0.2. Most samples plot within the bars representing the range for near equilibrium. Therefore the regional drift aquifer will be considered to be near equilibrium with respect to calcite.

Figure 14 shows the calcite saturation indices for the MRW drift ground water, including those data points within the 12 km buffered drift region. The saturation indices data from this aquifer range from -0.4 to +0.6. The median SI value is 0.2. Figure 14 shows that most of the samples are near equilibrium, and therefore, the ground water within the MRW will be considered to be near equilibrium with respect to calcite.

Figure 15 shows the SI data from the streams within the MRW. The majority of the SI values range from -1 to +1.5. The median SI value is +0.54. The median SI calcite value for streams in the MRW is just above the upper boundary of the saturated region (+0.42). From Figure 15 it can be seen that most samples lie within the supersaturated region, however a significant number lies within the near-equilibrium region. Therefore,

the streams within the MRW are dominantly supersaturated with respect to calcite; however, a significant portion lies within the near equilibrium region.

Figure 16 shows the SI data from lakes within the MRW. The SI data from the lakes range from -3.5 to $+2$. The median value for the lakes is 0.255 . The distribution is skewed toward undersaturated values. However, there are significant values in the near-equilibrium region and the supersaturated regions. The lakes do not show a dominant region but have significant numbers in all three regions.

Figure 17 shows the saturation indices for wetlands within the MRW including those data points in 12 km buffered region of the MRW. The SI data from the wetlands range from -3.7 to $+1.1$. The median SI value for calcite is -0.12 . The wetlands are skewed toward lower SI values. The wetlands are for the most part near-equilibrium to undersaturated with respect to calcite; however, there were a significant number of samples that are supersaturated with respect to calcite.

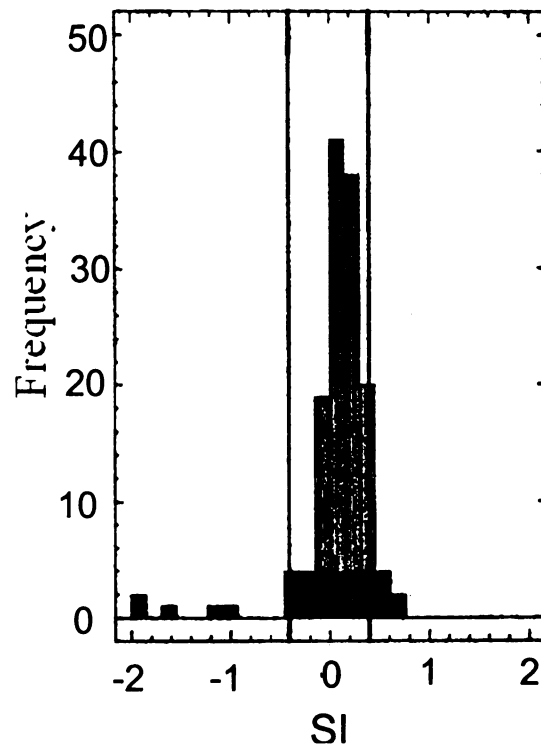


Figure 11. Calcite saturation indices from the Mississippian. Modified from Long et al. (Unpublished).

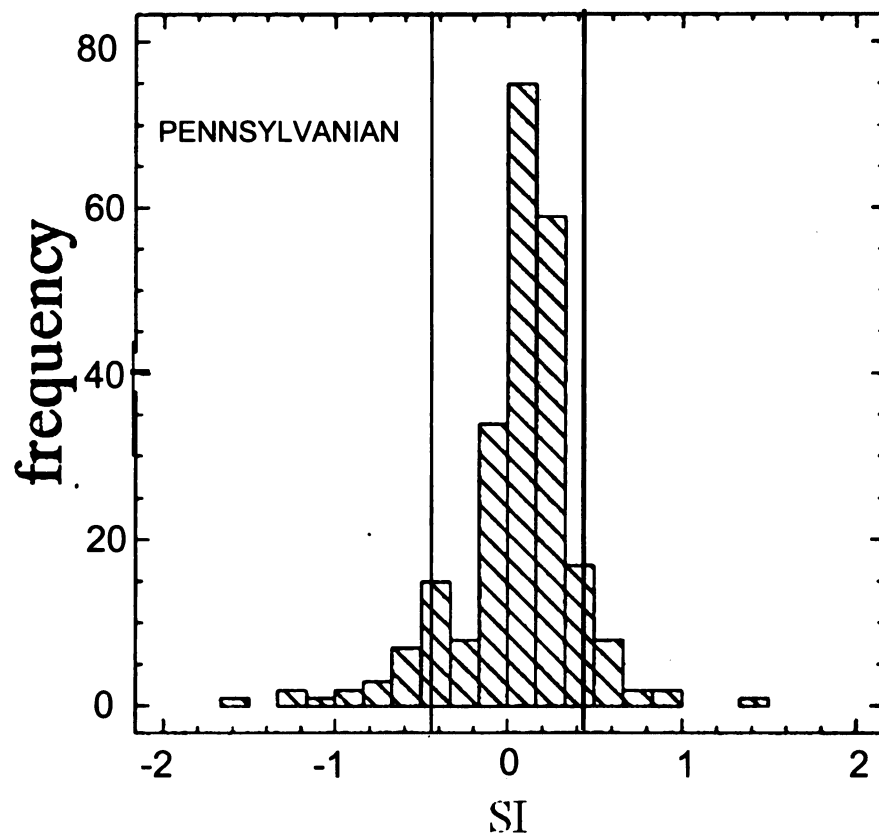


Figure 12. Calcite saturation indices for the Pennsylvanian. Modified from Meissner (1993).

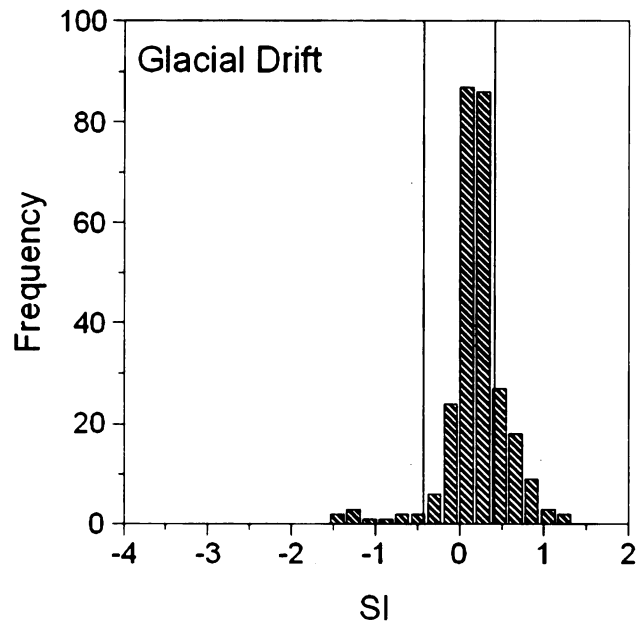


Figure 13. Calcite saturation indices for the glacial drift aquifer. Data are from the groundwater data set (Dannemiller and Baltusis, 1990; Wahrer, 1993; Meissner, 1993).

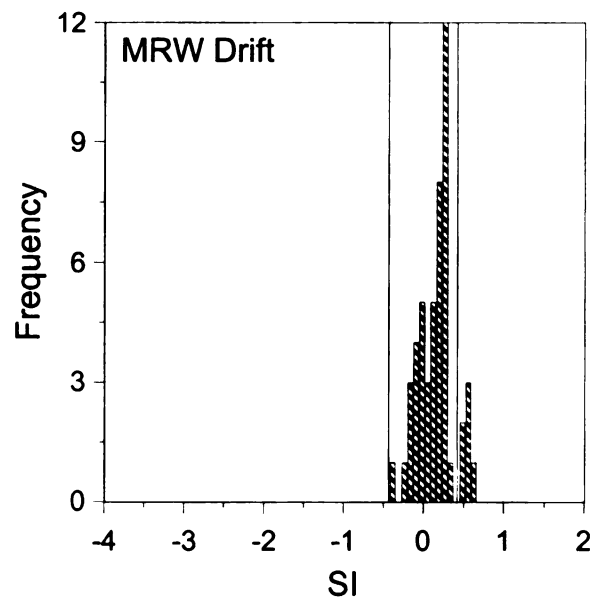


Figure 14. Ground water within the Muskegon River Watershed Drift. Data are from the ground water data set (Dannemiller and Baltusis, 1990; Wahrer, 1993; Meissner, 1993).

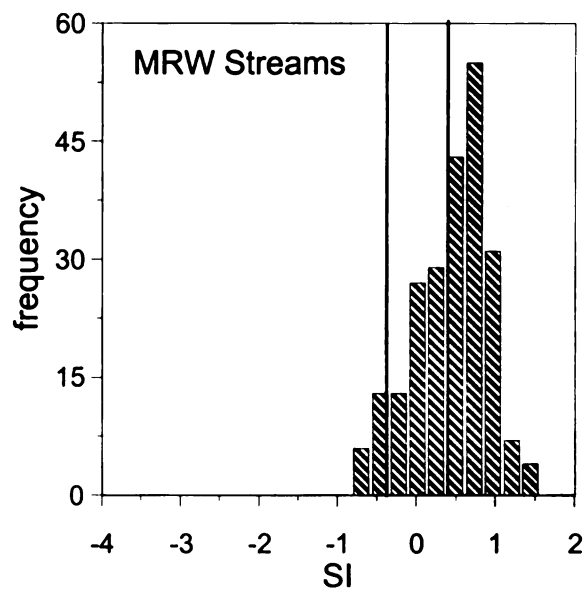


Figure 15. Calcite saturation indices for streams within the Muskegon River Watershed.

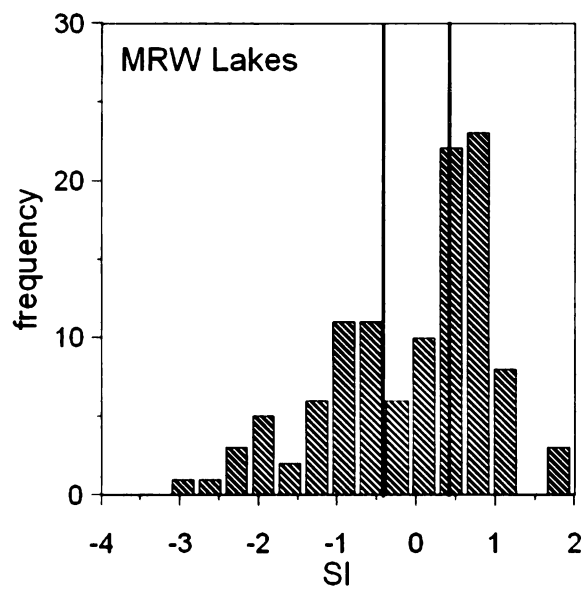


Figure 16. Calcite saturation indices for lakes within the Muskegon River Watershed.

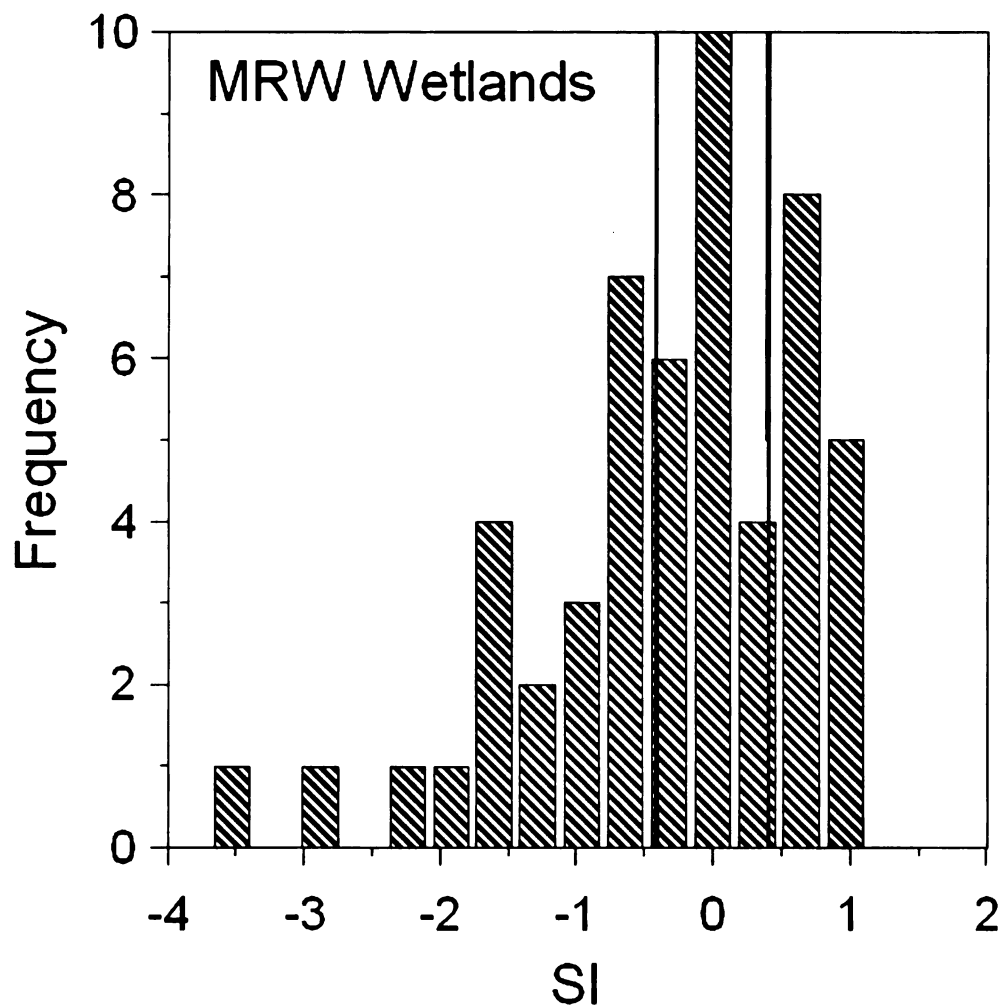


Figure 17. Calcite saturation indices for wetlands within the Muskegon River Watershed.

The water in the Pennsylvanian and Mississippian bedrock units are similar with respect to their distribution of calcite saturation indices. The Pennsylvanian (Figure 12) and the Mississippian (Figure 11) tends to be near-equilibrium with respect to calcite.

Both drift data sets are predominantly near-equilibrium with respect to calcite. The most supersaturated waters with respect to calcite are the stream waters. The lakes and wetlands are both widely distributed showing significant numbers of near equilibrium, supersaturated, and undersaturated samples.

Dolomite SI

Figure 18 shows the dolomite saturation indices for ground water in the Mississippian. Long (Unpublished) determined that the graph shows that a significant number of samples plot within the range considered to be near-equilibrium with dolomite; however, many samples plot below this in the undersaturated region as well.

Figure 19 shows the dolomite saturation indices for the Pennsylvanian. Meissner (1993) stated that the Pennsylvanian is slightly undersaturated with respect to dolomite. However, with the modifications (i.e. bars showing the region considered to be near-equilibrium) done to the graph the waters are approximately evenly split between the ranges considered to be near-equilibrium or undersaturated with respect to dolomite.

Figure 20 shows the dolomite saturation indices for water in the glacial drift. The Figure shows that most of the data lies between -2 to $+2$. The median SI value for the drift

aquifer is +0.05. Most samples plot within the range considered to be near-equilibrium with dolomite. This implies that most of the water within the regional drift aquifer is near-equilibrium with respect to dolomite.

Figure 21 shows the saturation indices for the drift aquifer within the buffered region of the MRW. The majority of SI values for dolomite in this aquifer ranges from -1 to +1 with a median value of -0.09. The figure shows that most of the samples within the MRW as well as within 12 km of the watershed are within the region considered to be near-equilibrium with dolomite.

Figure 22 shows the saturation indices for stream water in the MRW. The majority of the SI values for dolomite in these streams range from -2 to +3. The median SI value is +0.82. Although the median SI value is within the near-equilibrium range, there are a significant number of samples that are in the supersaturated range. Therefore, the stream waters within the MRW range from being near-equilibrium to supersaturated with respect to dolomite.

Figure 23 shows that the saturation indices for lakes in the MRW. The SI values for dolomite in the MRW lakes ranges from -6.4 to +3.7, with a median SI value of 0.19. The Figure shows that the lake samples are skewed toward undersaturated values; however, all three regions (i.e. undersaturated, near-equilibrium, and supersaturated) have a significant number of samples within them. Therefore, lakes within the MRW will be considered to range from undersaturated, through near-equilibrium, into supersaturated.

Figure 24 is a histogram showing the SI values for wetlands within the MRW, as well as within the 12km buffered region. The SI values for dolomite in the MRW range from -7.6 to +2.2. The median SI value is -0.5. All three SI regions (i.e. undersaturated, near-equilibrium, and supersaturated) have significant numbers of samples that plot within their respective regions. Therefore, the wetlands within the MRW will be considered to range from undersaturated to supersaturated with respect to dolomite.

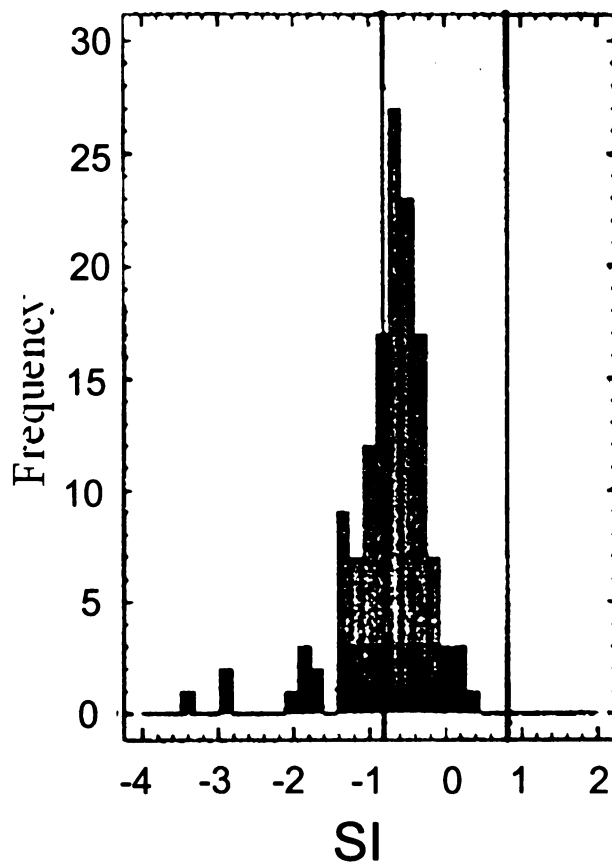


Figure 18. Dolomite frequency histogram of saturation indices in the Mississippian. Modified from Long et al. (Unpublished).

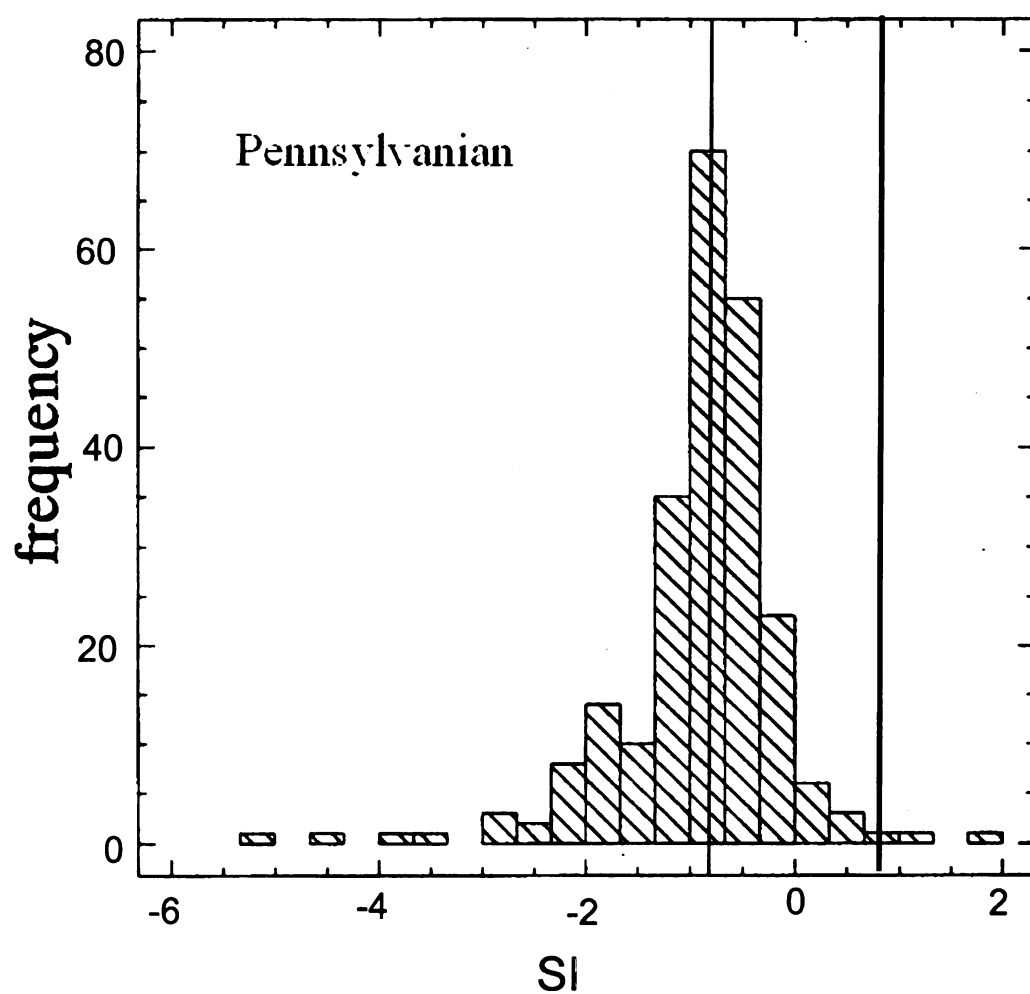


Figure 19. Dolomite frequency histogram for the Pennsylvanian. Histogram modified from Meissner (1993).

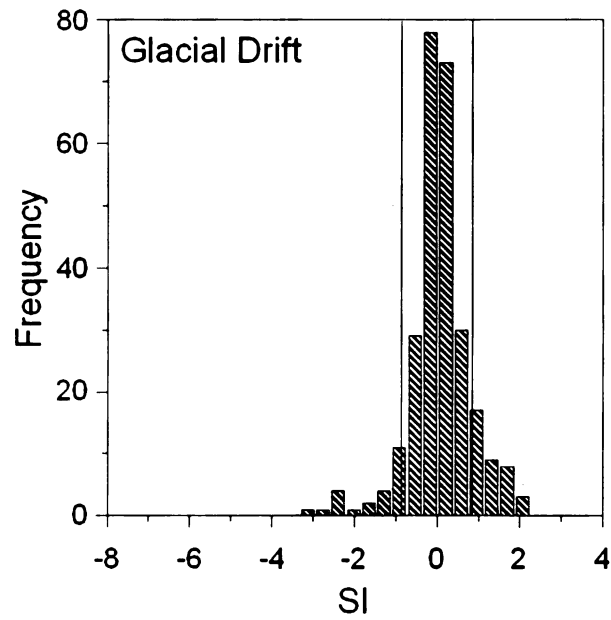


Figure 20. Dolomite frequency histogram for saturation indices for water in the glacial drift. Data from the ground water data set (Dannemiller and Baltusis, 1990; Wahrer, 1993; Meissner, 1993).

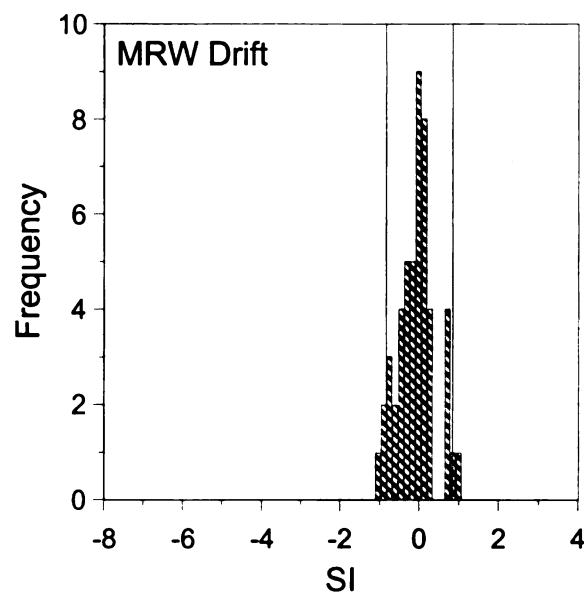


Figure 21. Dolomite frequency histogram of saturation indices of drift samples within the Muskegon River Watershed. Data are from the ground water data set (Dannemiller and Baltusis, 1990; Wahrer, 1993; Meissner, 1993).

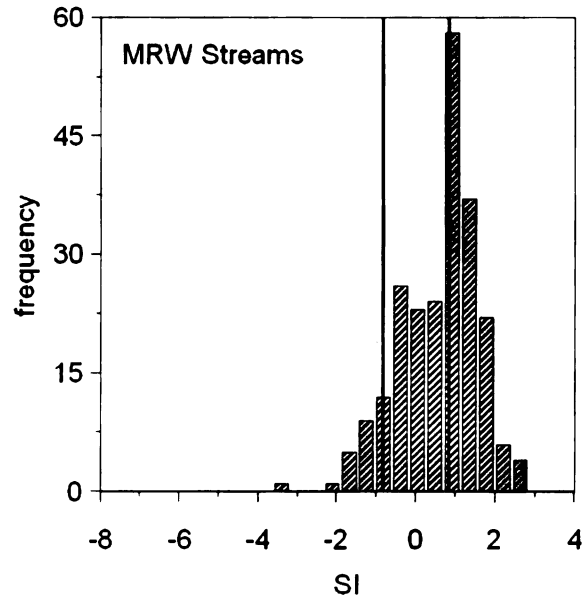


Figure 22. Dolomite frequency histogram for the streams in the Muskegon River Watershed.

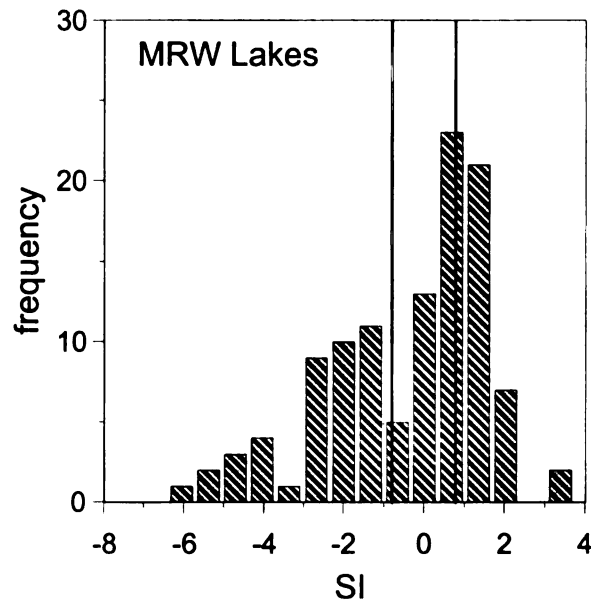


Figure 23. Dolomite frequency histogram of saturation indices for the lakes in the Muskegon River Watershed.

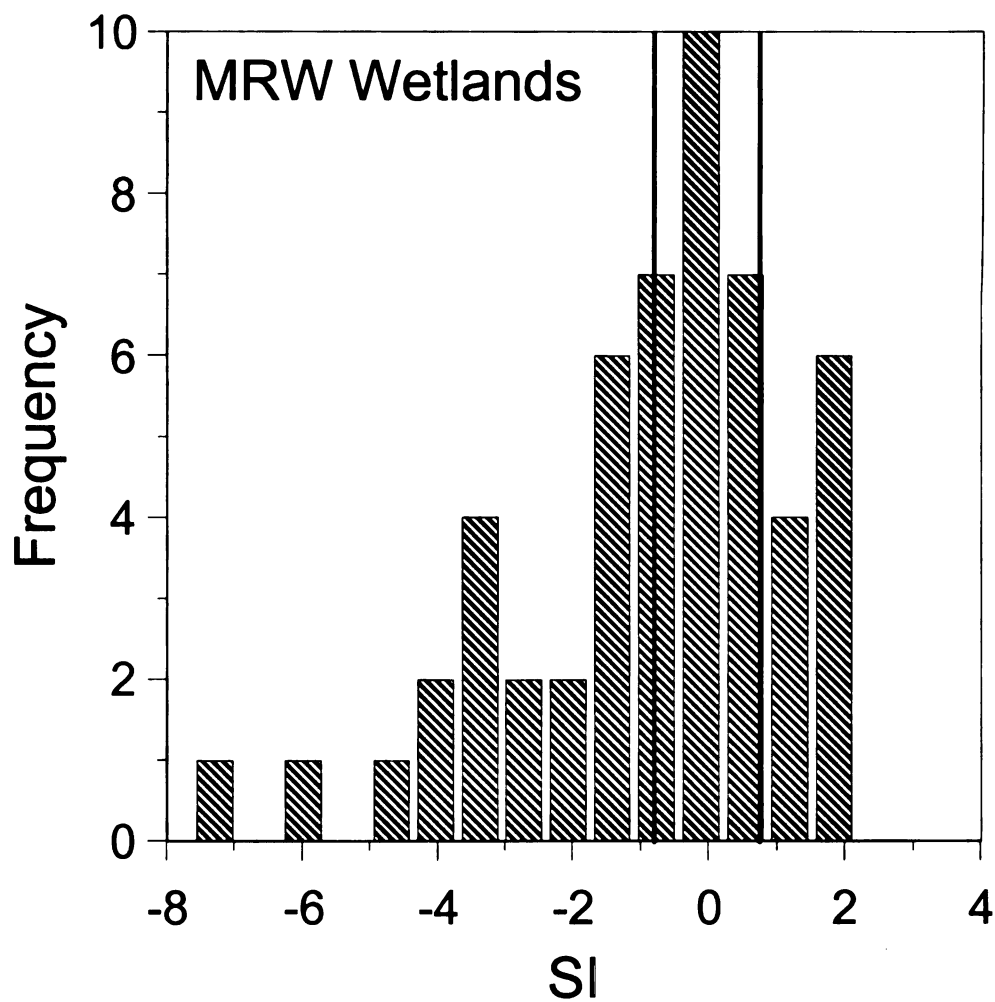


Figure 24. Dolomite frequency histogram of saturation indices for the wetlands within the Muskegon River Watershed.

The bedrock aquifers (i.e., Pennsylvanian and Mississippian) are both undersaturated and near-equilibrium with respect to dolomite saturation indices. The regional drift aquifer (Figure 20) and the water within the (Figure 21) MRW drift region are dominantly within the range considered to be near-equilibrium with dolomite. The streams (Figure 22) within the MRW are the most supersaturated with respect to dolomite out of all the different waters tested. The lakes (Figure 23) and wetlands (Figure 24) have similar distributions covering all three SI regions.

Gypsum SI

Figure 25 is a histogram showing the SI values for gypsum in the Mississippian. Long (Unpublished) described the distribution of SI values within the Mississippian as undersaturated with respect to this mineral except for a very few samples that could be considered to be near-equilibrium.

Figure 26 is a histogram showing the SI values for gypsum in the water within the Pennsylvanian. Meissner (1993) described the water in the Pennsylvanian as being undersaturated with respect to gypsum. The graph shown was modified from Meissner (1993), and verifies that the water in the Pennsylvanian aquifer is understaturated with respect to gypsum.

Figure 27 is a histogram showing the SI values for gypsum in the water within the glacial drift. Most of the SI values range from -3.5 to -0.5 . The median SI value is -2.1 . The average value for gypsum SI suggests that the water in the aquifer is in general

undersaturated with respect to gypsum. Almost all samples plot below the range of SI values considered to be near-equilibrium with gypsum. Therefore on average the water in the regional drift aquifer is considered to be dominantly undersaturated with respect to gypsum.

Figure 28 is a histogram showing the SI values for gypsum in the drift underlying the MRW. Most of the SI values range from -3.4 to -1.6 with a median value of -2.5 . All samples plot below the range representing near-equilibrium with respect to gypsum, and therefore will be considered undersaturated with respect to gypsum.

Figure 29 is a histogram showing the SI values for gypsum in streams within the MRW. The SI values range from -4.2 to -1.4 . The median SI value is -2.5 . All points lie below the range considered to be near-equilibrium with respect to gypsum. This shows that stream waters in the MRW tend to be undersaturated with respect to gypsum. The most saturated sample points ($SI = -1.3$ to -1.5) on the SI graph correspond to sites that are downstream of the MCWDS (a wastewater disposal facility).

Figure 30 is a histogram showing the SI values for gypsum in lakes within the MRW. The SI values range from -3.9 to -1 with a median value of -3 . All of the lake samples plot below the range representing near-equilibrium with gypsum. Therefore lakes in the MRW tend to be undersaturated with respect to gypsum.

Figure 31 is a histogram showing the SI values for gypsum in wetlands in the MRW. The SI values range from -4.6 to -2 . The median SI value is -3.2 . All of the wetland samples plot below the range representing near-equilibrium with gypsum. Therefore wetlands in the MRW tend to be undersaturated with respect to gypsum.

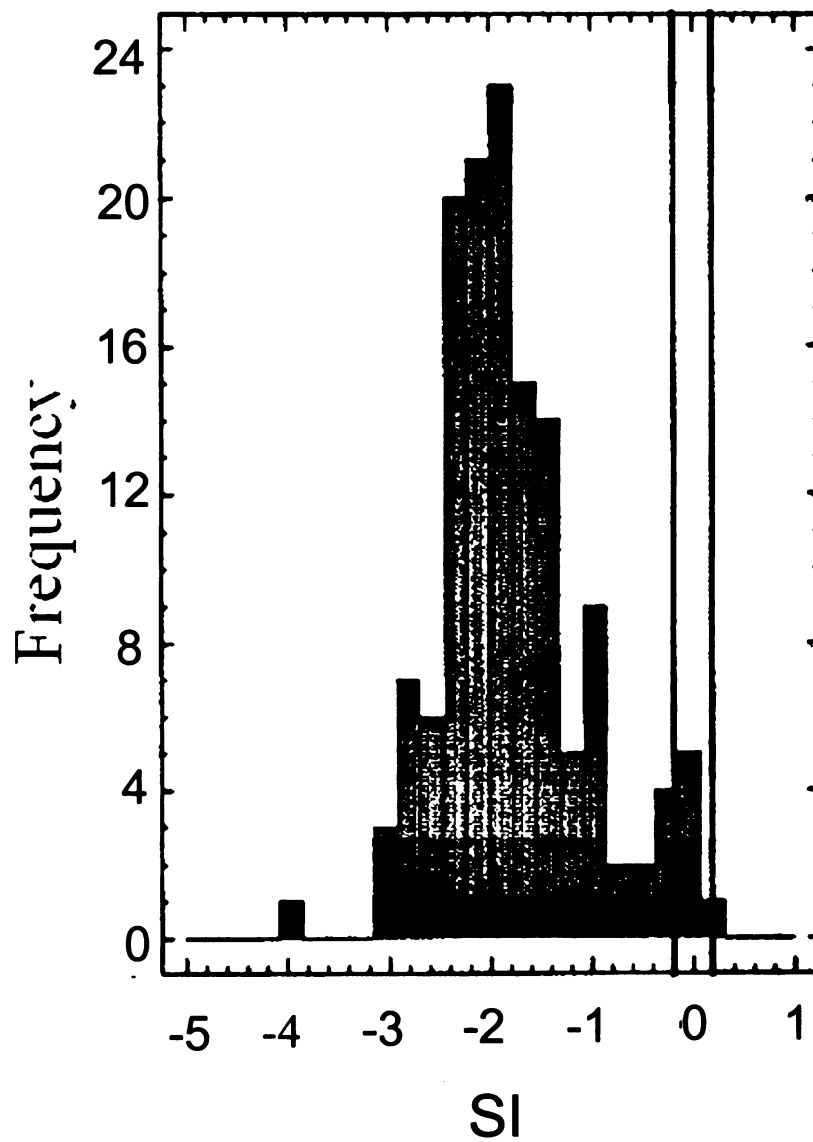


Figure 25. Gypsum frequency histogram for the Mississippian. Modified from Long et al. (Unpublished).

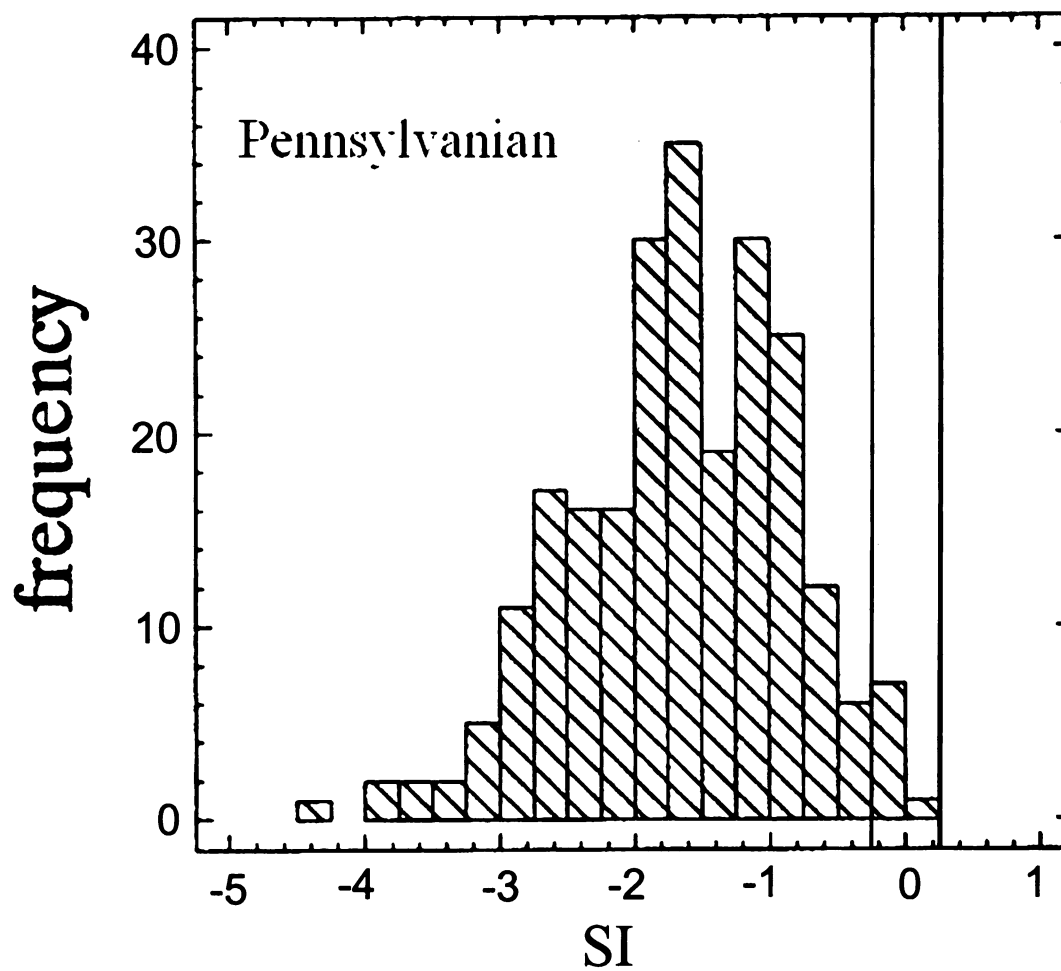


Figure 26. Gypsum frequency histogram for the Pennsylvanian. (Modified from Meissner, 1993).

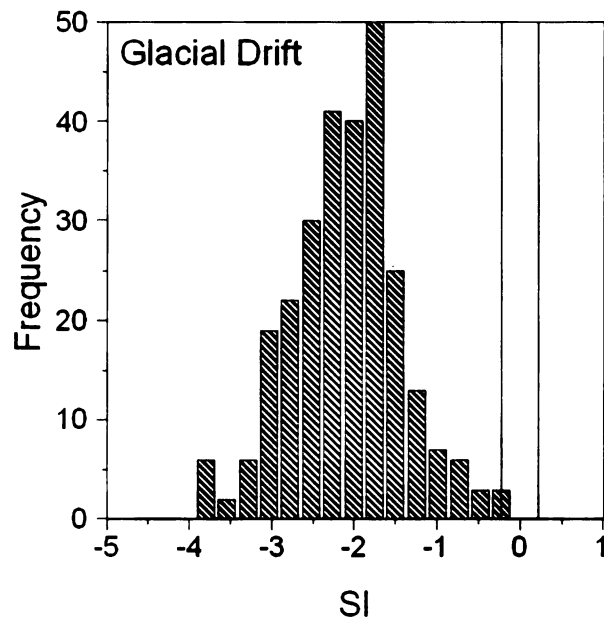


Figure 27. Gypsum frequency histogram for water in the glacial drift. Data from ground water data set (Dannemiller and Baltusis, 1990; Wahrer, 1993; Meissner, 1993).

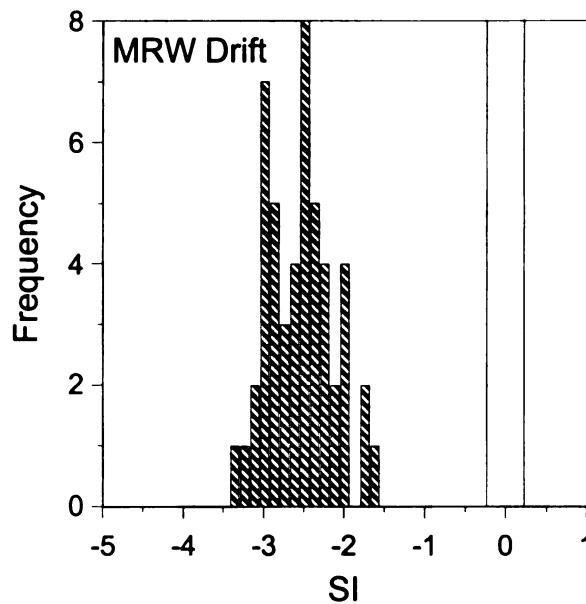


Figure 28. Gypsum frequency histogram of saturation indices for drift within the Muskegon River Watershed. Data are from the ground water data set (Dannemiller and Baltusis, 1990; Wahrer 1993; Meissner, 1993).

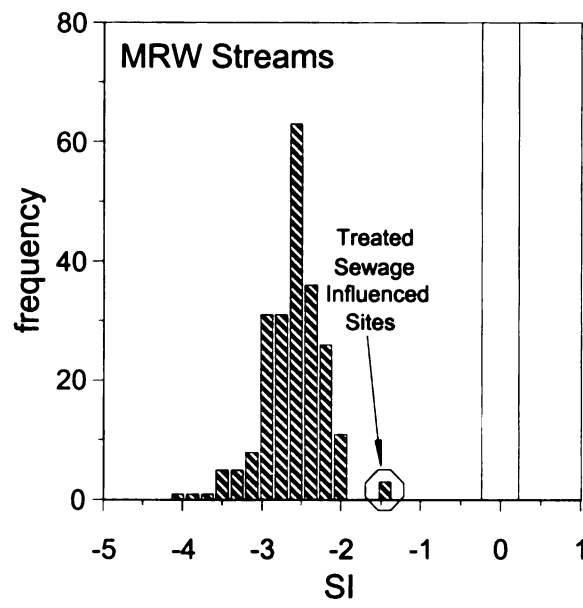


Figure 29. Gypsum frequency histogram for streams in the Muskegon River Watershed.

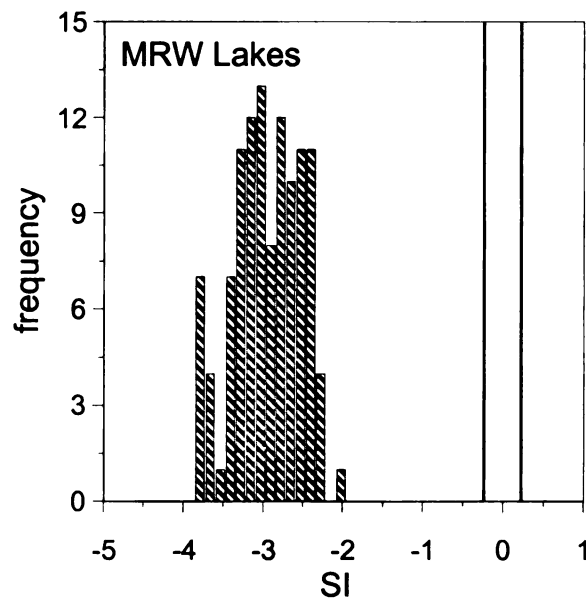


Figure 30. Gypsum frequency histogram for lakes in the Muskegon River Watershed.

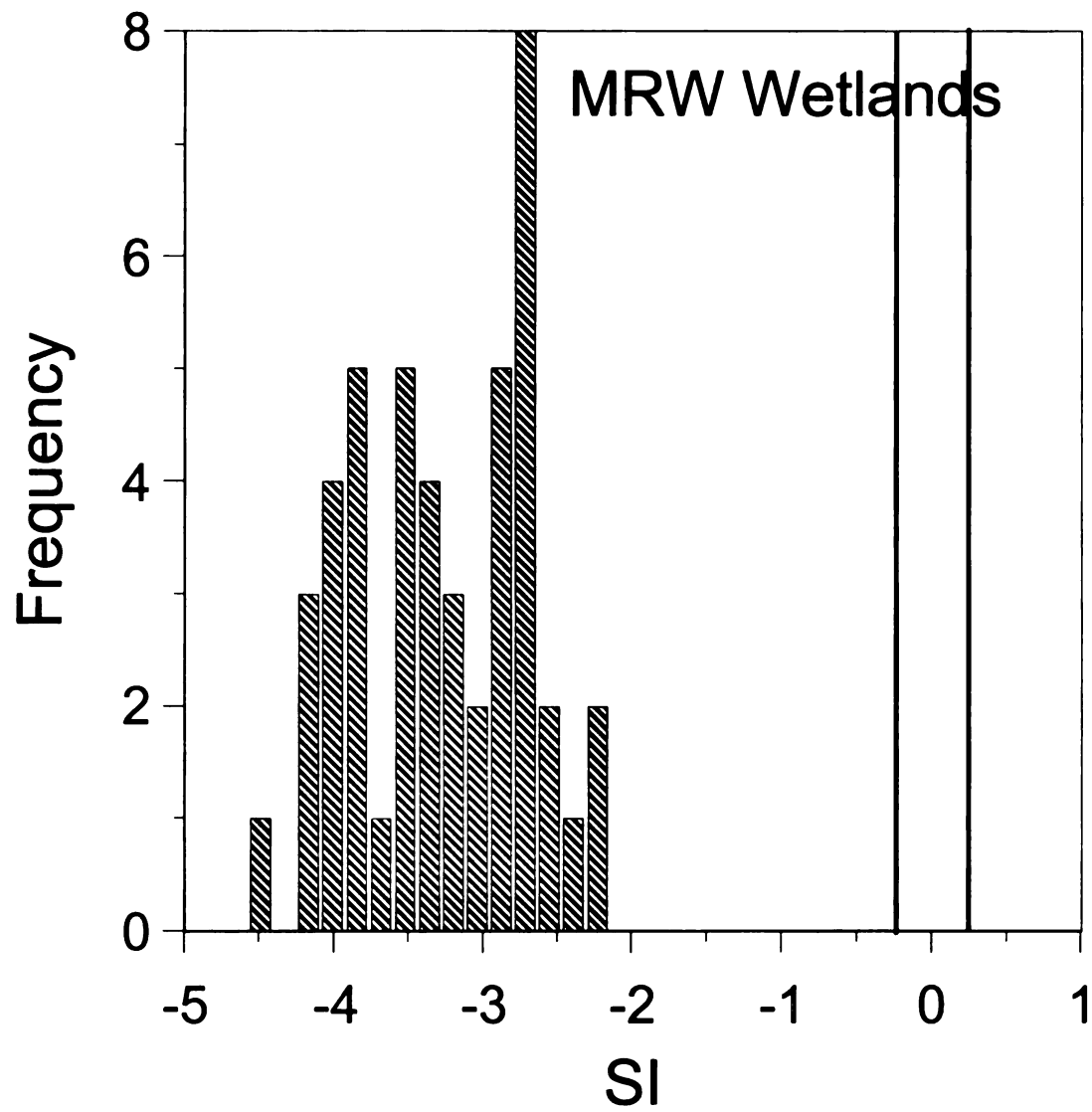


Figure 31. Gypsum frequency histogram of wetlands in the Muskegon River Watershed.

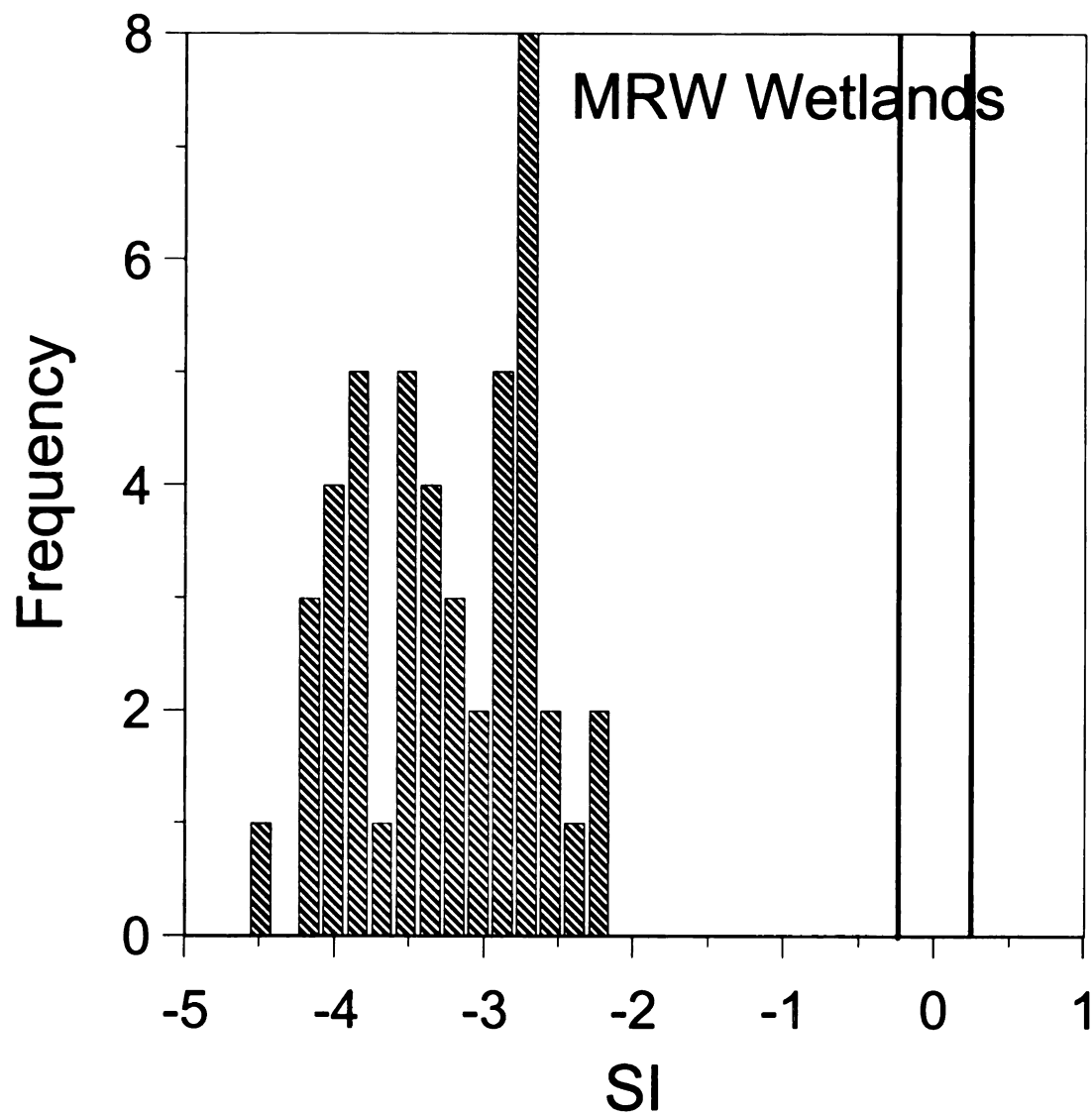


Figure 31. Gypsum frequency histogram of wetlands in the Muskegon River Watershed.

All of the waters tested were on average undersaturated with respect to gypsum. The Mississippian (Figure 25), Pennsylvanian (Figure 26), and glacial drift (Figure 27) are the least undersaturated with respect to gypsum. The ground water in the MRW (median SI = -2.5) (Figure 28) is more undersaturated than the regional aquifer (median SI = -2.1). The streams (Figure 29) are on average more undersaturated than all of the ground waters. The lakes (Figure 30) are more undersaturated than the streams and the wetlands are the least saturated of all the waters tested (median SI = -3.4).

Quartz SI

Figure 32 shows the quartz saturation indices for waters within the Mississippian bedrock. Long et al. (Unpublished) described the distribution as not normal with average SI values around $+0.5$. The average SI value is within the range considered to be supersaturated with respect to quartz; therefore it can be interpreted that quartz is supersaturated in the Mississippian.

Figure 33 shows the quartz saturation indices for waters within the Pennsylvanian. Meissner (1993) stated that the water in the Pennsylvanian tended to be supersaturated with respect to quartz. Despite the fact that the figure has been modified (i.e. bars showing the region considered to be near-equilibrium) the same conclusion is reached. Most samples plot above the near-equilibrium region, and therefore, the water is for the most part supersaturated with respect to quartz.

Figure 34 shows the quartz saturation indices for the regional drift water. Most of the SI values for the regional drift aquifer have SI values that range from +0.7 to -0.25. The median SI value is +0.37. Most of the values are above the range considered to be near-equilibrium with respect to quartz. There are a significant number of samples that do plot within the near-equilibrium range. Therefore, the water in the regional drift aquifer was predominantly near-equilibrium with respect to quartz.

Figure 35 shows the quartz saturation indices for drift within the MRW. Most of the drift samples have SI values for quartz that range from 0 to +0.6 with a median SI value of +0.34. Most of the values are above the range considered to be near-equilibrium with respect to quartz. There are a significant number of samples that do plot within the equilibrium range. Therefore, the drift water within the watershed and within the buffered is predominantly supersaturated with respect to quartz.

Figure 36 shows the quartz saturation indices for the stream water within the MRW. Most of the stream water data have SI values that range from -0.8 to +0.8. The median value is +0.08. The streams are nearly evenly split between the near-equilibrium region and the supersaturated region of the graph. Therefore, the water in the streams in the MRW is for the most part near-equilibrium to supersaturated with respect to quartz.

Figure 37 shows the quartz saturation indices for the lakes within the MRW. The lake data within the MRW has a quartz SI range between -2.6 and +0.4. The median lake data have a value of -0.60. The data for the most part are undersaturated with respect to

quartz; however, there is a significant amount of samples that are near-equilibrium with respect to this mineral. Therefore, the lakes in the MRW can be described as being for the most part undersaturated with respect to quartz; however, there are a significant number of samples that are near-equilibrium with this mineral.

Figure 38 shows the quartz saturation indices for wetlands within the MRW. The wetlands data within the MRW have a quartz SI range between -1.4 and $+0.32$. The median quartz SI value for a wetland in the MRW is -0.34 . The wetland data are nearly evenly distributed between SI values that are near equilibrium and values that are undersaturated. Therefore, wetlands in the MRW range from being near equilibrium to undersaturated with respect to quartz.

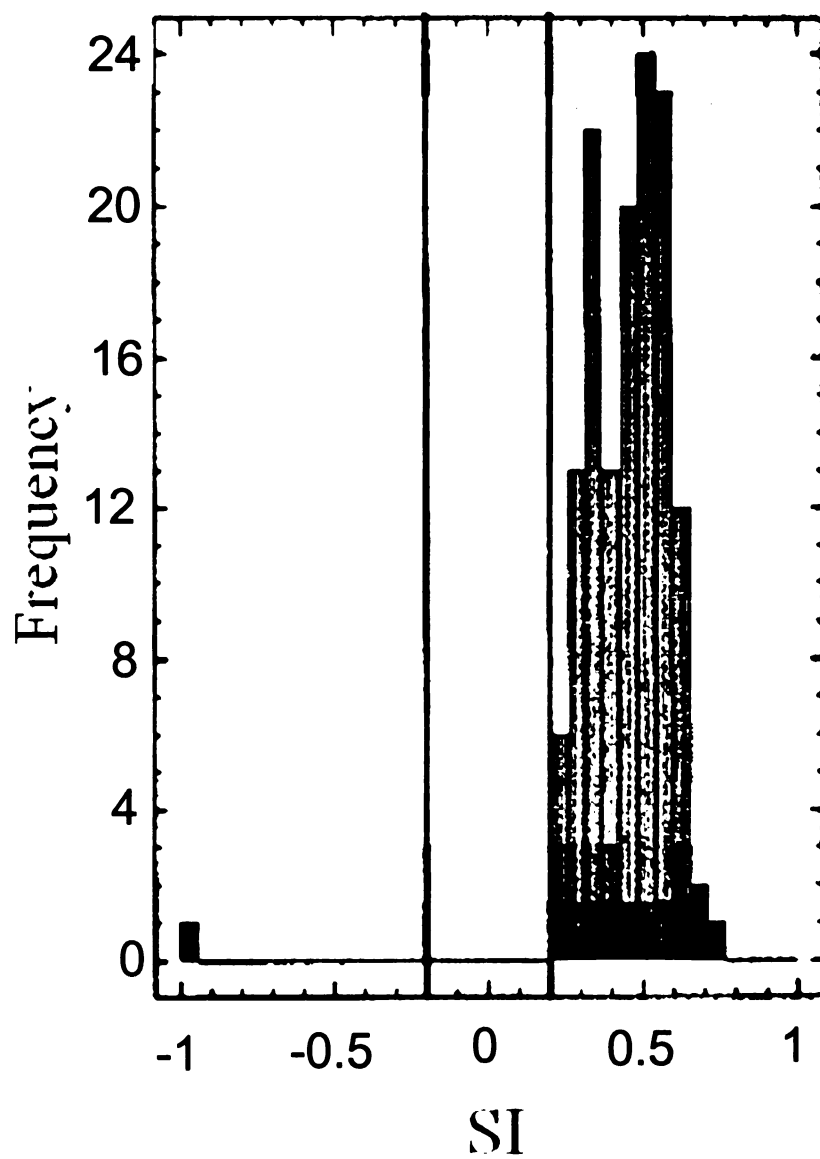


Figure 32. Quartz frequency histogram for samples within the Mississippian. Modified from Long (Unpublished).

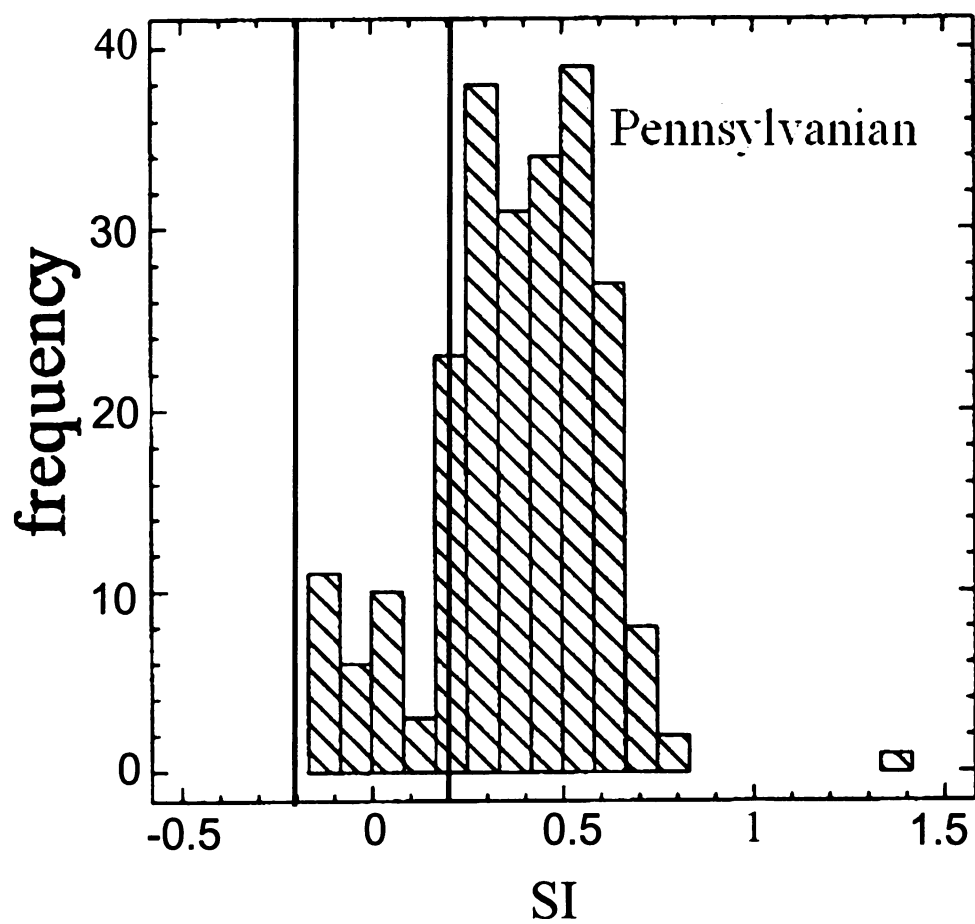


Figure 33. Quartz frequency histogram for the Pennsylvanian. Modified from Meissner (1993).

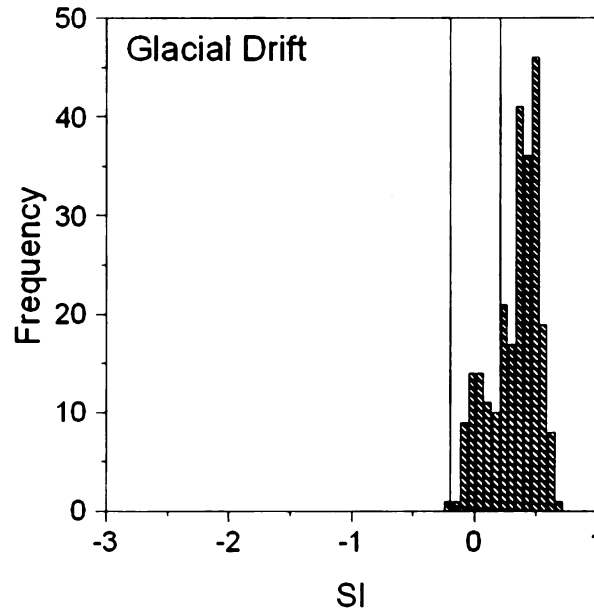


Figure 34. Quartz frequency histogram for water in the glacial drift. Data are from the ground water data set (Dannemiller and Baltusis, 1990; Wahrer, 1993; Meissner, 1993).

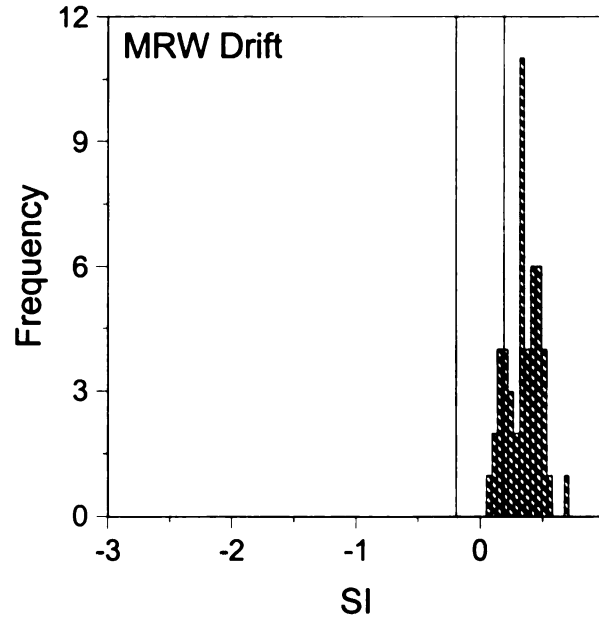


Figure 35. Quartz saturation indices frequency histogram for the glacial drift within the buffered region of the Muskegon River Watershed. Data are from the ground water data set (Dannemiller and Baltusis, 1990; Wahrer, 1993; Meissner, 1993).

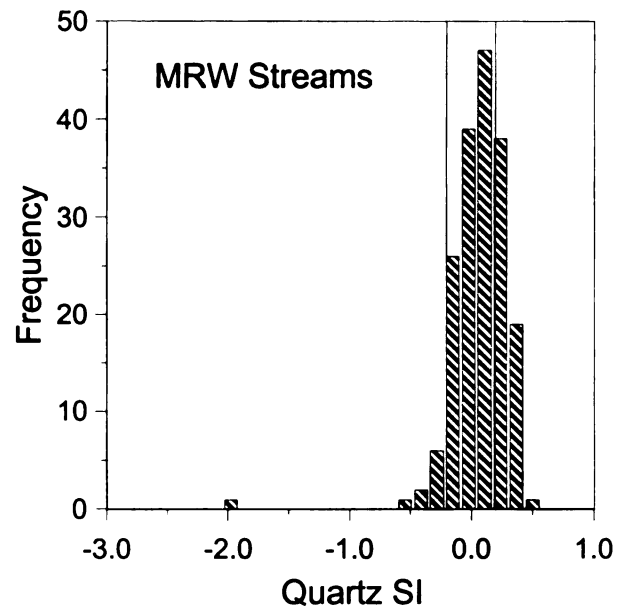


Figure 36. Quartz saturation indices histogram for streams in the Muskegon River Watershed.

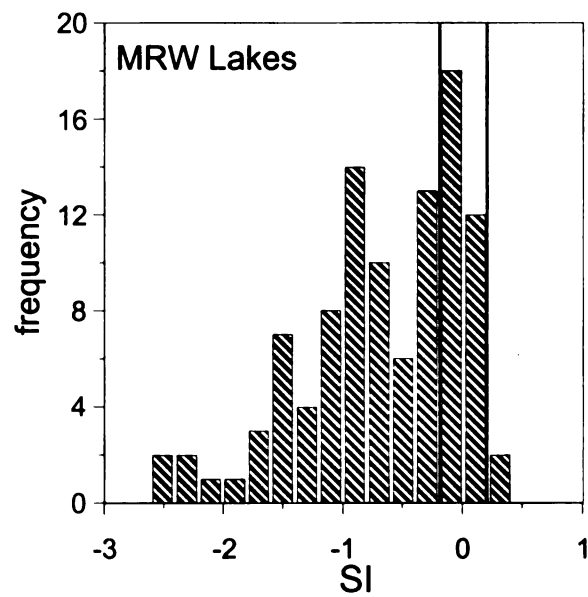


Figure 37. Quartz saturation indices histogram for lakes in the Muskegon River Watershed.

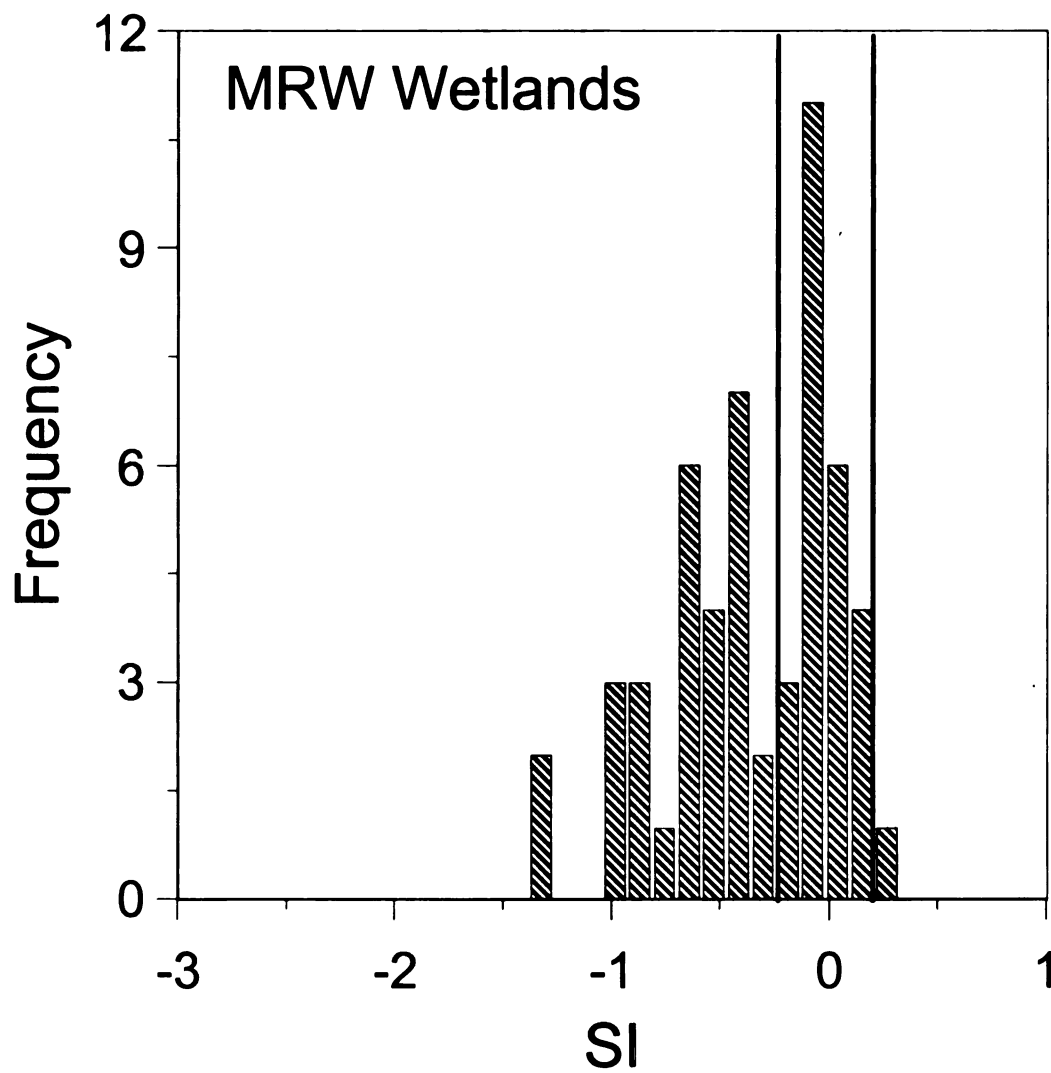


Figure 38. Quartz saturation indices histogram for wetlands in the buffered region of the Muskegon River Watershed.

The Mississippian bedrock (Figure 32), Pennsylvanian (Figure 33), Regional Drift aquifer (Figure 34), and the buffered MRW drift aquifer (Figure 35) are prevalently supersaturated with respect to quartz. The streams (Figure 36) are evenly split between being near-equilibrium and being supersaturated. The streams are the most supersaturated of the surface waters with respect to quartz. The wetlands (Figure 38) and the lakes (Figure 39) are, for the most part, undersaturated with a significant but a lesser amount in the region that are near-equilibrium with respect to this mineral.

Summary

Most of the water samples from the Mississippian (Figure 11) the Pennsylvanian (Figure 12), glacial drift (Figure 13), and the MRW drift (Figure 14) are near-equilibrium with respect to calcite. As rainwater percolates into the ground it gains CO_2 that dissolves up more calcite and then comes to equilibrium. The ground water then emerges into the surface environment supplying streams, lakes, and wetlands with water that is equilibrated to conditions that have a higher concentration of CO_2 than the surface water conditions. As a result CO_2 is released out of the water and the surface water becomes supersaturated with respect to calcite. In order to come back to equilibrium the water precipitates out calcite. The streams (Figure 15) are the most supersaturated of the all of the environments. The other two surface waters (i.e., lakes (Figure 16) and wetlands (Figure 17)) contain all 3 different regions (supersaturated, near-equilibrium, undersaturated). The turbulence in the streams as well as the degassing due to Henry's law (loss of CO_2) causes the streams to loose CO_2 (Herman and Lorah, 1987).

Biological activity (photosynthesis) also can cause a decrease in CO₂ concentration. The lakes and the wetlands have a much more spread out distribution than the other hydrologic regions because they not only have a ground water input but a very significant amount of water that has equilibrated to surface conditions and maybe even become undersaturated with respect to calcite. The effect of biological activity, turbulence, and Henry's Law precipitation may follow. Calcite has been known to precipitate out of lakes (Otsuki and Wetzel, 1974; Strong and Eadie, 1978). The wetlands and the lakes were sampled throughout the late spring and summer. The productivity may have been different though the spring and summer and thereby affecting the amount of CO₂ in the water. This, in turn, changes the solubility of calcite. Effler (1984) stated that the amount of CO₂ consumed by a lake varies seasonally and varies the most in the most productive parts of the lake.

Dolomite saturation indices are undersaturated to near-equilibrium in the bedrock (Figure 18 and Figure 19). The regional drifts (Figure 20) as well as the MRW drift (Figure 21) have saturation indices that tend to plot in the near-equilibrium region. The streams (Figure 22) are supersaturated with respect to dolomite. The lakes (Figure 23) and wetlands (Figure 24) cover all three saturation index regions (i.e., supersaturated, undersaturated, and near-equilibrium) just like calcite.

The bedrock units (Figure 25 and Figure 26), and the regional drift (Figure 27) are the most saturated of the hydraulic domains with respect to gypsum. Ground water in the

MRW Drift (Figure 28) is less saturated than that in the regional drift (Figure 27). The stream water (Figure 29) and the MRW Drift (Figure 28) have about the same distribution of gypsum SI and therefore are about the same in saturation with respect to gypsum. The stream waters (Figure 29) are the most saturated of the surface waters with respect to gypsum. The most saturated of the streams are sample locations located downstream of the MCWDS. The wetlands (Figure 31) and lakes (Figure 30) are the two least saturated with respect to gypsum of all the hydraulic domains. The lakes (Figure 30) are slightly more saturated than the wetlands (Figure 31). This may be the result of sulfate-reducing bacteria removing the sulfate from the water, and thereby decreasing the concentration of sulfate in the water. This process, in turn, decreases the SI value for gypsum. Sulfate reduction can occur in swamps, bogs, soils, and lacustrine sediments (Drever 1997). Sulfate reduction has been known to occur in calcium carbonate dominated lakes in the Midwestern United States (Kalff, 2002).

The bedrock aquifers (Figure 32 and Figure 33) and the drift waters (Figure 34 and Figure 35) tend to be supersaturated with respect to quartz. The streams (Figure 36) tend to be near-equilibrium to supersaturated. The lakes (Figure 37) and wetlands (Figure 38) tend to be undersaturated to near-equilibrium. Kolak (2000) also noticed that streams in the Saginaw Bay Watershed were in general more saturated than lakes and wetlands with respect to quartz. One of the mechanisms to remove silica from the water involves diatoms (Hurley et al., 1985). Diatoms are a type of phytoplankton that remove dissolved silica from the water by making silicate shells (Kalff, 2002). Phytoplankton are photosynthetic and therefore need sunlight to live. Therefore, it is expected that surface

waters such as lakes, streams and wetlands would have a lower SI for silica than ground waters because diatoms cannot exist in ground waters do to lack of sunlight. Streams are the most saturated of the surface waters because streams, which are always moving, are getting a constant flow of ground water. As a result, the water in the streams have not had as long of a time for diatoms to remove silica as compared to wetlands and lakes in which the water sits for a longer period of time.

In summary, the dolomite and calcite saturation indices are very similar. In both calcite and dolomite, the surface waters have a more spread out distribution of saturation indices than the ground waters. This could be the result of the ground water having a more stable environment than the surface waters. The ground water would have time to come into equilibrium with slight differences in temperature. However, the surface water environment has fluctuating temperatures throughout the day. The ground water entering into the surface waters will experience a large drop in the partial pressure of CO_2 that will cause a temporary supersaturation with respect to this mineral. The surface waters also have biological processes (photosynthesis), which can remove CO_2 causing a temporary saturation of calcite till precipitation occurs. Quartz, in general, is more supersaturated in ground waters than surface waters. This is most likely the result of the presence of sunlight in surface waters, which allows photosynthetic silica secreting organisms such as diatoms (Kalf, 2002) to extract out silica from the water. These organisms need sunlight to live and therefore do not effect ground water. In general,

ground waters are more saturated in gypsum than the surface waters. This maybe the result of sulfate reducing bacteria in the surface waters reducing the sulfate to H_2S .

Chapter 4

Chemical Graphical Data

Introduction

The following graphs are presented in this chapter to give insight into the processes controlling ground water and surface water chemistry in the MRW. Elevated Cl (M) concentrations have been identified in surface waters and ground waters of the MRW. The source of Cl in the watershed will be explored using Na/Cl (M) histograms and tables, as well as logarithmic Na and Cl graphs. Histograms and tables of Na/Cl (M) ratios will be compared to the Na/Cl ratios of known sources of Cl to the watershed. The logarithmic Na vs. Cl graphs of surface waters and drift ground water will be compared to regions suspected of brine upwelling, bedrock units known to contain saline waters, and a seawater evaporation curve. The processes controlling Ca in the different hydrologic domains within the watershed will be explored using graphs of Ca vs. Mg.

Na/Cl Histograms and Charts

Sodium to chloride histograms, graphs, and tables can be used to gain insight into the origin of the chloride in the ground water. When using Na/Cl (M) ratios to determine the source of Cl, the assumption is made that Cl and Na act conservatively throughout the watershed. Road salt, which is dominantly composed of the mineral halite, is used throughout the watershed to melt ice on roads. Halite has a Na/Cl (M) ratio of 1. The Na data and Cl data each have an error of 10 percent. The error is additive when combining the Na and Cl data in a fraction. As a result, the error in the Na/Cl (M) fraction is 20

percent. Therefore, if the Na/Cl (M) ratio of the water being examined were between 0.8 and 1.2 then that water has a Na/Cl (M) ratio that would be consistent with the dissolution of halite. Stoessell (1997) used mass ratios, one of those ratios being Na/Cl (M), to determine, which oilfield brine was leaking into a shallow aquifer in Louisiana. Wilson (1989) compiled average values for different solutes in oilfield brines in Michigan. From that data, Na/Cl (M) ratios were determined and showed that oilfield brines in Michigan have, average ratios between 0.7 and 0.17 (Table 2), Na/Cl (M) ratios less than 0.8. Therefore samples with Na/Cl (M) less than 0.8 will be considered to have Na/Cl (M) ratios consistent with that of a oilfield brine. If these oilfield brines have entered into the shallow drift, the waters affected should have Na/Cl (M) ratios approaching this range. However, these formations are not in contact with glacial drift in the MRW and would have to enter into the environment through anthropogenic routes such as wastes from oil and gas production and application of brines to roads. Wayland (2000) used similar Na/Cl ratios to help give evidence for whether the Cl in the watershed is from an oilfield brine, halite, or septic systems and animal wastes. Another possible source of Cl to the ground water are septic systems and sewage treatment plants. A study of two septic systems in Canada revealed that the septic system effluent has an average Na/Cl (M) ratio between 2.5 and 3.3 (Robertson et al., 1991). Water samples taken from downstream of the Muskegon County Wastewater Disposal System (MCWDS) revealed that the stream draining the facility has a Na/Cl (M) ratio between 1.4 and 2.5. In this chapter these two sources (septic and treated sewage) will be combined as septic/treated sewage. Therefore water samples with the Na/Cl (M) greater than 1.2 will be considered to have Na/Cl (M) ratios consistent with that of treated

sewage/septic systems. The Na/Cl (M) ratio from natural sources of Cl and Na are suspected to be within this range as well. The drift contains Na bearing minerals such as plagioclase (Mariam and Mokma, 1996; Mariam and Mokma, 1995). A study by Jin et. al., (2005) revealed that soil water in Michigan that has come into contact with plagioclase should result in a water that has Na concentrations between 0.7 and 3 mg/L. Rainwater in the MRW has been found to have Na concentrations that range from 0.054 to 0.066 mg/L (NADP, 2004). Compared to the dissolution of plagioclase, rainwater brings in an insignificant portion of Na into the aquifer. Chloride bearing minerals were not mentioned in the two different mineralogical analysis of two different soils in Michigan (Mariam and Mokma, 1996; Mariam and Mokma, 1995). As a result, Cl concentrations should be less than Na concentrations since Cl bearing minerals were not known to occur in a significant amount in the drift and rain water may be the only significant natural source of Cl to the watershed, excluding brine upwelling. Rainwater, a natural source of Cl, near the Muskegon River watershed has been found to contain about 0.10 mg/L Cl. The fact that Cl bearing minerals are not known to occur within the drift in the watershed and little Cl comes into the watershed as rain as well as the fact that Na bearing minerals are known to occur within the watershed, the amount of naturally dissolved Na should be greater than the naturally occurring Cl. As a result the Na/Cl (M) ratios derived from plagioclase dissolution and precipitation would probably be within the range of treated sewage/septic systems.

The RASA study showed that ground water samples, samples taken in the RASA study region in Michigan, had definable trends when Cl concentrations were greater than 10

mg/L (Long, 2005). Ground water with Cl concentrations below 10 mg/L Cl tended to not have definable trends. Those samples below 10 mg/L Cl were classified as being within a background level of Cl a level at which multiple sources of Cl are significant throughout the region of study. Above the 10 mg/L Cl, definable trends become apparent. Those definable trends are a result of the more dominant sources, high Cl sources, showing their Na/Cl ratios. Tables showing the percentage of samples that plot within the Na/Cl ratios of the possible sources discussed above are included to show what ranges are most common. One column shows all of the samples a second column shows only samples with Cl concentrations over 10 mg/L. This was done in order to see if samples over 10 mg/L Cl plotted in a different range of Na/Cl values than samples that had any level of Cl.

A graph showing Na/Cl (M) vs. Cl (ppm) has been provided to show the Na/Cl (M) ratio of stream samples that either directly drain the MCWDS or are directly downstream of it (Figure 39). The graph also shows the relationship between the Na/Cl (M) ratios of the stream samples and the ratios of septic system effluent. If septic systems and treated sewage were effecting the streams in a significant amount, besides those directly downstream of the MCWDS, more samples with high Cl within the range of septic systems and treated sewage would be shown. If the stream samples directly downstream of the MCWDS are ignored, the range of Na/Cl (M) ratios that have the highest Cl concentrations are those between 0.4 and 1.1. Graphs of the Na/Cl (M) vs. Cl (ppm) were made for the MRW drift, SBW drift, SBW streams, regional drift, Pennsylvanian bedrock waters, and Mississippian bedrock waters and show similar trends: the samples

with the highest Cl concentrations have Na/Cl ratios less than 1.1, and therefore were not included in this thesis. Although the SBW drift, Pennsylvanian, Mississippian, and regional drift have similar trends in distribution of samples within the ranges of Na/Cl (M), the concentration of Na (M) and Cl (M) were much higher in these hydrologic domains than that found in the MRW drift or the MRW streams. In general, the samples that have Na/Cl (M) ratios within the range of treated sewage/septic systems have a lower concentration of Cl than the samples that have Na/Cl (M) ratios within the range of halite or brines. As mentioned earlier, the natural background Na/Cl (M) ratios will plot within this range as well. These sources will produce a natural range of Na/Cl that may not be consistent due to varying degrees of sodium bearing minerals in the drift. The upwelling of saline waters from the bedrock layers into the drift layers is also possible.

The Mississippian and the Pennsylvanian bedrock contain saline waters and both units underlie the glacial drift in the MRW. The SBW is underlain by Pennsylvanian bedrock. The hypothesis is that upwelling from bedrock layers below is causing the increase in Cl concentration in the drift and surface waters in the MRW. Therefore the distribution of Na/Cl (M) ratios of the Mississippian and Pennsylvanian bedrock needs to be compared to the MRW drift and MRW surface waters.

The following Na/Cl (M) histograms show three different ranges. The Na/Cl (M) range consistent with the dissolution of halite (0.8 to 1.2) is shown on the histograms as the area between the two black vertical lines. Samples that plot with Na/Cl (M) values greater than 1.2, the region consistent with treated sewage/septic systems and plagioclase

dissolution/atmospheric precipitation, will be shown on the graph as those samples that plot to the right of the halite region. The region that plots to the left of the halite region, samples that have Na/Cl (M) ratios less than 0.8, will be samples that have Na/Cl (M) ratios consistent with oil field brines.

Water in the Pennsylvanian (Figure 40 and Figure 41) bedrock, with Na/Cl ratios less than 4.0, shows a distribution of samples that are generally centered around the halite dissolution region. However table 3 reveals that if all samples, as well as samples with Cl concentrations greater than 10 mg/L, are grouped into the three ranges the most dominant range is actually the treated sewage/septic system and/or plagioclase dissolution/precipitation. Which makes water from the Pennsylvanian impossible to determine from water from the treated sewage/septic systems and or plagioclase dissolution with lesser amounts dissolved halite and oilfield brines. Water from the Mississippian bedrock (Figure 42 and Figure 43) tends to plot in the oilfield brine region. Table 4 reveals that this trend becomes even more dominant when only the samples with Cl concentrations greater than 10 mg/L are used. However, a significant number of samples plot with in the region that would be consistent with the dissolution of halite and treated sewage/septic systems and/or plagioclase dissolution/atmospheric precipitation. The similarity between the Mississippian bedrock water and the oilfield brines is to be expected because the Mississippian bedrock is known to contain saline waters (Westjohn and Weaver, 1998). Therefore determining the difference between the Mississippian waters and the oil field brines are not possible on Na/Cl (M) ratios alone.

It has been hypothesized that the brines in the Michigan basin are from evapoconcentrated seawater. When seawater is concentrated one of the minerals that can precipitate out is halite. As halite precipitates out, the seawater loses Na and Cl. The seawater contains more Cl than Na and as precipitation continues a larger percentage of Na is lost as compared to Cl. This has the effect of decreasing the Na/Cl (M) ratio with further evaporation of seawater. This gives the characteristic hook on the logarithmic charts of the seawater evaporation curve at the onset of halite precipitation.

Formation	Na/Cl (M)
Berea	0.50
Traverse	0.61
Dundee	0.64
Richfield	0.27
Detroit R.	0.17

Table 2. Table of the average Na/Cl (M) of different formation waters in the Michigan basin. Data was taken from Wilson (1989).

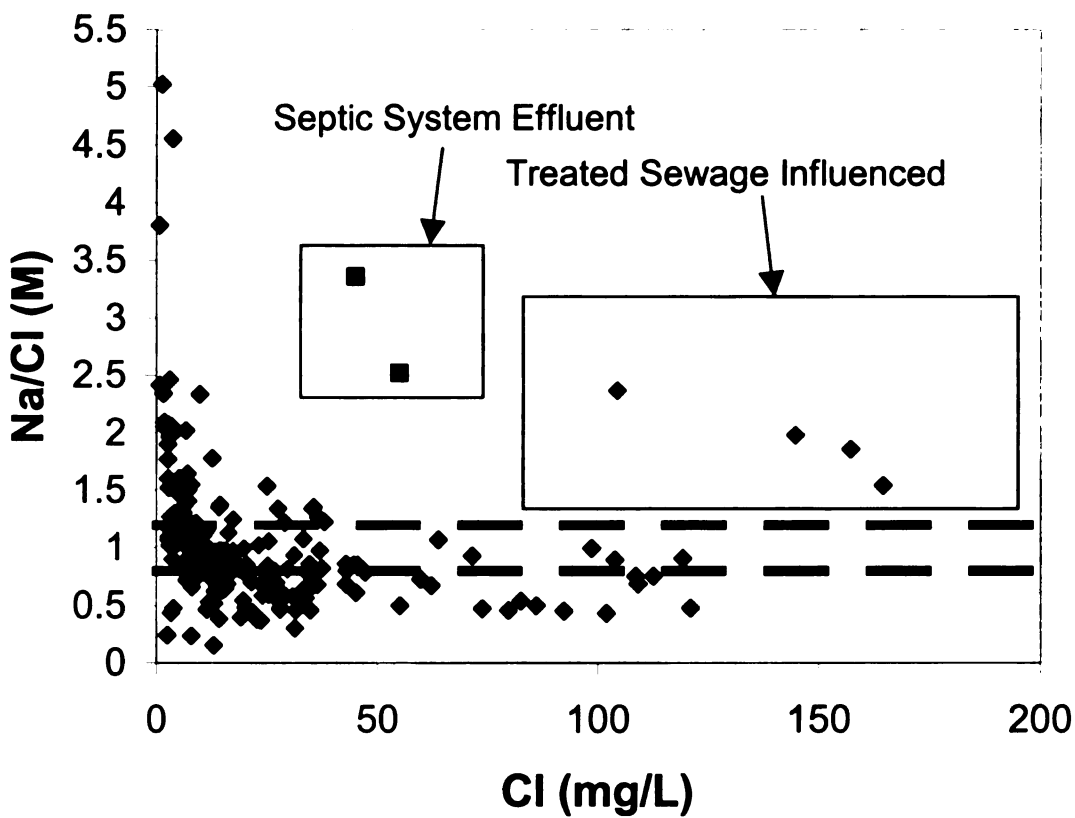


Figure 39. Graph of Na/Cl (M) vs. Cl ppm for streams within the Muskegon River Watershed. A box surrounds sewage sites downstream of the Muskegon County Wastewater Disposal System. Septic System Effluent Data from Robertson et al. (1991).

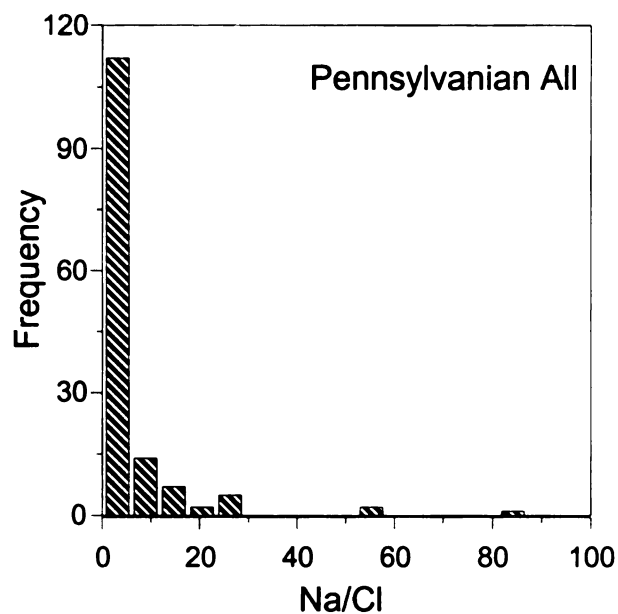


Figure 40. The Na/Cl (M) ratio for ground water within the Pennsylvanian bedrock aquifer. Data are from the ground water data set (Dannemiller and Baltusis, 1990; Wahrer, 1993; Meissner, 1993).

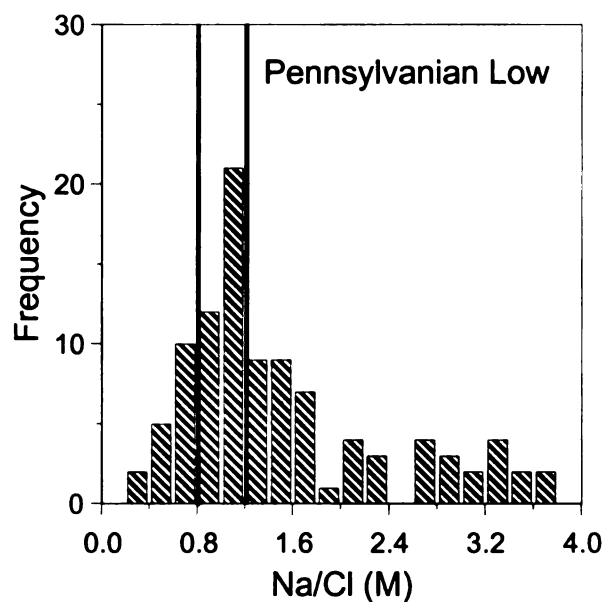


Figure 41. The Na/Cl (M) ratio for groundwater within the Pennsylvanian with a ratio of 3.8 or less. Data are from the ground water data set (Dannemiller and Baltusis, 1990; Wahrer, 1993; Meissner, 1993).

	All Samples	Samples with Cl > 10 mg/L
Na/Cl < 0.8	12%	17%
0.8 < Na/Cl < 1.2	23%	30%
Na/Cl > 1.2	64%	53%

Table 3. Table showing the percentage of samples that plot within different ranges of Na/Cl (M) values for ground water samples from the Pennsylvanian bedrock aquifer. Data are from the ground water data set (Dannemiller and Baltusis, 1990; Wahrer, 1993; Meissner, 1993).

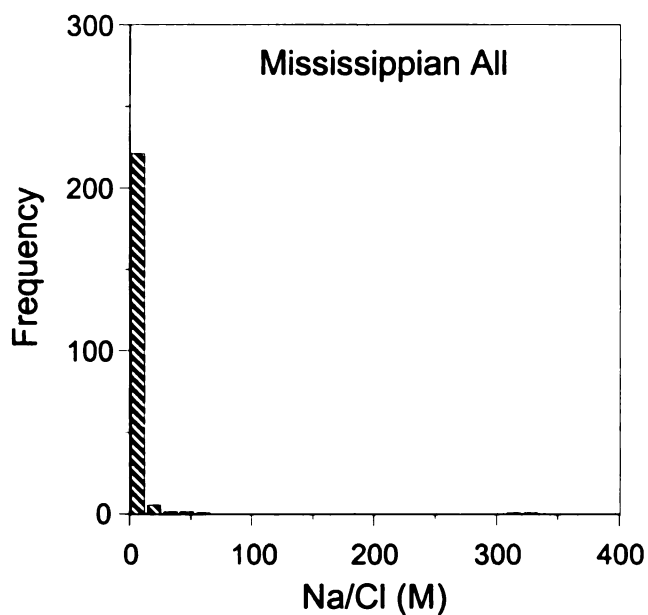


Figure 42. Na/Cl (M) ratio for groundwater within the Mississippian. Data are from the ground water data set (Dannemiller and Baltusis, 1990; Wahrer, 1993; Meissner, 1993).

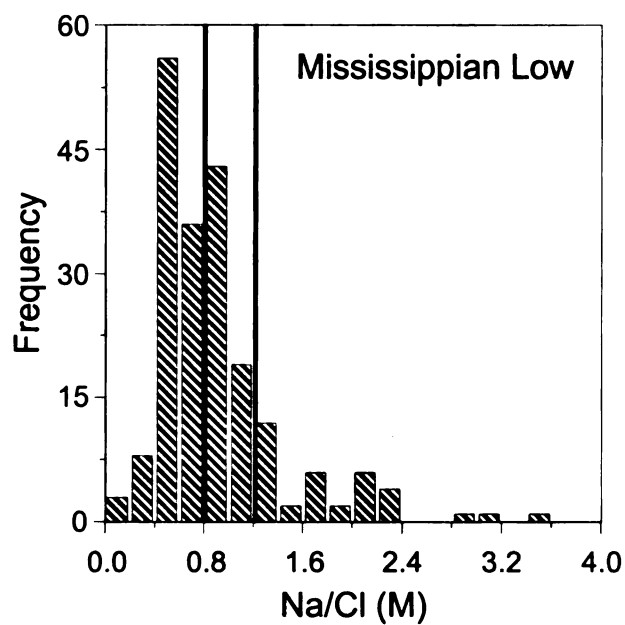


Figure 43. Na/Cl (M) ratios for groundwater within the Mississippian with a ratio less than 3.8. Data are from the ground water data set (Dannemiller and Baltusis, 1990; Wahrer, 1993; Meissner, 1993).

	All Samples	Samples with Cl > 10 mg/L
Na/Cl < 0.8	44%	51%
0.8 < Na/Cl < 1.2	27%	30%
Na/Cl > 1.2	29%	19%

Table 4. Table showing the percentage of samples that plot within different ranges of Na/Cl (M) values for ground water samples from the Mississippian bedrock aquifer. Data are from the ground water data set (Dannemiller and Baltusis, 1990; Wahrer, 1993; Meissner, 1993).

Na/Cl (M) ratios for bedrock aquifers and MRW watershed

Figures 44 and 45 are histograms containing the Na to Cl (M) ratios for ground water located in the drift and within the 12km buffered boundary of the MRW. A significant number of samples plot within all three different ranges. Which would support the idea that oilfield brines, halite dissolution, and treated sewage/septic and/or plagioclase dissolution/precipitation are all having an effect on the MRW drift. Table 5 shows that most samples in the Drift have Na/Cl (M) ratios greater than 1.2. However if just samples with Cl concentrations greater than 10 mg/L are considered then most samples have Na/Cl (M) ratios less than 0.8. The difference in the distribution of all samples and only samples with Cl concentrations greater than 10 mg/L may be a function of the influence of natural sources of Na and Cl. Natural sources of Na and Cl should have relatively low levels of both Na and Cl and should plot with Na/Cl ratios greater than 1.2.

Figure 46 and 47 are Na/Cl (M) histograms for streams within the MRW. Figure 47 shows that (for samples with Na/Cl (M) ratios less than 4.0) the frequency of samples increases towards the 0.8 to 1.0 interval, at which the frequency is the highest. This shows that the dominant peak is within the dissolution of halite region, although, significant number of samples plot within the region that would be consistent with an oilfield brine. Table 6 shows that most samples plot with Na/Cl ratios between 0.8 and 1.2. When only samples with Cl concentrations greater than 10 mg/L are used the two dominant ranges are less than 0.8 and 0.8 to 1.2. The percentage of samples with the Na/Cl (M) ratios greater than 1.2 decreases when only samples with Cl concentrations greater than 10 mg/L are considered; this is similar to the trend found in the MRW drift.

Figure 48 is a histogram of the Na/Cl (M) ratios of lake water samples in the MRW. The histogram shows that the frequency of samples increases towards the interval of 0.6 to 0.8 where the frequency is highest. The interval 0.6 to 0.8 is located within the range that would be consistent for an oilfield brine. Table 7 shows that most samples have Na/Cl (M) ratios less than 0.8 and slightly fewer have Na/Cl (M) ratios between 0.8 and 1.2. A slightly smaller percentage of samples plot above 1.2 Na/Cl (M) ratio when only samples above 10 mg/L are considered, this is similar to trend found in the MRW streams, and MRW drift. The two regions with the most samples located within them are the Na/Cl (M) region consistent with that of an oilfield brine and the region consistent with the dissolution of halite.

Figure 49 is a histogram of Na/Cl (M) ratios of wetland water samples in the MRW. The histogram shows the frequency of samples increases towards the 0.8 to 1.0 interval, where the frequency is the highest, located within the region that would be consistent with halite dissolution. Table 8 shows that most samples plot with Na/Cl values less than 0.8, with a lesser but still considerable amount of samples that have Na/Cl values between 0.8 and 1.2. Samples with Cl concentrations greater than 10 mg/L have a lower percentage of samples with Na/Cl (M) ratios greater than 1.2, than when all of the samples are considered. This trend was apparent in the MRW Drift, MRW Streams, and MRW lakes is apparent in the MRW wetlands as well.

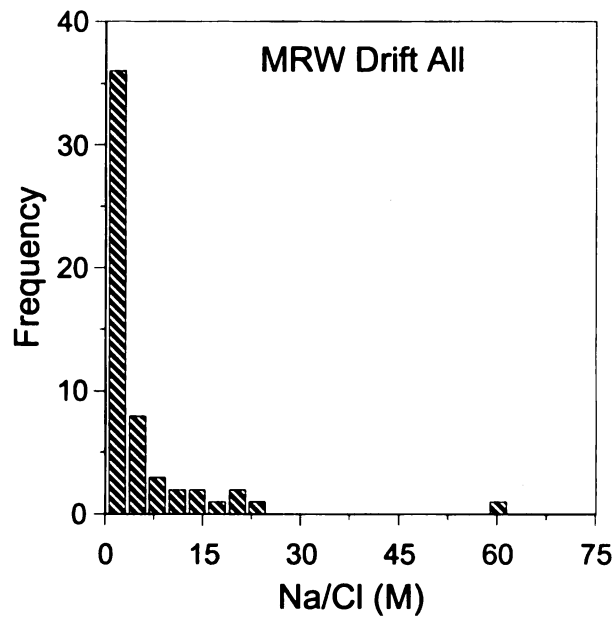


Figure 44. Frequency histogram of Na/Cl (M) ratios for ground water wells within the Muskegon River Watershed Drift. Data are from the ground water data set (Dannemiller and Baltusis, 1990; Wahrer, 1993; Meissner, 1993) and includes drift data within 12 km of the watershed.

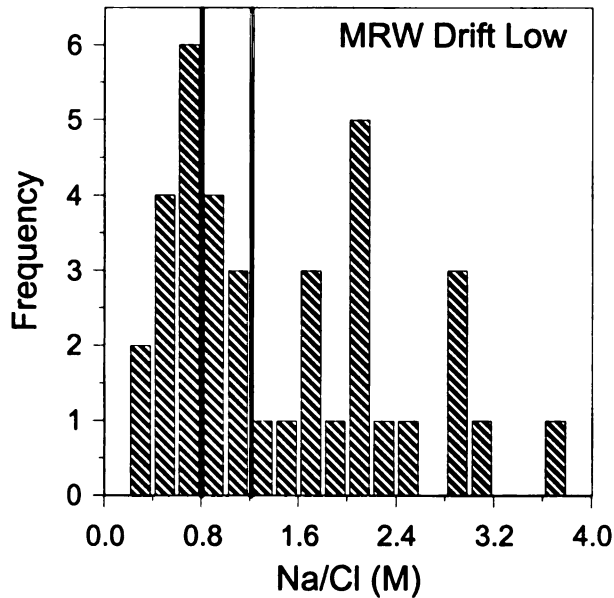


Figure 45. Frequency histogram of Na/Cl (M) ratios for ground water wells within the Muskegon River Watershed Drift that have ratios below 3.8. Data are from the ground water data set (Dannemiller and Baltusis, 1990; Wahrer, 1993; Meissner, 1993).

	All Samples	Samples with Cl > 10 mg/L
Na/Cl < 0.8	21%	47%
0.8 < Na/Cl < 1.2	13%	35%
Na/Cl > 1.2	66%	18%

Table 5. Table showing the percentage of samples that plot within different ranges of Na/Cl (M) values for ground water samples within the MRW drift. Data are from the ground water data set (Dannemiller and Baltusis, 1990; Wahrer, 1993; Meissner, 1993).

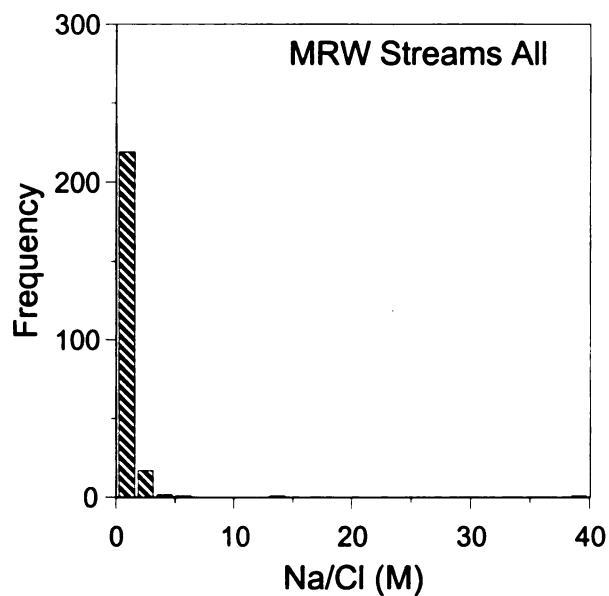


Figure 46. Na/Cl (M) ratios for stream water within the Muskegon River Watershed.

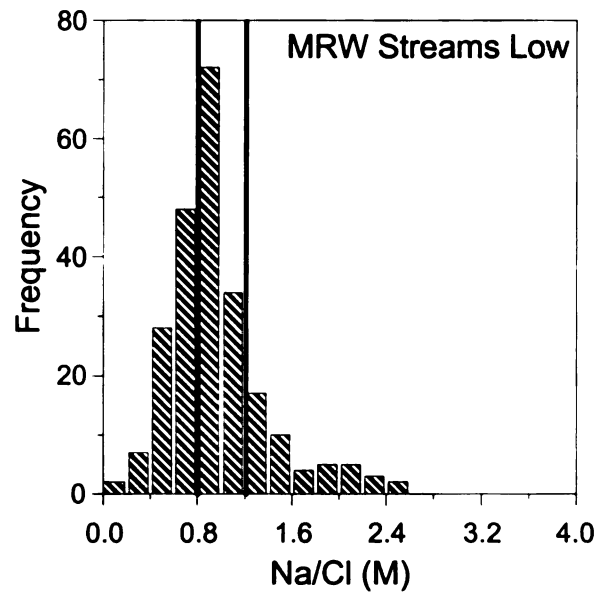


Figure 47. Na/Cl (M) ratios for stream water within the Muskegon River Watershed with Na/Cl less than 3.8.

	All Samples	Samples with Cl > 10 mg/L
Na/Cl < 0.8	35%	46%
0.8<Na/Cl<1.2	44%	45%
Na/Cl >1.2	21%	9%

Table 6. Table showing the percentage of samples that plot within different ranges of Na/Cl (M) values for stream water samples in the MRW.

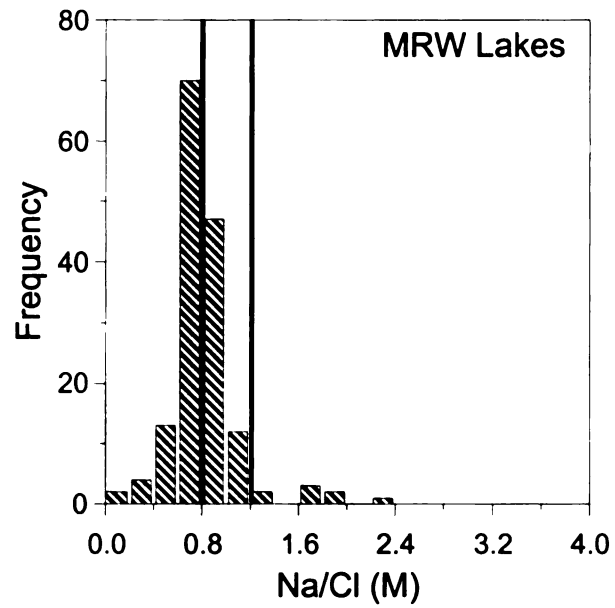


Figure 48. Na/Cl (M) ratios for lake water within the Muskegon River Watershed.

	All Samples	Samples with Cl > 10 mg/L
Na/Cl < 0.8	57%	60%
0.8 < Na/Cl < 1.2	38%	39%
Na/Cl > 1.2	5%	1%

Table 7. Table showing the percentage of samples that plot within different ranges of Na/Cl (M) values for lake water samples in the MRW.

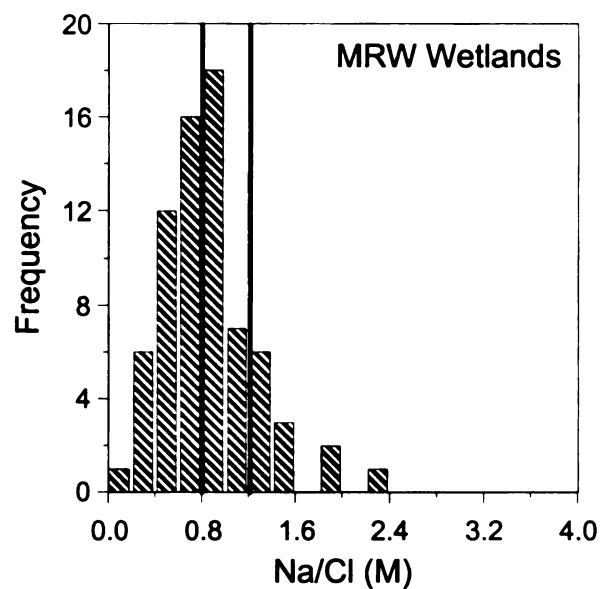


Figure 49. Na/Cl (M) ratios for wetland water within the Muskegon River Watershed.

	All Samples	Samples with Cl > 10 mg/L
Na/Cl < 0.8	47%	67%
0.8<Na/Cl<1.2	34%	30%
Na/Cl >1.2	19%	3%

Table 8. Table showing the percentage of samples that plot within different ranges of Na/Cl (M) values for wetland water samples in the MRW.

Na/Cl ratios for SBW Drift and SBW streams

If the processes controlling Cl in the Drift in the MRW are similar to the processes controlling Cl in the Drift in the SBW, then the Na/Cl (M) ratios should be similar between these two watersheds. Both watersheds overlie bedrock units that are known to contain saline waters. The glacial drift under the SBW is an area known to have saline waters migrating from the underlying bedrock into the shallow drift aquifer. The glacial drift within the Michigan Lowlands (part of the Michigan Lowlands is located within the MRW) contains waters that have elevated Cl levels.

Figures 50 and 51 show Na/Cl (M) ratios for drift waters in the Saginaw Bay Watershed. The histogram shows that the highest peaks are located within the region that is consistent with the dissolution of road salt. However table 4 shows that when all samples are considered most samples plot with Na/Cl ratios consistent with treated sewage/septic systems and/or plagioclase dissolution/atmospheric precipitation. Table 9 shows that most samples have Na/Cl (M) ratios less than 1.2. However, when only samples with Cl concentrations greater than 10 mg/L are considered Na/Cl (M) ratios between 0.8 and 1.2 are the most popular. The least popular Na/Cl (M) range is less than 0.8 this was true when all samples were considered as well as samples with Cl concentrations greater than 10 mg/L.

Figures 52 and 53 show Na/Cl (M) ratios for streams within the SBW. The interval with the highest frequency is 0.6 to 0.8. The histogram appears to converge on this peak with peaks that are closer to this peak with a higher frequency than those that are farther away. Table 10 shows that most stream samples in the SBW plot with Na/Cl (M) ratios less than 0.8. The second most popular Na/Cl (M) ratio is 0.8 to 1.2 with Na/Cl (M) ratios greater than 1.2 being the least significant range.

The Pennsylvanian bedrock underlies the SBW drift. If brines are upwelling into the near surface aquifer, then the Na/Cl (M) ratios found in the SBW drift should be similar to the Na/Cl (M) ratios found in the Pennsylvanian bedrock. If that water has entered into the surface waters, then the streams and lakes should have Na/Cl (M) histograms that are similar to those found in the Pennsylvanian as well. Both the SBW drift and the Pennsylvanian bedrock water have very similar Na/Cl (M) histograms. Both the SBW drift and the Pennsylvanian bedrock water have their highest frequency peaks within the range considered to be from halite dissolution. When all samples are considered both the SBW drift and Pennsylvanian bedrock aquifer tend to be dominated by Na/Cl (M) ratios greater than 1.2. However the SBW drift, when just considering samples with Cl concentrations greater than 10 mg/L, is dominated by samples with Na/Cl (M) ratios between 0.8 and 1.2. Streams within the SBW however have Na/Cl (M) ratios that plot more within the range that would be consistent with an oilfield brine. This is shown both in the histograms as well as the tables. It was expected that all three would be the same if brines were upwelling and effecting the drift as well as the surface waters. However, it appears that other things are influencing the water that is entering into the streams. This

could be the result of oilfield brines entering into the shallow aquifer, from oil and gas exploration, prevented from going into the deeper drift aquifer by the presence of layers of lacustrine clays. The MRW drift is underlain by both Pennsylvanian bedrock as well as Mississippian bedrock. If water is upwelling from the bedrock layers below, then the Na/Cl (M) MRW drift histogram should look like either the Na/Cl (M) histogram from the Pennsylvanian or the Mississippian bedrock. The MRW drift is dominated by samples within the range of the dissolution of halite (0.8 to 1.2). However when just samples with Cl concentrations greater than 10 mg/L are considered water with Na/Cl (M) ratios consistent with the dilution of a brine (less than 0.8) appear to be as equal importance as that of dissolution of halite. Water from the Mississippian bedrock, when all samples are considered, plots for the most part within the range of a diluted brine. When only samples with Cl concentrations greater than 10 mg/L are used the most common ranges of Na/Cl values are less than 0.8 (consistent with diluted oilfield brine). The Na/Cl (M) ratio range of 0.8 to 1.2 (consistent with dissolution of halite) is of lesser importance. The MRW drift also has peaks within the region that would be consistent with halite dissolution; however, Pennsylvanian bedrock water plots within this region as well and therefore may be a possible source of Cl. Since the Mississippian is in direct contact with the drift in portions of the watershed and oilfields are located within the watershed as well, both are possible contributors to Cl in the drift. The MRW (Figure 48) lakes histogram is the most similar to the Marshall with the highest frequency interval 0.6 to 0.8 Na/Cl (M). This is also within the region consistent with oilfield brine. Table 8 also shows that most MRW lakes samples plot within the range consistent with oilfield brine, which is within the range consistent with water from the Mississippian bedrock.

The MRW Wetlands (Figure 49) and the MRW stream (Figure 46 and Figure 47) are more like the Pennsylvanian (Figure 40 and Figure 41) bedrock water, with their highest frequency Na/Cl (M) ratios plotting between 0.8 and 1.2. However table 4 shows that the Pennsylvanian has a different distribution of samples than the MRW streams, MRW lakes, and wetlands. The water within the Pennsylvanian have Na/Cl (M) ratios greater than 1.2. This is evidence against upwelling of Pennsylvanian water into the surface waters of the MRW.

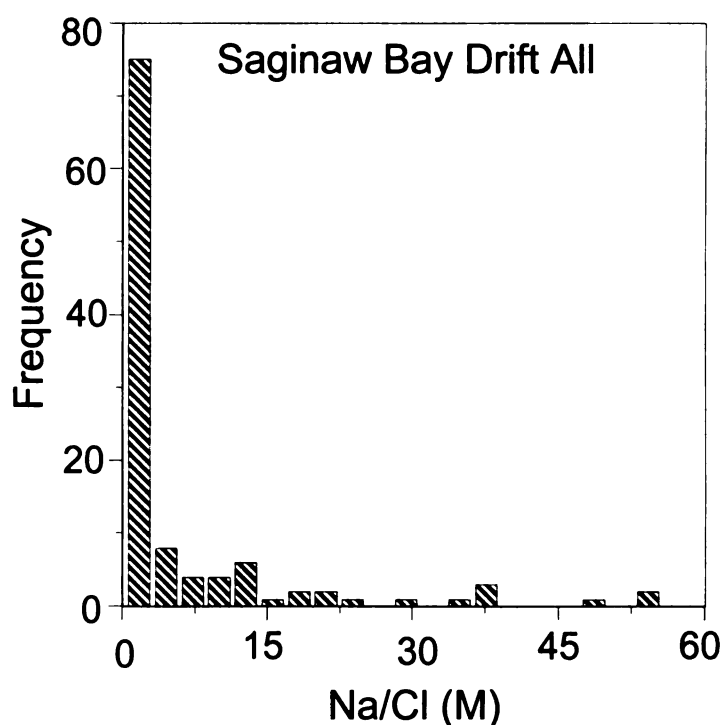


Figure 50. Na/Cl (M) ratios of groundwater in the Saginaw Bay Watershed. Data are from the ground water data set (Dannemiller and Baltusis, 1990; Wahrer, 1993; Meissner, 1993).

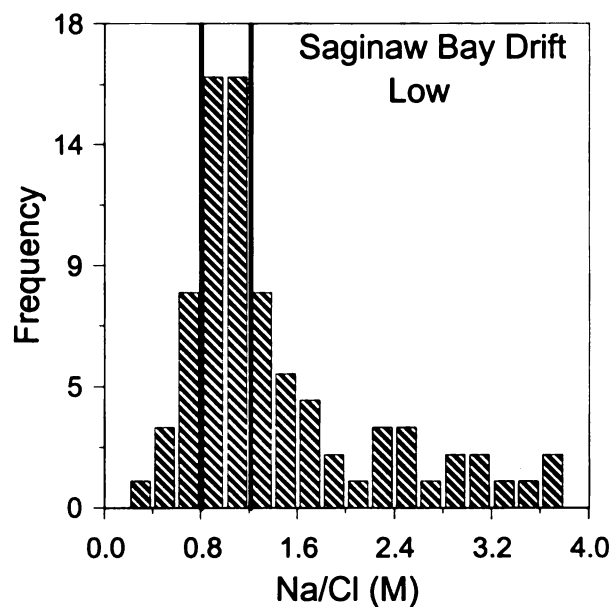


Figure 51. Na/Cl (M) ratios of groundwater in the Saginaw Bay Watershed with Na/Cl (M) ratios less than 3.8. Data are from the ground water data set (Dannemiller and Baltusis, 1990; Wahrer, 1993; Meissner, 1993).

	All Samples	Samples with Cl > 10 mg/L
Na/Cl < 0.8	11%	16%
0.8 < Na/Cl < 1.2	29%	46%
Na/Cl > 1.2	60%	38%

Table 9. Table showing the percentage of samples that plot within different ranges of Na/Cl (M) values for Drift water samples in the SBW. Data are from the ground water data set (Dannemiller and Baltusis, 1990; Wahrer, 1993; Meissner, 1993).

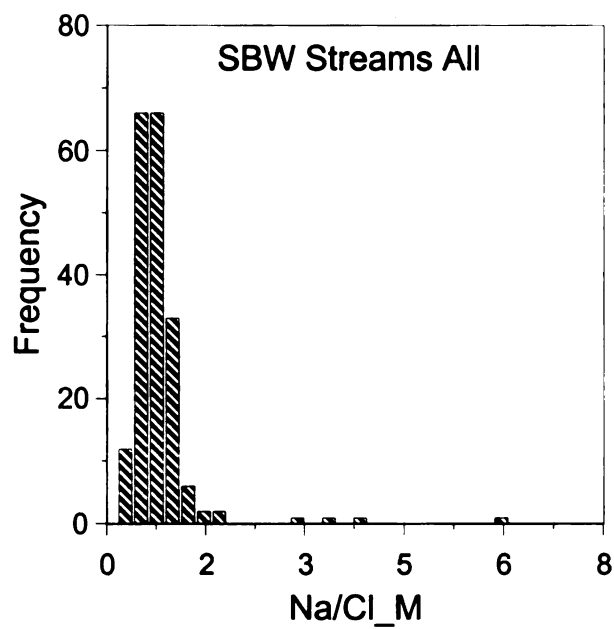


Figure 52. Cl/Na (M) ratios for streams in the Saginaw Bay Watershed. Data are from (Kolak, 2000).

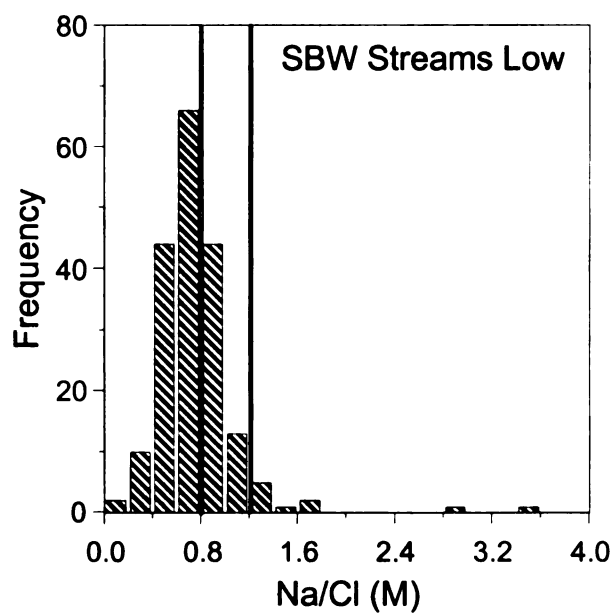


Figure 53. Cl/Na (M) ratios for streams in the Saginaw Bay Watershed with Na/Cl ratios less than 3.8. Data are from Kolak (2000).

	All Samples	Samples with Cl > 10 mg/L
Na/Cl < 0.8	64%	66%
0.8 < Na/Cl < 1.2	30%	29%
Na/Cl > 1.2	6%	5%

Table 10. Table showing the percentage of samples that plot within different ranges of Na/Cl (M) values for stream samples in the SBW. Data are from Kolak (2000).

Logarithmic Na vs. Cl Graphs

Carpenter (1978) stated that during evaporation, the ionic ratios between different ions in natural water should stay the same if the ions in a system are conservative (i.e., they do not precipitate or react with the surrounding substrate). Carpenter (1978) derived a logarithmic formula to express this relationship and it is written as Equation 1 below.

$$\text{Log B} = \text{Log A} + \text{Log k} \quad (1)$$

The variables A and B are concentrations of conservative ions dissolved in water. The letter k represents equilibrium constant. The graphing of two conservative ions using this formula results in a straight line with a one to one slope. Any deviation from this slope means that the concentration of one or both of the ions is being effected by precipitation or reaction with the surrounding substrate.

Figure 54 is a plot that compares bedrock water to the seawater evaporation curve.

Although, very similar plots have been made by Wharar (1993) and Meissner (1993) a

new plot was made due to the very slight differences in the classification of the different bedrock units. The argument is that the brines in the Michigan basin are from evapoconcentrated seawater. The brines have infiltrated into the overlying drift aquifer and have mixed with the much more dilute water in the drift. If the ions graphed are conservative through the mixing process, the ratios between the two conservative ions should not vary until the dilution of the brine is so great that the contribution of the conservative ions from the dilute water is having a significant effect on the ratio of the two ions in the mixed water. The Mississippian, Pennsylvanian, and glacial drift waters all have the same trend showing evidence of mixing between a dilute end member and a saline end member. The glacial drift and the Pennsylvanian waters plot in a trend along the seawater evaporation curve, however, neither hydrologic region contains waters that are concentrated enough to overlap with the seawater evaporation curve. However, some Mississippian waters are more highly concentrated and plot on the seawater evaporation curve past the point of halite precipitation. All of the drift and bedrock water exhibit scatter at lower concentrations, mostly due to various degrees of water-rock interactions and the effects of human activities, Wahrer (1993).

Figure 55 shows the log concentration of Na vs. Cl of the ground water in the MRW drift as well as the Pennsylvanian bedrock aquifer and the ground water drift. All of the hydrologic regions represented in Figure 55 show a distribution of points that show more variation at lower Na and Cl concentrations and less variation at higher concentrations. The result is a distribution of points that resemble a teardrop shape. All of the hydrologic regions represented in Figure 55 show a distribution of points that taper off

towards the seawater evaporation curve at higher concentrations of Na and Cl except for the MRW drift. Although the MRW drift plots within the same region of the graph as the other data sets it does not clearly show a trend tapering off towards the seawater evaporation curve. The ground water data from the Pennsylvanian and ground water drift data sets have samples that have much higher concentrations of Cl and Na than the MRW drift. This suggests that some of the geochemical processes that are going on in the bedrock and the regional glacial drift may also occur in the MRW Drift water. However, the processes occurring within the MRW may not be occurring to the extent as those same processes occurring in the regional glacial drift and the bedrock. The MRW drift data do not clearly indicate mixing between with saline waters and fresh meteoric waters due to the lack of high Cl samples in the MRW drift data set.

Figure 56 shows the log concentration of Na and Cl in the MRW streams, MRW Drift, and the seawater evaporation curve. The figure shows that the MRW drift data overlie the MRW stream data, indicating the influence of ground water on stream water chemistry. Combining the assumption that the ground water feeds the stream water with the observation that the stream water and the MRW drift ground water plot in the same regions (i.e., have similar values) the interpretation can be made that the two ions act conservatively going from ground water to the streams. The four most concentrated points in the stream data are sites downstream of treated sewage inputs to the streams. These points also plot noticeably higher in the Na than the rest of the stream data. The MRW streams for the most part plot along the halite dissolution line. If the MRW drift was the main contributor to the Cl concentrations at low concentrations of Cl then the

MRW streams should have a similar distribution of samples at low concentrations of Cl as the MRW drift does. However, the MRW streams tend to plot along a straight line, along the halite dissolution line at low concentrations of Na and Cl, and do not show a scatter at low concentrations that the MRW drift does. This supports the alternative hypothesis that the source of Cl in the streams is from the dissolution of halite.

Figure 57 shows log concentrations of Na (M) vs. Cl (M) of water for lakes in the MRW, MRW Drift, and regional drift data sets, as well as the seawater evaporation curve. The data from the MRW lakes plot within the same area as that from the MRW drift and the regional drift. However the lakes plot with a tighter trend, with less scatter than the drift data sets and the river data set. The lakes plot along the halite dissolution curve and do not show the scatter at low concentrations of Na and Cl that the MRW drift does. This supports the alternative hypothesis that the excess Cl in the MRW lakes is from the dissolution of halite

Figure 58 shows a log concentration of Na (M) vs. Cl (M) of water for the data from the wetlands in the MRW as well as from the data from the drift in the MRW, regional drift, and seawater evaporation curve. The point along the seawater evaporation curve at which halite precipitation occurs is labeled on this chart. The data for the wetlands in the MRW, MRW Drift, and regional drift all plot in the same general area. However, the MRW wetlands tend not to have as much scatter as the regional drift and the MRW drift has at lower concentrations. At higher concentrations of the Na and Cl the drift data sets and the MRW wetlands are more similar. This figure also shows the halite dissolution

line. The wetlands plot along the halite dissolution line and do not show the scatter at low concentrations of Na and Cl that the MRW drift does. This is consistent with the alternative hypothesis that the source for Cl in the wetlands is from dissolution of halite.

Figure 59 shows that the MRW Drift, MRW Streams, and the SBW Drift all plot within the same region on the graph. This would suggest that the processes occurring within them are similar. However, the samples within the SBW are in general more concentrated than the samples found in the MRW. Although the area on the graph that represents the MRW drift is shaped like a tear drop like the regional drift, the MRW drift has few high Cl samples so the trend or direction that the high Cl samples are going is suspect. Therefore the interpretation that the MRW drift is trending towards the seawater evaporation curve like the other regional drift will not be made due to insufficient data. The MRW streams and the SBW streams plot within the same region on the graph. They both trend along the halite dissolution line on the graph. This would suggest that the source of Cl to both the streams in the SBW and the MRW is the dissolution of halite.

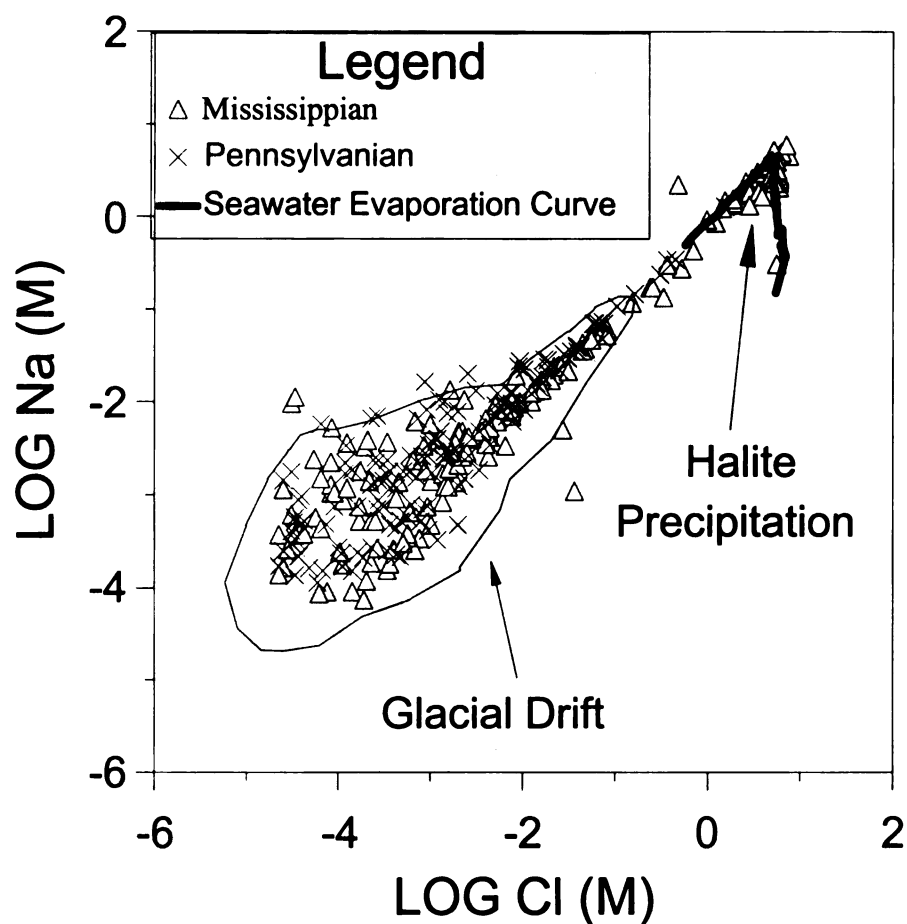


Figure 54. Graph showing the relationship between the log molar concentrations of Na and Cl in the Pennsylvanian, Mississippian, seawater evaporation curve (McCaffery et al., 1987), halite dissolution line, and the envelope on the graph where the water from the glacial drift plot. Ground water data are from the ground water data set (Dannemiller and Baltusis, 1990; Wahrer, 1993; Meissner, 1993).

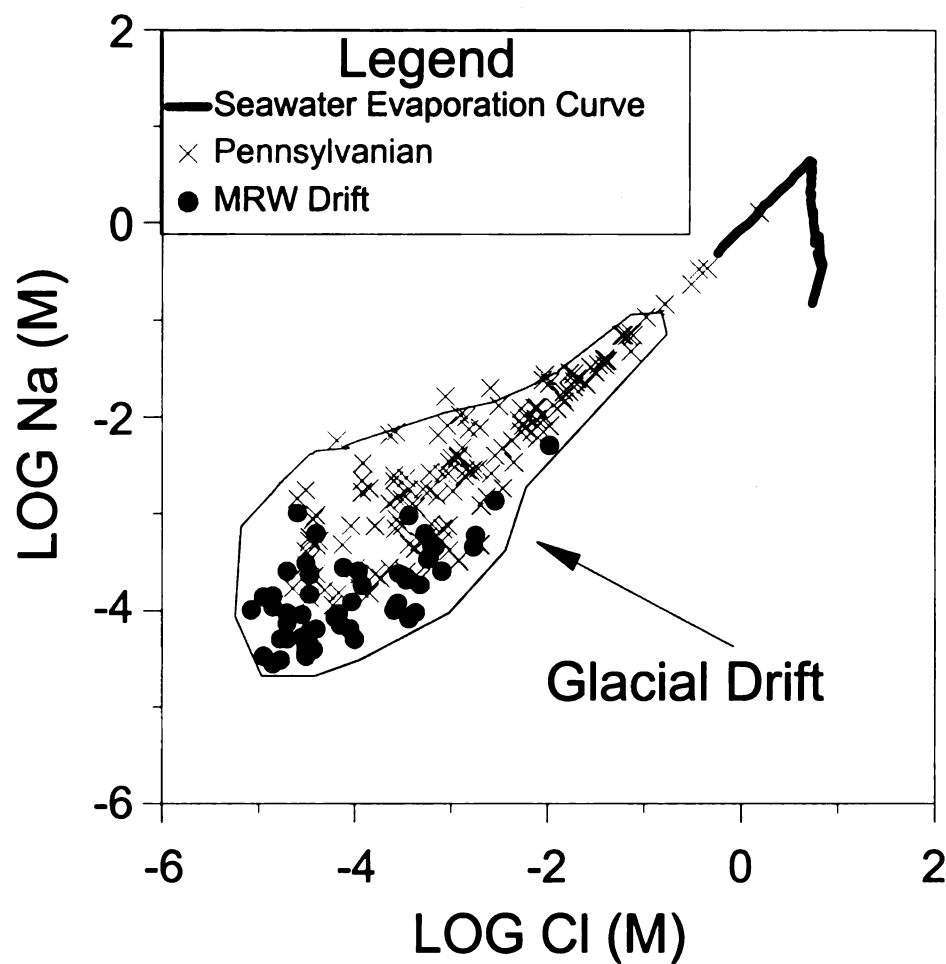


Figure 55. Graph showing the relationship between the log molar concentrations of Na and Cl in the Muskegon River Watershed Drift, Pennsylvanian bedrock, seawater evaporation curve (McCaffery et al., 1987), and the envelope on the graph where the glacial drift plot. Ground water data are from the ground water data set (Dannemiller and Baltusis, 1990; Wahrer, 1993; Meissner, 1993).

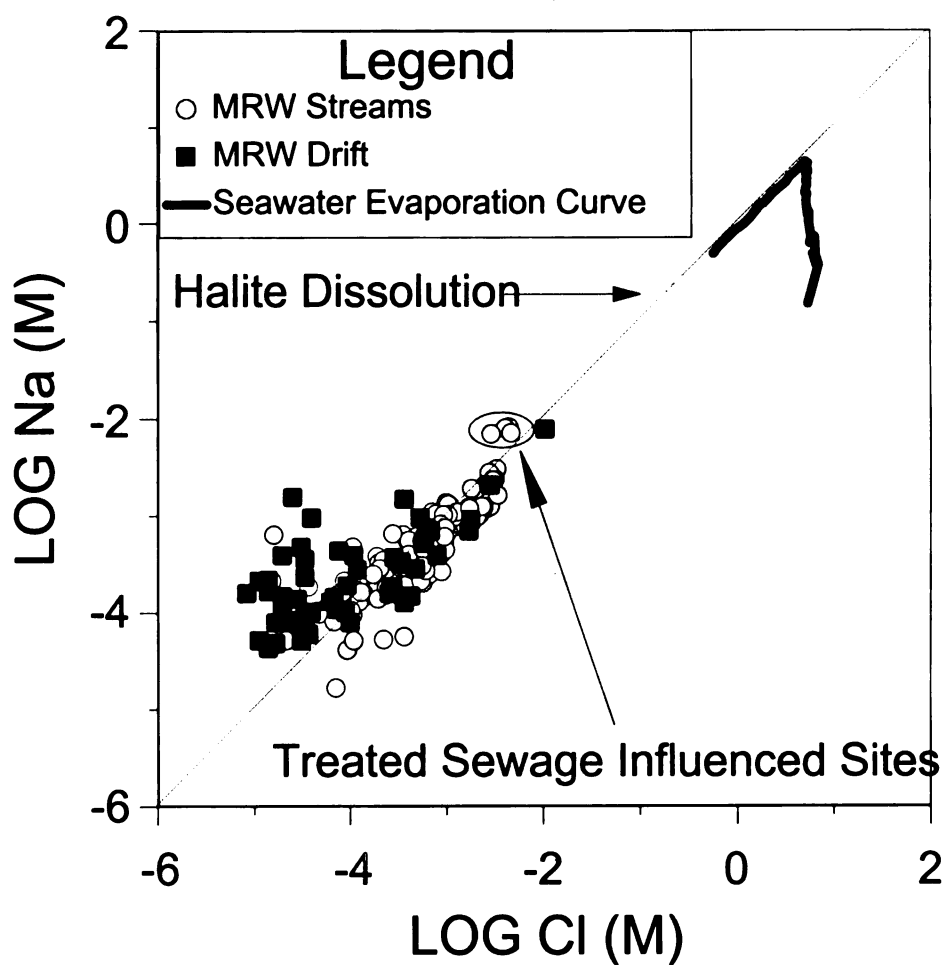


Figure 56. Graph showing the relationship between the log molar concentrations of Na and Cl in the Muskegon River Watershed streams, Muskegon River Watershed drift, halite dissolution line, and the seawater evaporation curve (McCaffery et al., 1987). Ground water data are from the ground water data set (Dannemiller and Baltusis, 1990; Wahrer, 1993; Meissner, 1993).

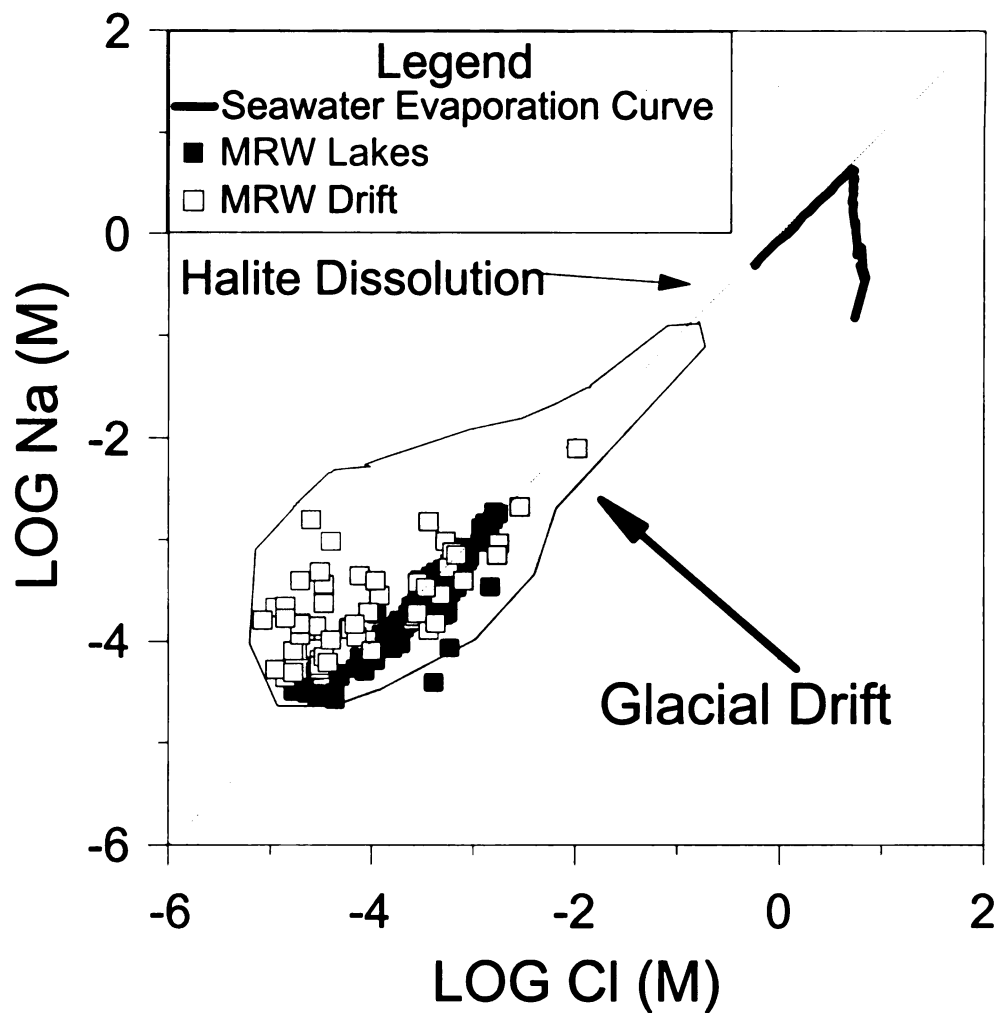


Figure 57. Graph showing the relationship between the log molar concentrations of Na and Cl in the Muskegon River Watershed lakes, regional drift, Muskegon River Watershed drift, halite dissolution line, seawater evaporation curve (McCaffery et al., 1987), and the envelope on the graph where the glacial drift plot. The Muskegon River Watershed Drift data includes data up to 12km outside of the Muskegon River Watershed boundary. Ground water data are from the ground water data set (Dannemiller and Baltusis, 1990; Wahrer, 1993; Meissner, 1993).

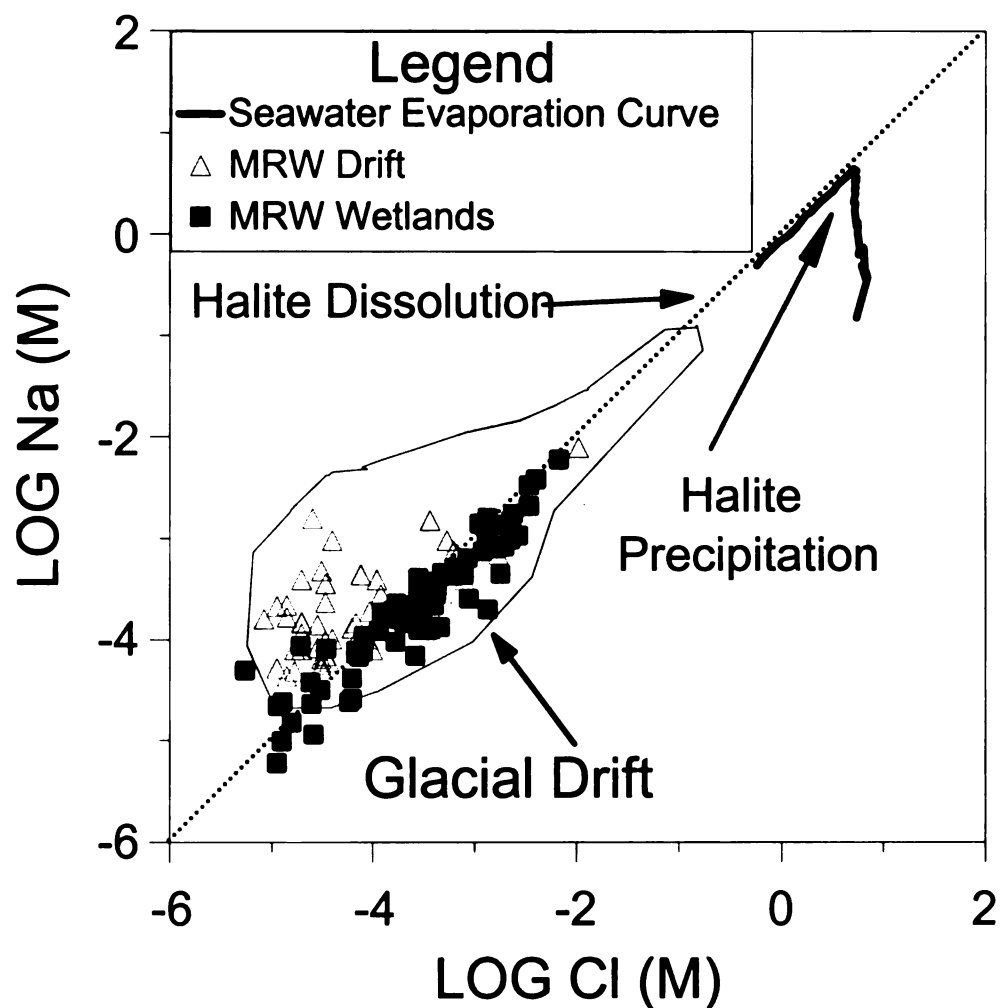


Figure 58. Graph showing the relationship between the log molar concentrations of Na and Cl in the Muskegon River Watershed wetlands, Muskegon River Watershed drift, dissolution of halite, seawater evaporation curve (McCaffery et al., 1987), and the envelope on the graph where the glacial drift plot. Ground water data are from ground water data set (Dannemiller and Baltusis, 1990; Wahrer, 1993; Meissner, 1993).

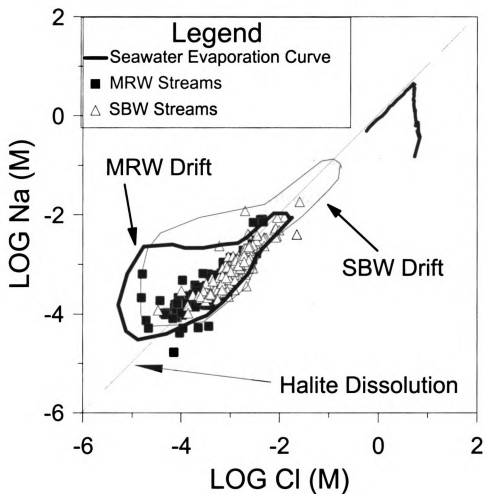


Figure 59. Graph showing the relationship between the Saginaw Bay Watershed drift, regional drift, Muskegon River Watershed drift, halite dissolution, seawater evaporation curve (McCaffery et al., 1987), and the envelopes on the graph where the MRW and SBW drift plot. Ground water data are from the ground water data set (Dannemiller and Baltusis, 1990; Wahrer, 1993; Meissner, 1993).

In summary, the SBW data show evidence for mixing between ground water in the glacial drift and the bedrock layers beneath. The mixing is shown in the way in which glacial drift samples on the logarithmic graphs have a similar distribution of samples to the bedrock units underlying the SBW (i.e., Pennsylvanian). Wahrer (1993) made the same conclusion on the same line of evidence in the Saginaw Lowland Area, region that makes up most of the SBW. The streams overlying the SBW do not show the same scatter as the SBW drift samples do at low concentrations of Na and Cl. The streams samples trend along the halite dissolution line, which gives evidence for the waters being from the dissolution of halite. Although, the MRW drift samples overly the glacial drift and bedrock units, it does not extend far up towards the seawater evaporation curve, which does not support mixing with a saline end member (i.e., bedrock units underneath). The SBW drift however extends up towards and almost to the seawater evaporation curve, which supports the hypothesis that there is a saline source for dissolved ions in the SBW (Long, 1989; Wahrer, 1993). The MRW streams, MRW lakes, and MRW wetlands overlie the MRW drift, however; they do not show the same scatter at the lower concentrations as the MRW drift does. The MRW surface waters and SBW streams plot close to the halite dissolution line, which is evidence for halite dissolution as the source of Na and Cl to the surface waters. This interpretation is tempered by the fact that the seawater evaporation line plots with a very similar slope to the halite dissolution line. On the logarithmic charts they are indistinguishable in slope until the onset of precipitation of halite out to seawater. A more accurate interpretation is that there is substantial evidence for halite as being the source of Na and Cl to the surface waters at low levels of Na and Cl. If brine upwelling were the source of Cl at low levels to the surface waters

than the graphs should look graphs from the bedrock layers beneath. The graphs of surface waters do look like graphs from the bedrock layers as concentration of Na and Cl increases. Therefore the low level Cl and Na found in the surface waters is possibly from road salt however the higher concentrations of Cl and Na maybe from brines. Either brines naturally upwelling or from oil and gas exploration.

Calcium vs. Magnesium

Insight into the geochemical evolution of the surface water chemistry can be further gained from the study of Ca and Mg. This part of the chapter explores the molar relationship between Ca and Mg using X Y graphs. The element Mg (M) will be plotted on the X-axis since it is more conservative in surface waters and as a result will not precipitate out (e.g., MgCO_3) in an appreciable amount (Otsuki and Wetzel, 1974).

Calcium on the other hand is known to precipitate out of lakes (Muller, et al., 1972; Strong and Eadie, 1978) as well as streams (Herman and Lorah, 1987).

A major source for Ca and Mg to the ground water within Michigan is the dissolution of dolomite. Possible sources of dissolved Ca to ground water are calcite and aragonite.

The chemical formula for dolomite is $\text{MgCa}(\text{CO}_3)_2$ and, therefore, contains both Ca and Mg in a one to one molar ratio. If dolomite were to dissolve congruently, i.e. there is no preference between the liberation of Mg or Ca from the dolomite, then ground water would have a 1 Mg for 1 Ca molar ratio in the water. Therefore when samples are plotted on a graph of Ca (M) vs. Mg (M) they should plot along a slope of 1.

If the Ca and Mg in the watershed are from an equilibrium reached between dolomite and calcite (CaCO_3) then the water should have sample points that have a ratio of 1.36. This ratio was determined by using the geochemical modeling program PHREEQC (Parkhurst, 1995). The program AquaChem (1998) was used to make loading geochemical data into PHREEQC and obtaining results from PHREEQC easier. The starting parameters before equilibration to dolomite and calcite was a pH of 7, a temperature of 25°C , a p_e of 4, and a density of one. PHREEQC then equilibrates the water to calcite and dolomite with a set concentration of dissolved CO_2 . The concentration of CO_2 in ground water typically varies between $10^{-1.5}$ and $10^{-2.5}$ atmospheres (Drever, 1997). As a result of the variability in dissolved CO_2 in ground water, different models were run with all parameters being the same except for different values of CO_2 . It was found that although the concentration of Ca and Mg changed with the concentration of dissolved CO_2 in the water, the ratio between the Ca and Mg stayed the same.

The Ca to Mg ratio after the equilibrium between calcite and dolomite was reached is represented on the charts as a solid line with a slope equal to that ratio of Ca to Mg (1.36). The congruent dissolution of dolomite is represented on the graph as a stippled line with a slope of 1. The lines were moved left to right as necessary on the chart to explore the relationship of the data trend to the calculated slopes.

In some cases, creating two graphs for a data set was necessary. Glacial drift as well as the Pennsylvanian ground waters contained samples that were significantly higher in Ca (M) and Mg (M) than the majority of the data. As a result, it was difficult to see how the best-fit line fit the data in the lower region of the graph where most of the data were usually plotted. In order to see how most of the data were plotted with respect to the calcite/dolomite equilibrium line (slope of 1.4) and the dolomite dissolution line (slope of 1), a second graph was made that contained the points in the lower region of the graph.

Figures 60 and 61 show Ca vs. Mg values for ground water within the Mississippian bedrock unit. The slope of the best-fit line is 2.14 with a r^2 value of 0.809. All samples appear to be tightly correlated and appear to follow the same trend in Figure 60. However, at Ca concentrations less than 0.005 (M) (Figure 61) some of the data fit the dolomite equilibrium line and others fit the calcite/dolomite equilibrium line. Both of these lines have slopes much lower than the overall best-fit line.

Figure 62 is a graph of the Ca vs. Mg values for ground water within the Pennsylvanian bedrock unit. The slope of the best-fit line is 2.62 with a r^2 value of 0.950. Figure 63 is a graph of the Ca vs. Mg values for ground water within the Pennsylvanian with Ca values less than .0032 (M). There appears to be a significant increase in scatter at about 0.0025 (M) Ca and 0.001 (M) Mg.

Figure 64 is a graph of Ca (M) vs. Mg (M) values for the glacial drift. The data have a slope of 1.93 and a r^2 value of 0.76. Most samples in the glacial drift aquifer are below a Ca concentration of 0.005 (M) with just a few above this concentration. Figure 64 is a graph of Ca (M) vs. Mg (M) values for the glacial drift data with Ca (M) values lower than 0.005 (M). The data have a slope of 1.56 with a r^2 value of 0.742. The graph shows a tight cluster of points that plot, from the origin to approximately 0.0025 (M) Ca (M) and 0.0015 Mg (M), along a trend with a slope very similar to the calcite/dolomite equilibrium line. Above this point the data becomes more scattered.

Figure 65 is a graph of Ca (M) vs. Mg (M) for the MRW drift. The slope is 1.63 and the data have a r^2 value of 0.67. The graph shows a tight cluster of samples from the origin to a Ca concentration of 0.0025 and a Mg concentration of 0.0015. Figure 66 is a graph of Ca (M) vs. Mg (M) for streams within the Muskegon River Watershed. The slope of the data is 1.4 with a r^2 value of 0.65. All of the data plot well below the Ca concentration of 0.003. The calcite/dolomite equilibrium line appears to fit the data better than the congruent dissolution of dolomite line. The graph shows a cluster of samples up to a Ca concentration of 0.0025 and a Mg concentration of 0.0015. Figure 67 is a graph of Ca (M) vs. Mg (M) for lakes within the Muskegon River Watershed. The slope of the data is 1.4 with a r^2 value of 0.75. The samples plot below 0.002 Ca and 0.00125 Mg. The calcite/dolomite equilibrium line fits the data better than the dolomite congruent dissolution line. Figure 68 is a graph of Ca (M) vs. Mg (M) for wetlands

within the Muskegon River Watershed. The slope of the data is 1.58 with a r^2 value of 0.67. The MRW wetland samples plot below 0.0025 Ca and 0.00125 Mg. The samples appear to follow the calcite/dolomite equilibrium line more than the congruent dolomite dissolution line.

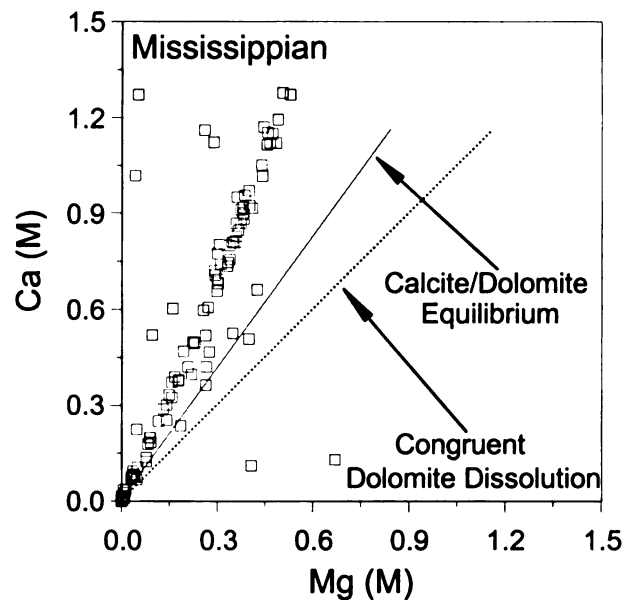


Figure 60. Graph of Ca (M) vs. Mg (M) for ground water samples within the Mississippiian bedrock. Data are from ground water data set (Dannemiller and Baltusis, 1990; Wahrer, 1993; Meissner, 1993).

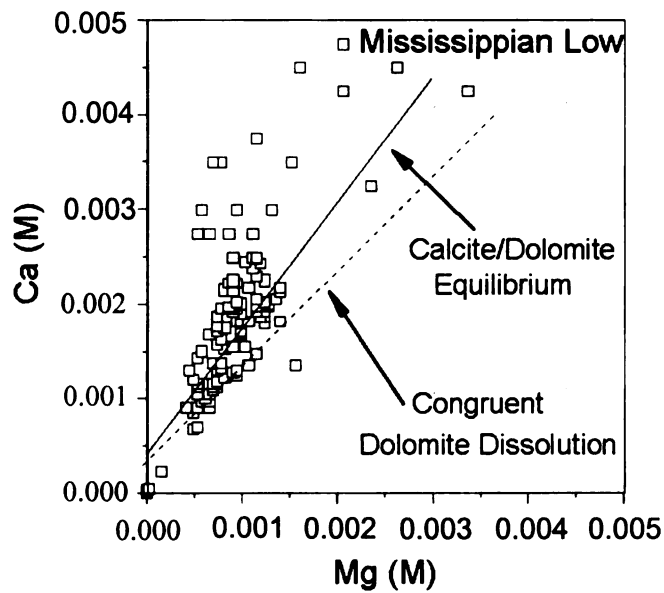


Figure 61. Graph of Ca (M) vs. Mg (M) for ground water samples within the Mississippiian bedrock with Ca(M) concentrations less than 0.005. Data are from ground water data set (Dannemiller and Baltusis, 1990; Wahrer, 1993; Meissner, 1993).

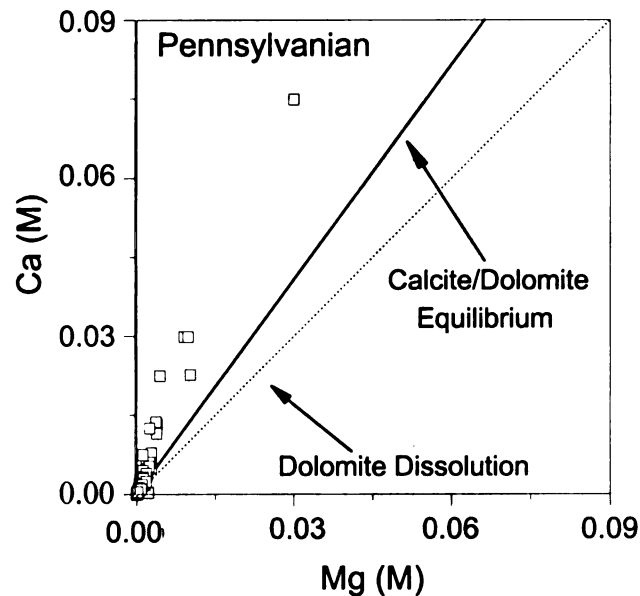


Figure 62. Graph of Ca (M) vs. Mg (M) for ground water samples within the Pennsylvanian bedrock. Data are from the ground water data set (Dannemiller and Baltusis, 1990; Wahrer, 1993; Meissner, 1993).

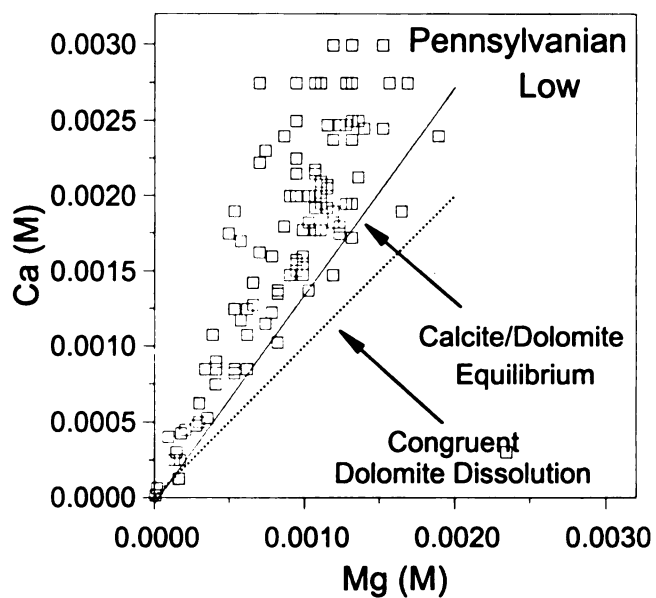


Figure 63. Graph of Ca (M) vs. Mg (M) for the Pennsylvanian with Ca (M) concentrations lower than 0.00032 (M). Data are from the ground water data set (Dannemiller and Baltusis, 1990; Wahrer, 1993; Meissner, 1993).

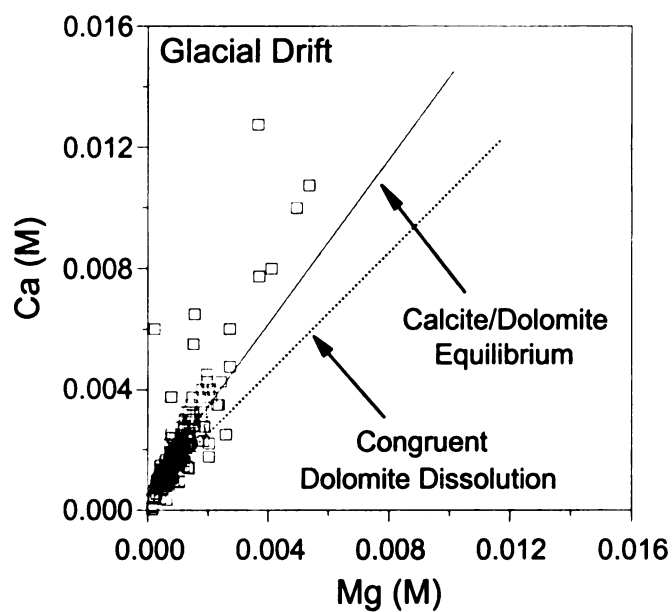


Figure 64. Graph of Ca (M) vs. Mg (M) for ground water samples within the glacial drift. Data are from the ground water data set (Dannemiller and Baltusis, 1990; Wahrer, 1993; Meissner, 1993).

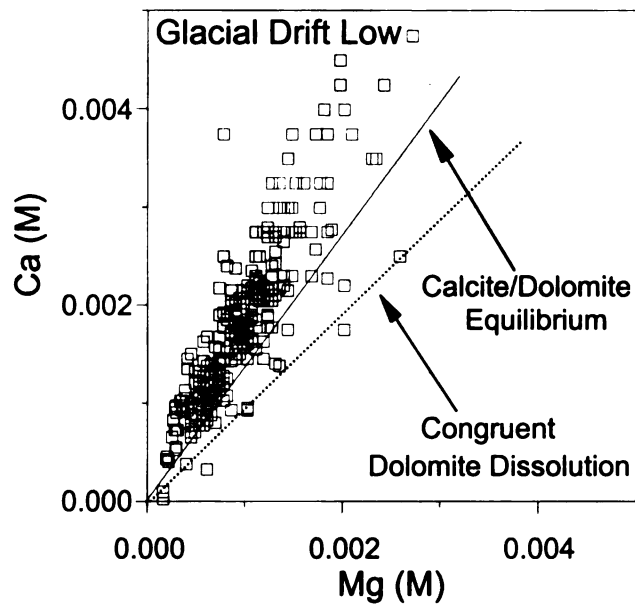


Figure 65. Graph of Ca (M) vs. Mg (M) for ground water samples within the regional drift with Ca concentrations below 0.005 (M). Data are from the ground water data set (Dannemiller and Baltusis, 1990; Wahrer, 1993; Meissner, 1993).

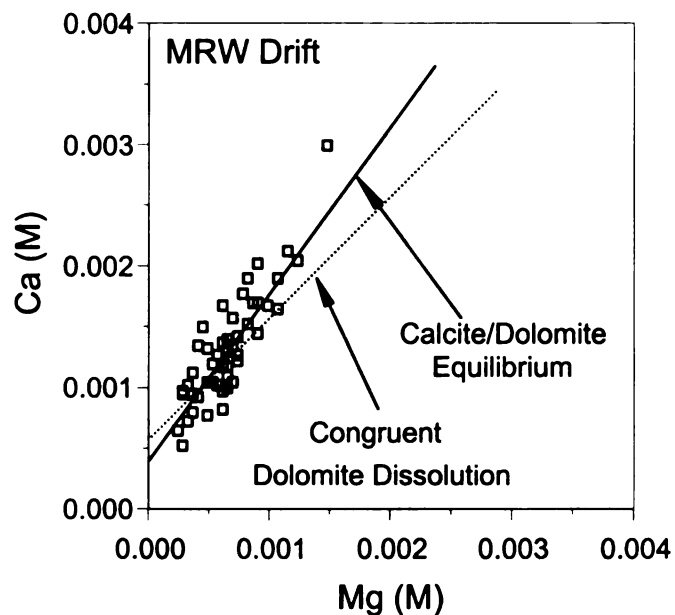


Figure 66. Graph of Ca (M) vs. Mg (M) for the Muskegon River Watershed buffered Drift. Data are from ground water data set (Dannemiller and Baltusis, 1990; Wahrer, 1993; Meissner, 1993).

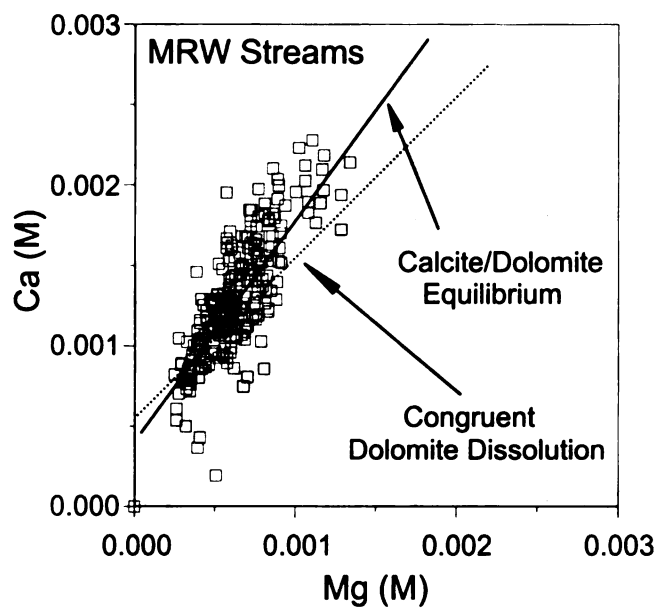


Figure 67. Graph of Ca (M) vs. Mg (M) for streams within the Muskegon River Watershed.

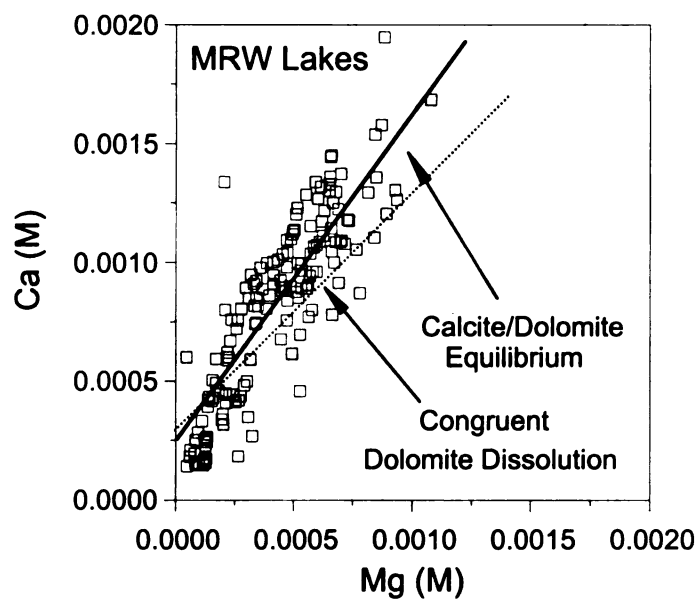


Figure 68. Graph of Ca (M) vs. Mg (M) for lakes within the Muskegon River Watershed.

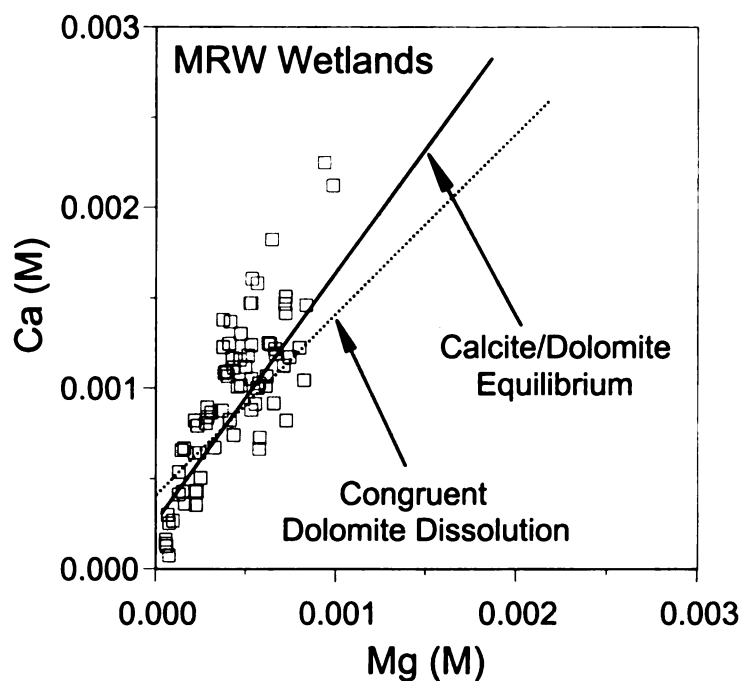


Figure 69. Graph of Ca (M) vs. Mg (M) for wetlands within the Muskegon River Watershed.

In general, the surface waters and drift waters plot along the line representing the equilibrium between calcite and dolomite than the bedrock waters. The bedrock waters plot with a slope that is significantly higher than the calcite dolomite equilibrium line.

The cluster of data points that represent streams (Figure 67) in the MRW plot up to 0.001 (M) Mg until the Ca (M) concentration exceeds 0.00175 (M). Once the Ca (M) concentration exceeds 0.00175 (M) the Mg (M) concentration can exceed 0.001 (M). The reason for this trend is unclear.

The amount of calcite/dolomite dissolution and therefore Ca concentrations in surface waters is controlled by dissolved carbon dioxide, and temperature. Rainwater entering into the ground has a partial pressure of $10^{-3.5}$ atmospheres for CO₂. However, as the rainwater percolates through the ground, it comes into contact with soil gases that are more concentrated in CO₂ than the rainwater; as a result, the rainwater absorbs more CO₂. The soil and unsaturated zone are enriched in CO₂ because of the degradation of organic matter and the respiration of plants (Hem, 1985). Water with more dissolved CO₂ can dissolve up more calcite than water with less CO₂ (Drever, 1997). As a result, the water with more dissolved CO₂ will have more dissolved calcite in it than the water with less dissolved CO₂. However, when the ground water enters into the surface water domain, ground water has more dissolved CO₂ in it than the atmosphere, it then comes into contact with the atmosphere and loses CO₂, due to Henry's Law. The pH of the water increases and as a result the mixed water may become supersaturated with respect to calcite. The water may then start to precipitate calcite. Degassing of CO₂ may also occur by the agitation of water. Water emerging as springs into streams will flow downstream and encounter turbulence. The turbulence will speed up the amount of CO₂ out gassing and as a result encourage the precipitation of CaCO₃ (Herman and Lorah, 1987). Dissolved CO₂ can also be removed through photosynthesis. Photosynthesis has

been used to explain an increase in the calcite saturation indices of lakes. The photosynthetic organisms uptake the CO_2 and as a result, the Ph of the water increases. This, in turn, makes the water more supersaturated with respect to calcite. (Effler, 1984; Effler et al., 1981; Effler et al., 1982). The amount of CO_2 consumed in the lake varies seasonally with the greatest variation found in the most productive parts of the lake (Effler, 1984). The highest calcite saturation occurs in the warm summer months (Effler, 1984; Effler et al., 1985). In a Ca polluted lake in New York, Effler et al. (1985) correlated particulate Ca deposition to primary productivity. It is primary productivity that removes the CO_2 from the water.

The paragraph above states the different mechanisms that could remove or add Ca to water. If the assumption is made that Mg is conservative and the Ca/Mg ratio of ground water entering the surface water is constant, then the amount of calcium removed or added to the water should be noticeable within the Ca/Mg ratio or slope of the graph.

The fact that the bedrock waters plot with a steeper slope than the surface waters is to be expected from the explanation above. However, the fact that the MRW drift waters and the surface waters plot with a very similar slope is not to be expected. The MRW Drift water (Figure 66) should theoretically plot with a significantly steeper slope due to the precipitation of calcite that should occur in surface water conditions. The bedrock aquifers as well as the regional drift aquifer graphs of Ca vs. Mg have steeper slopes than the surface water graphs. Therefore, it does not appear that a significant amount of

calcite precipitation is occurring between the drift and the surface waters. If precipitation was occurring then the slope should be less in the surface waters than in the drift waters.

Summary

The Na/Cl (M) histograms revealed that the surface waters and the drift waters in the MRW have Na/Cl (M) ratios that can be explained by the dissolution of halite, oilfield brines, and treated sewage/septic. Alternatively, the Na/Cl (M) ratios found in the surface waters and drift waters could be explained by the upwelling of saline water from the Pennsylvanian and Mississippian formations as well as plagioclase dissolution/atmospheric precipitation. The histograms of surface waters within the MRW (i.e., lakes, wetlands, streams) do not show many samples that plot with a Na/Cl (M) ratio that would be consistent with treated sewage/septic and/or plagioclase dissolution/atmospheric precipitation. Samples in the MRW surface waters tend to plot in the oilfield brine and halite dissolution regions of the histograms. The SBW watershed, one in which it is suspected that saline waters are upwelling and interfering with the shallow aquifer, shows that the Na/Cl (M) histograms for the Pennsylvanian, the bedrock unit underlying the SBW, and the SBW drift are very similar. However, the SBW streams are more shifted towards lower Na/Cl values when compared to the SBW drift and the Pennsylvanian. The MRW drift and the MRW lakes have very similar distributions, however the MRW streams plot more into the halite dissolution range of Na/Cl (M) values. The SBW drift samples plot in the range consistent with halite dissolution, or possibly from the Pennsylvanian bedrock aquifer. However, the MRW drift plots more in the oilfield brine region, or the Marshall region. The fact that the

MRW drift plots in the region consistent with the water from the Marshall, and the fact that the MRW drift in some locations overlies the Marshall, is consistent with the brine upwelling theory.

The distributions of samples on logarithmic Na vs. Cl charts are different for surface waters and drift waters. The MRW drift shows more scatter in the lower Na and Cl values than the surface waters. The scatter at low Na and Cl concentrations found in the MRW drift are similar in shape to the other SBW drift, glacial drift, and bedrock water. However, the MRW drift does not have as highly concentrated Na and Cl samples that these other regions have. The scatter at the low Na and Cl values is probably due to plagioclase dissolution and atmospheric precipitation. The surface waters in the MRW cluster around the halite dissolution line. This would support the alternative hypothesis that the source of Cl in the MRW is halite and not the upwelling of saline waters in bedrock layers below. However, care must be taken in this interpretation because although the ground waters have more scatter at low Na and Cl values than surface waters their samples become more and more similar with increasing Na and Cl values. The fact that the MRW drift and the MRW surface waters are different at the low Na and Cl concentrations only points to differences in the origin of Na and Cl in samples with low concentrations of Na and Cl and not samples at higher levels of Na and Cl. The fact that halite dissolution and the seawater evaporation line are parallel in slope shows that the two are indistinguishable till Na and Cl concentrations are high enough in seawater to allow for halite precipitation. Therefore halite dissolution maybe the source of Cl at lower concentrations in surface waters however, at higher concentrations it maybe brines.

The source of brines is probably coming from the surface because if it were from the bedrock layers below the Na and Cl values for surface waters, even at low concentrations of Na and Cl, would be more similar to the low Na and Cl concentrations from bedrock layers below. If brines were applied on the surface such as brining of roads or disposal of brines in pits during oil and gas exploration then just the high Na and Cl samples from the bedrock layers would be shown. It was shown in the histograms that many of the surface waters have Na/Cl (M) ratios consistent with oilfield brine. These same samples were plotted on the logarithmic charts and although it can be seen that many samples plot slightly below the halite dissolution line, consistent with an oilfield brine, the logarithmic chart do not express the slight differences in Na and Cl concentrations to the degree needed to confidently determine whether the water has Na and Cl concentrations within the range of an oilfield brine or the dissolution of halite. Therefore the trend in the surface waters may be either from halite dissolution or from oil and gas exploration.

The plots of Ca (M) vs. Mg (M) reveal that the bedrock drift ground water and the regional drift ground water in general have more dissolved Ca with respect to Mg than the surface waters and drift within the MRW. The surface waters and the samples from the Mississippian, samples with Mg (M) concentrations less than 0.001 (M), plot with a similar slope to that of the calcite/dolomite equilibrium line. This is evidence that Ca and Mg are controlled by the equilibrium between calcite and dolomite. All of the different waters tested showed a cluster of samples below 0.001 (M) Mg. Points with concentrations above approximately 0.001 (M) Mg tend to be more spread out than what is below 0.001 (M) Mg. The reason for this is unknown. However, it does suggest that

the processes controlling the concentrations of Ca and Mg are different after 0.001 (M) Mg. It also suggests that processes controlling Ca and Mg concentrations are similar to those occurring within the bedrock, the drift, as well as surface waters.

Chapter 5

Piper diagrams

Introduction

Piper diagrams are useful for determining if the water observed is from one source or mixture of two distinct sources. The Piper diagram can also be used to classify natural waters. The Piper diagram is composed of a cation triangle, an anion triangle, and a quadrilateral. The cation triangle shows the relative proportions of the major cations in water (i.e., Ca, Mg, Na+K). The anion triangle shows the relative proportions of major anions in water (i.e., Cl, SO₄, HCO₃). The quadrilateral combines the information on the cation and anion triangle. A point on the quadrilateral is made by drawing a line from a sample point on the cation triangle, parallel to the Mg axis, up into the quadrilateral. The same sample used to draw the line on the cation triangle is found on the anion triangle and used to draw a line parallel to the SO₄ axis into the quadrilateral. The location where the two lines intersect on the quadrilateral represents the anion and cation chemistry of that sample. Water can be classified based on the relative proportions, in equivalents/Liter, of the major ions (i.e., Cl, SO₄, HCO₃, Ca, Mg, and Na+K) (Figure 70). The data points will plot in areas that represent the dominant major ions if a dominant ion exists. A dominant ion exists if that ion contains more than 50 percent of the total major cations or anions (Drever, 1997). The classification of that water (hydrochemical facies) is composed of the name of the dominant cation and anion if one or both exist (Figure 70).

If the water being tested is the result of two chemically distinct waters mixing, a straight line (this line is called a tie line) comprising the different data points will be shown in the cation and anion triangle of the Piper diagram (Figure 70). If a straight line does form from the data points, it is not conclusive that the water being studied is the result of two waters mixing; however it strongly suggests it (Drever, 1997). An end member is water that has not mixed with the other water. Samples of end member waters may or may not have been taken however, the mixing line that is the result of two end members mixing indicates that the two end members exist. If any samples of either end member were taken these samples should plot at either end of the tie line. The samples that are the result of mixing of these two end members should plot between these points on the line.

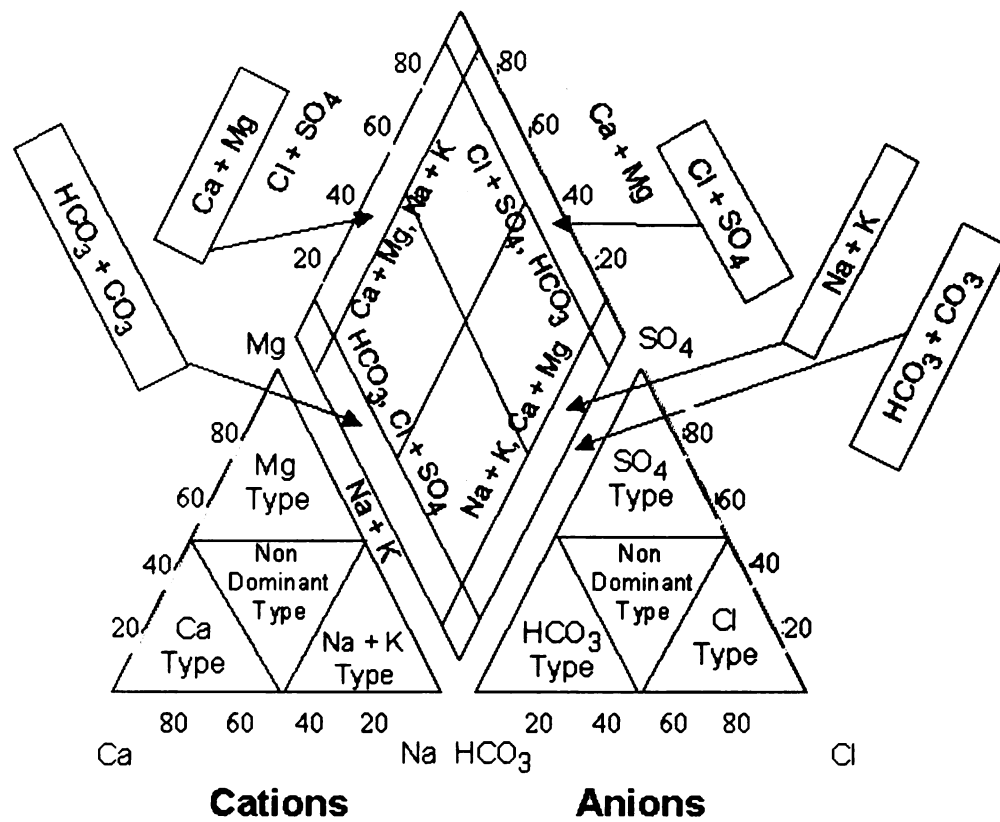


Figure 70. Piper diagram showing the different hydrochemical facies (Piper, 1944; Drever, 1997).

Excess Cl has been found in the shallow aquifer in Bay County. It has been hypothesized by Long et al. (1988) that the source of the saline waters to the drift aquifer are the bedrock layers below. Bay County is underlain by the Pennsylvanian, which contains saline waters as well as fresh waters. Badalamenti (1992) noticed that there was a linear trend between surface waters in Bay County and brines (Marshall, Berea, and Dundee Formations) in the Michigan Basin, and that this suggested that there was mixing between the two systems. The Pennsylvanian lies above the Mississippian and is the lower most aquifer in contact with the glacial drift in the Saginaw Bay Watershed and Bay County regions. The MRW is underlain by both the Pennsylvanian and the Mississippian bedrock. Both of these aquifers contain saline waters. If the MRW is experiencing the same upwelling as Bay County, the Piper diagrams should show the same trends as Bay County and the bedrock aquifers below it.

Piper Diagrams

Figure 71 is a Piper diagram of the Pennsylvanian bedrock unit. Meissner (1993) has described the Pennsylvanian as having three principle hydrologic facies. The principle hydrochemical facies for the Pennsylvanian bedrock and unit by Meissner (1993) are Ca-HCO₃, Ca-SO₄, and Na-Cl. Figure 71 shows a trend in the cation triangle from Ca dominant end member to a Na+K dominant end member water. The anion triangle shows two different trends. One of the trends runs from HCO₃ dominant end member to a Cl dominant end member. The other trend runs from HCO₃ dominant end member to a SO₄ dominant end member.

Figure 72 is a Piper diagram of the Mississippian. A trend is present on the cation triangle between a Ca rich end member and a Na+K rich end member. The trend runs across the entire cation triangle. The trend in the anion triangle runs from the HCO_3 end member to a Cl end member. The dominant hydrochemical facies are Ca- HCO_3 and Na+K-Cl.

Figure 73 is a Piper diagram of water in the glacial drift. The cation triangle shows a trend that runs at an angle between a Ca end member and a Na+K end member water. The anion triangle shows a trend between a HCO_3 end member and a SO_4 end member water and another trend that runs from the HCO_3 dominant end member to a Cl dominant end member water.

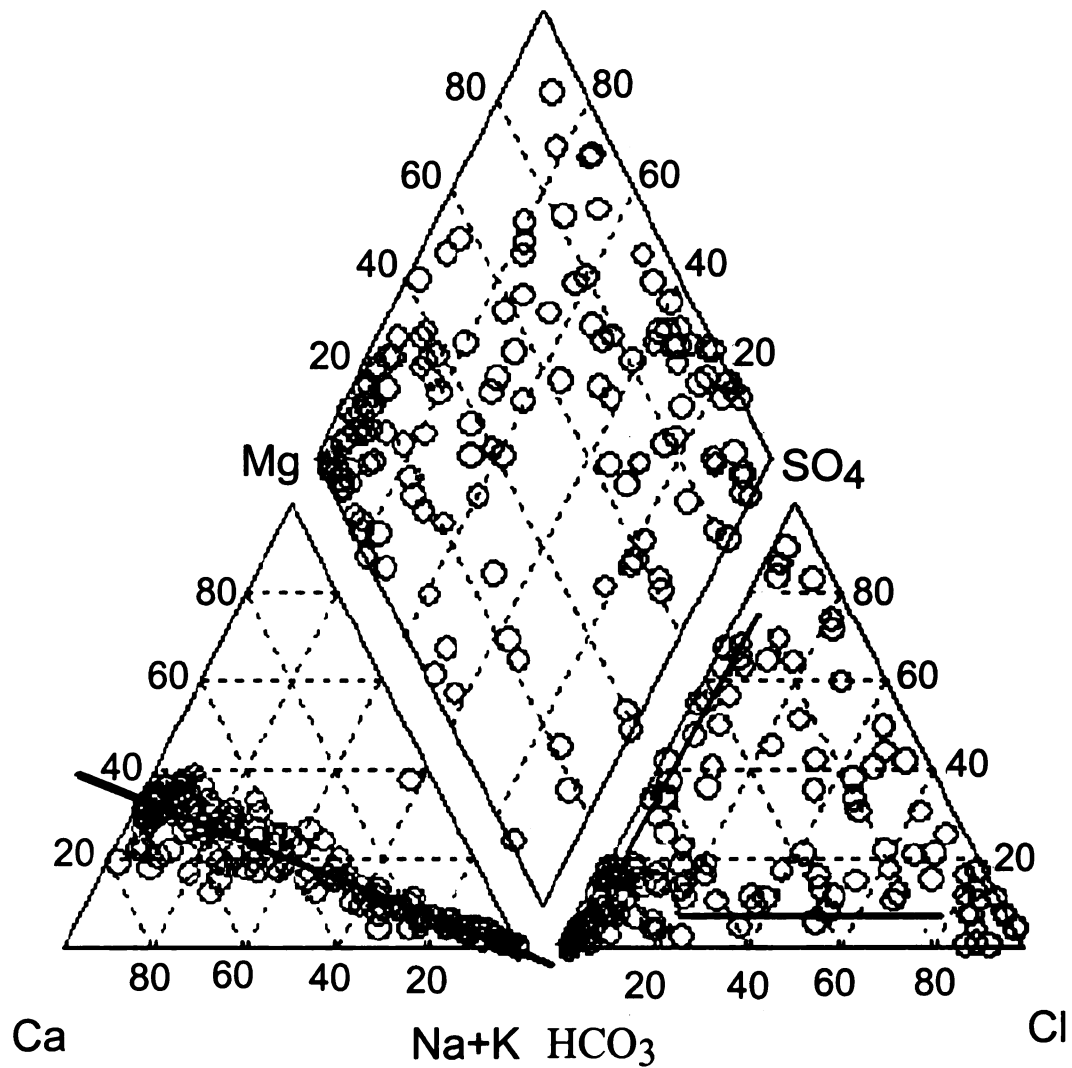


Figure 71. Piper diagram of the ground water in the Pennsylvanian bedrock. Data are from ground water data set (Dannemiller and Baltusis, 1990; Wahrer, 1993; Meissner, 1993).

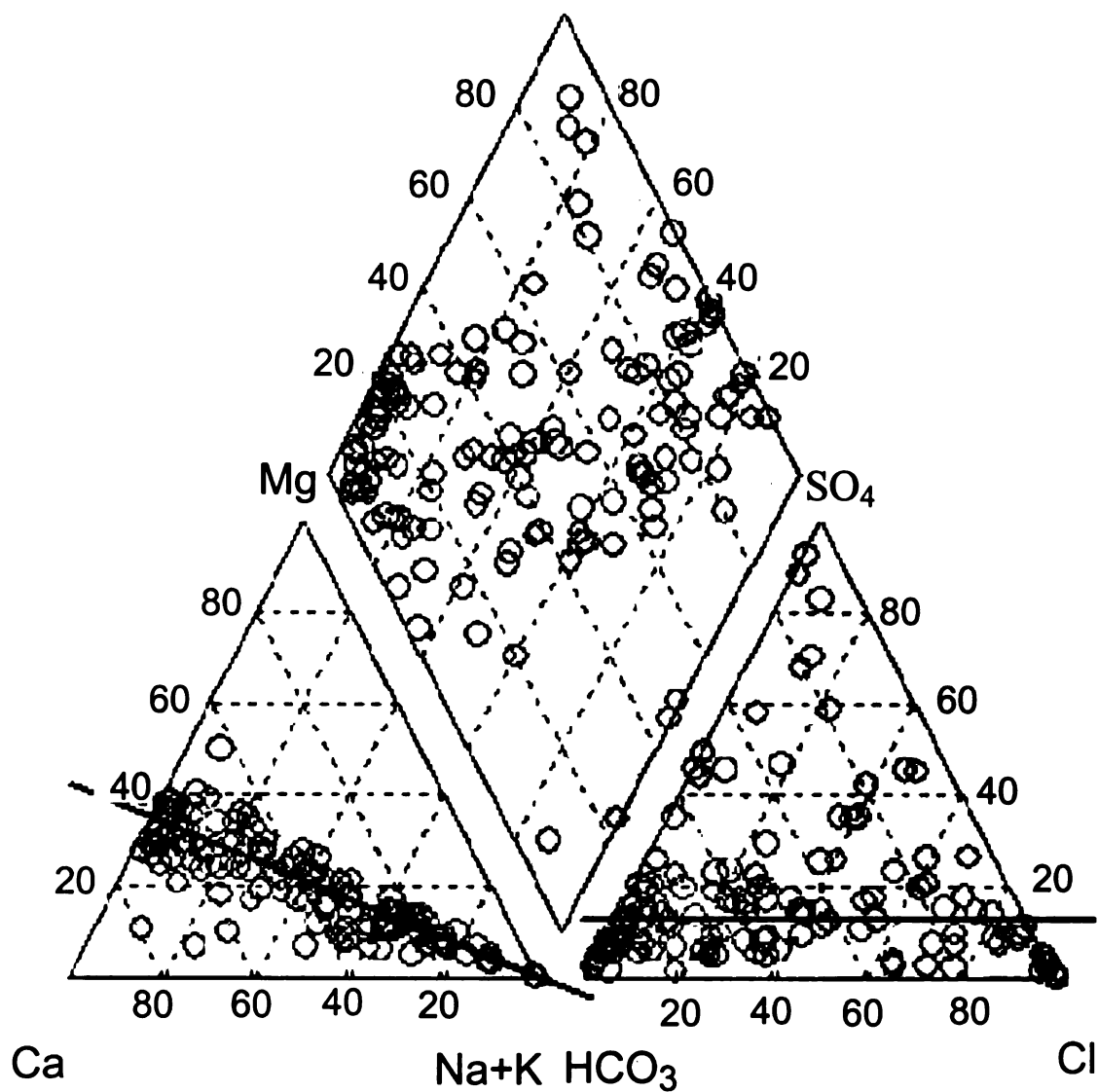


Figure 72. Piper diagram of the ground water in the Mississippian bedrock. Data from the ground water data set (Dannemiller and Baltusis, 1990; Wahrer, 1993; Meissner, 1993).

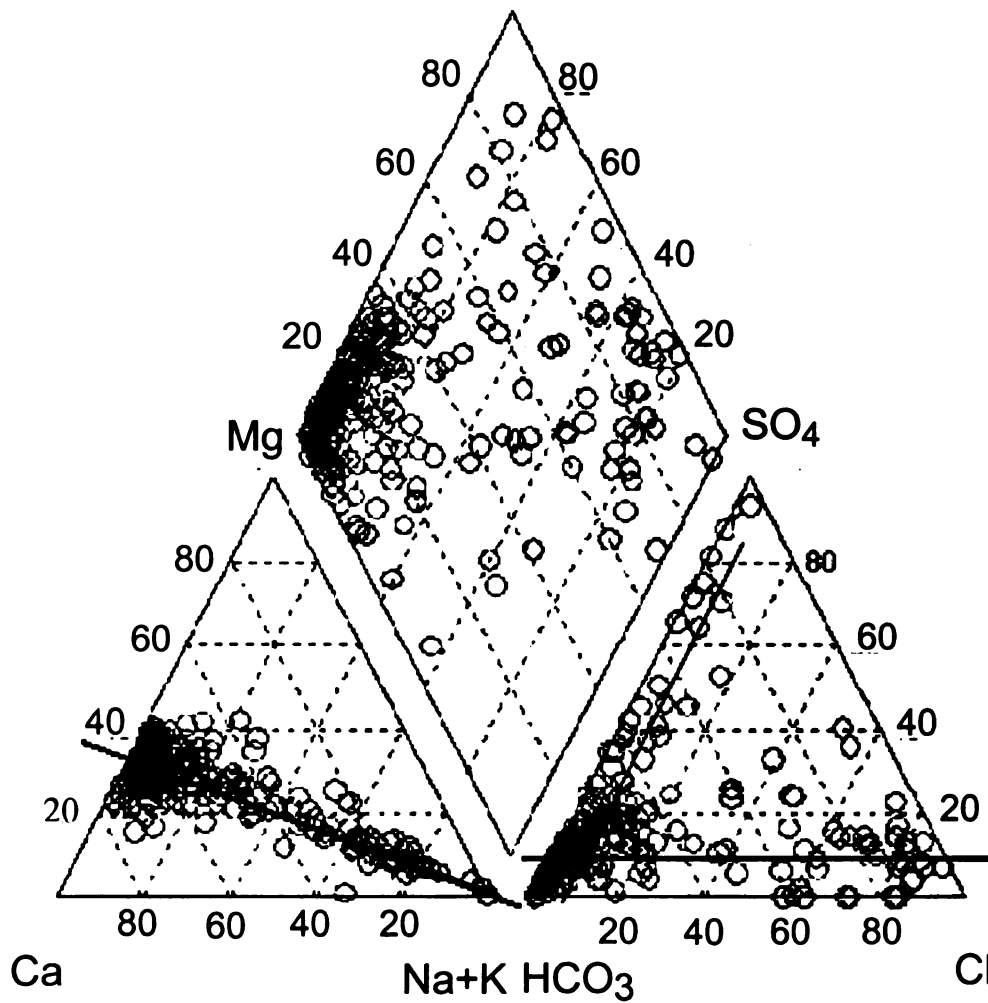


Figure 73. Piper diagram of the ground water in the glacial Drift. Data are from the ground water data set (Dannemiller and Baltusis, 1990; Wahrer, 1993; Meissner, 1993).

Figure 74 is a Piper diagram of the drift ground water within the Muskegon River Watershed. The cation triangle shows a trend that is for the most part clustered around the Ca end of the cation triangle but tapers off towards the Na+K end of the triangle. The anion triangle shows a trend from the HCO_3 end of the triangle toward the Cl end of the triangle. The most common type hydrochemical facies within the MRW would be a Ca- HCO_3 type with some amount of Na+K-Cl type water. The ground water within the Muskegon River Watershed can be described as dominantly Ca- HCO_3 facies.

Figure 75 is a Piper diagram of the ground water samples within the glacial drift of the Saginaw Bay Watershed. There is a trend in the cation triangle that runs between a Ca end member water and a Na+K dominant end member water. The anion triangle shows a trend between a HCO_3 end member and a Cl end member. The anion triangle has another trend that runs between the HCO_3 end of the anion triangle and the SO_4 dominant end of the triangle.

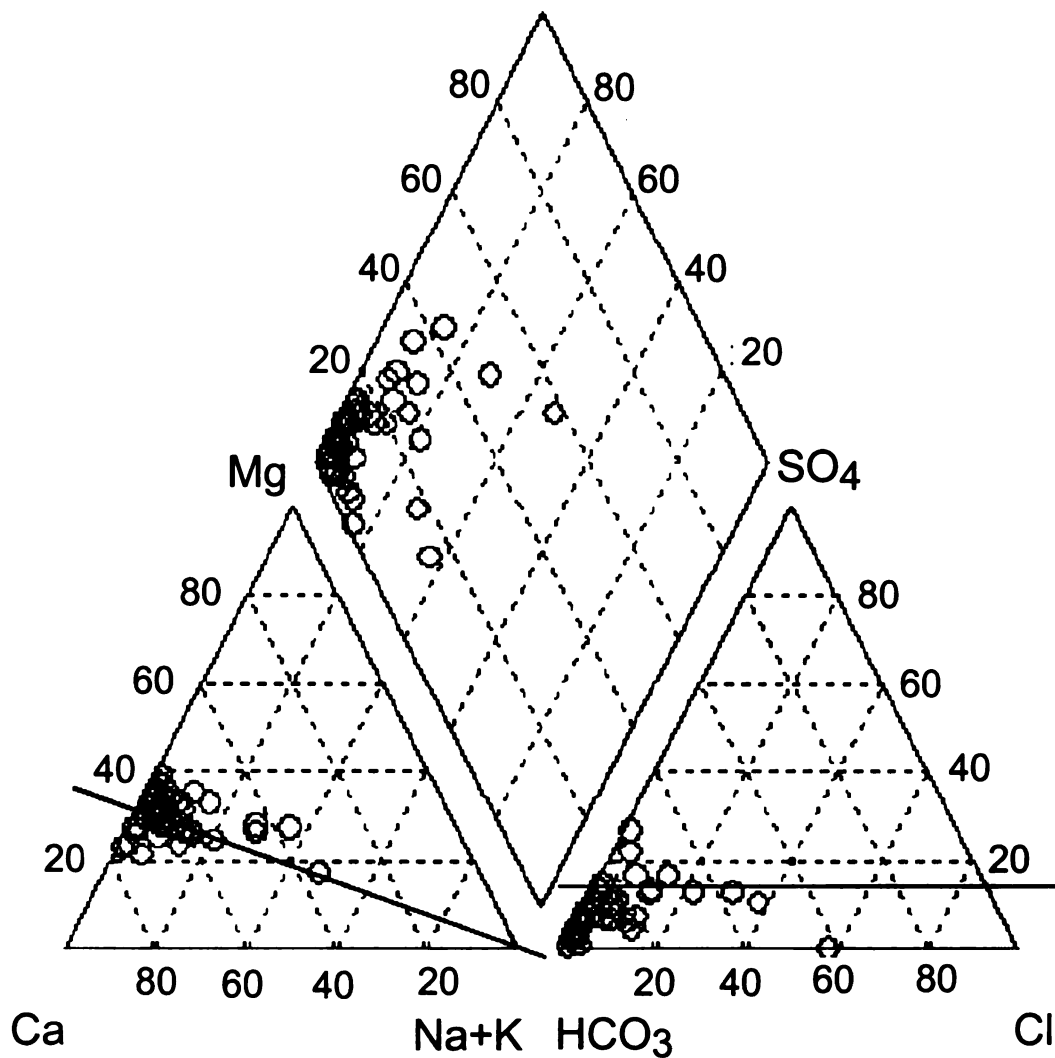


Figure 74. Piper diagram of ground water samples within the buffered region Muskegon River Watershed Drift. Data are from the ground water data set (Dannemiller and Baltusis, 1990; Wahrer, 1993; Meissner, 1993).

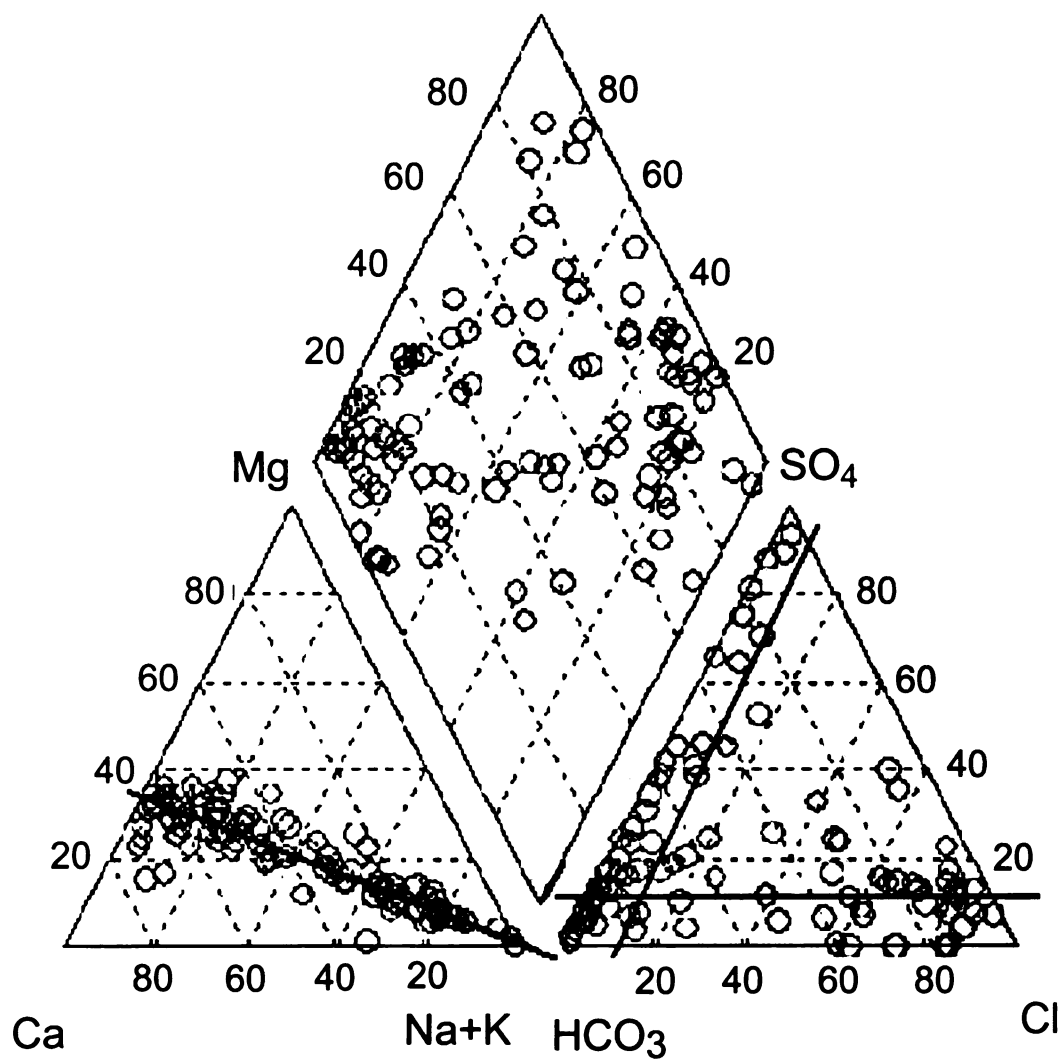


Figure 75. Piper diagram of ground water samples within the glacial drift of the Saginaw Bay Watershed. Data are from the ground water data set (Dannemiller and Baltusis, 1990; Wahrer, 1993; Meissner, 1993).

Figure 76 is a ternary diagram of the stream waters within the Saginaw Bay watershed. Kolak (2000) took the stream samples at base flow. He observed a mixing trend between samples that plot in the Ca dominant end of the ternary diagram and the samples that plot towards the Na+K end of the ternary diagram. Kolak (2000) interpreted that this trend may be the result of saline waters in the glaciofluvial aquifer entering into the surface waters. There appears to be two trends in the ternary diagram; one of the trends runs horizontally across the ternary diagram. The other trend runs between the Ca end and the Na+K end of the trilinear diagram.

Figure 77 shows the stream water data within the MRW. Most of the samples plot in the Ca dominant end of the cation triangle. However, some of the samples plot in the nondominant and the Na+K dominant areas. A trend line can be drawn showing the transition from a Ca dominant water to a nondominant water and then to a Na+K dominant water. The anion triangle shows a trend between the HCO_3 end of the triangle and the Cl end of the triangle. The anion triangle shows a trend that runs between the HCO_3 corner of the triangle toward the SO_4 and Cl side of the triangle. If this line were projected it would intersect at approximately equal equivalents of SO_4 and Cl. This trend line passes through the stream sites that are downstream of the Muskegon County Wastewater Disposal System and may as a result show reveal other streams that are influenced by sewage as well. In general, streams in the MRW watershed can be

classified as fitting within the Ca-HCO_3 hydrochemical facies. One sample did plot within the Na+K-Cl facies.

Figure 78 shows the lake water data within the MRW. The lake data show a trend in the cation triangle that runs horizontally between 20 and 40 percent equivalents Mg. The samples taken from the lakes tend to plot within the Ca dominant end of the cation triangle. The anion triangle of the Piper shows a trend that runs between the Cl dominant end of the triangle and the HCO_3 end of the triangle. The lakes in the MRW can be classified as a Ca-HCO_3 type water.

Figure 79 shows a Piper diagram for wetlands within the MRW. Although most samples in the cation triangle plot in the Ca dominant end, some plot in the nondominant region and the Na+K region of the triangle. The samples that plot in these different regions form a trend line across the cation triangle from the Ca dominate region to the Na+K dominant region. Most samples on the anion triangle plot in the HCO_3 dominant end of the triangle; however, some plot in the nondominant region and the Cl dominant region. The samples that plot in these different regions form a trend line between a HCO_3 dominant water to a Cl dominant water. The Power Plant Pond samples plot the closest to the Cl vertex of the anion triangle, and reveals that the Power Plant Pond has the highest equivalent percentage of anions of all of the wetlands tested. It also plots closest

to the Na+K vertex of the anion triangle. The wetlands are for the most part Ca-HCO₃

type water; however, two samples were Na+K-Cl type water.

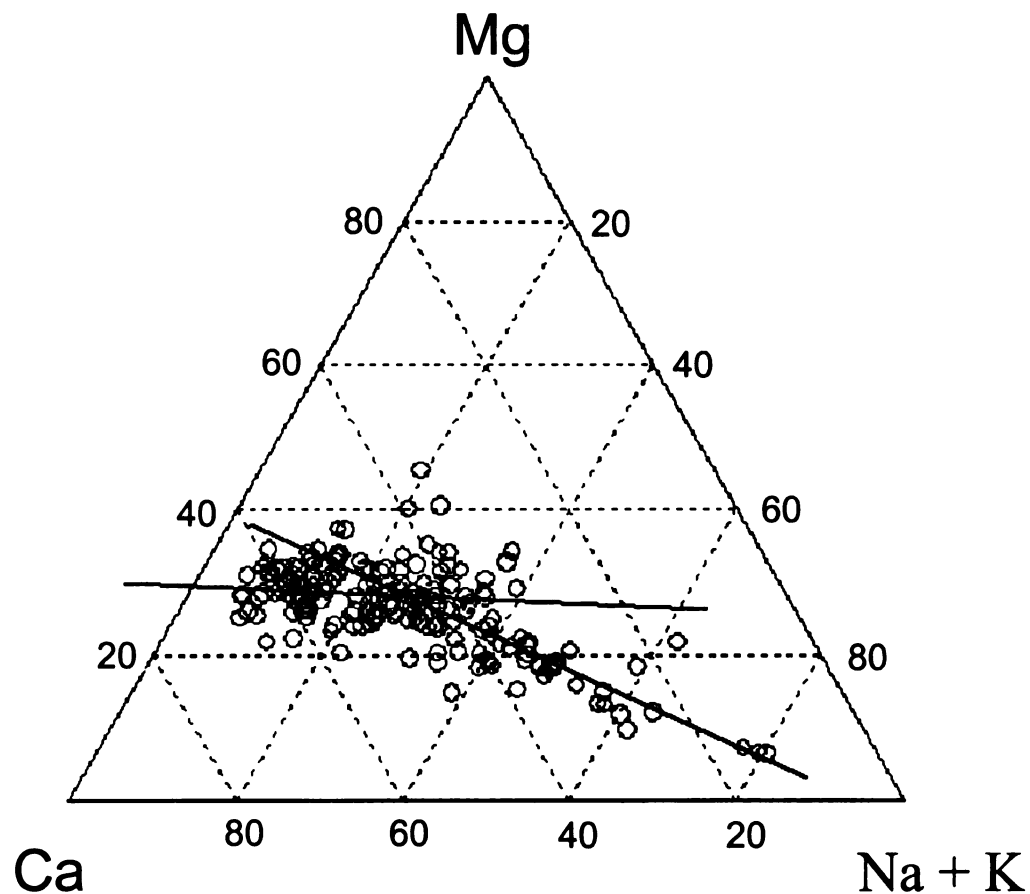


Figure 76. Ternary Diagram for base flow river data from the Saginaw Bay Watershed. The data were modified (i.e. lake data removed) from the RIV3 data set from Kolak (2000).

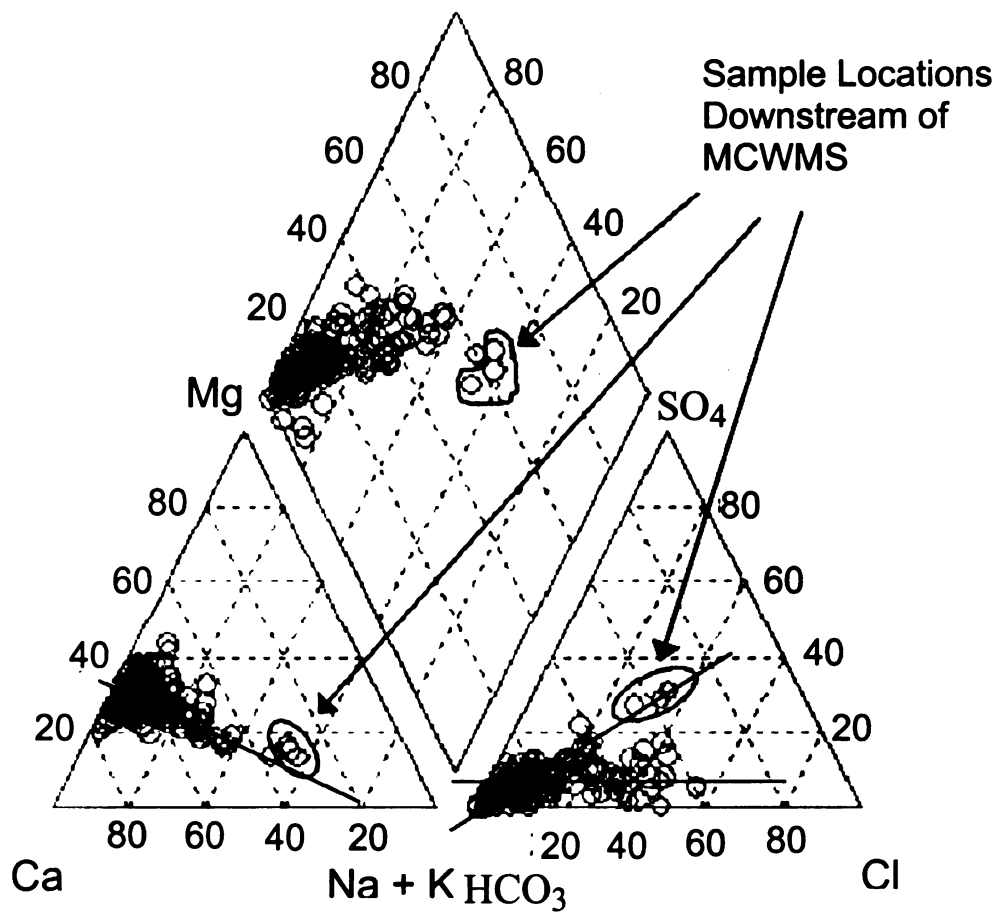


Figure 77. Piper diagram of the stream water within the Muskegon River Watershed. The data points in which sewage were expected to influence the stream water were circled.

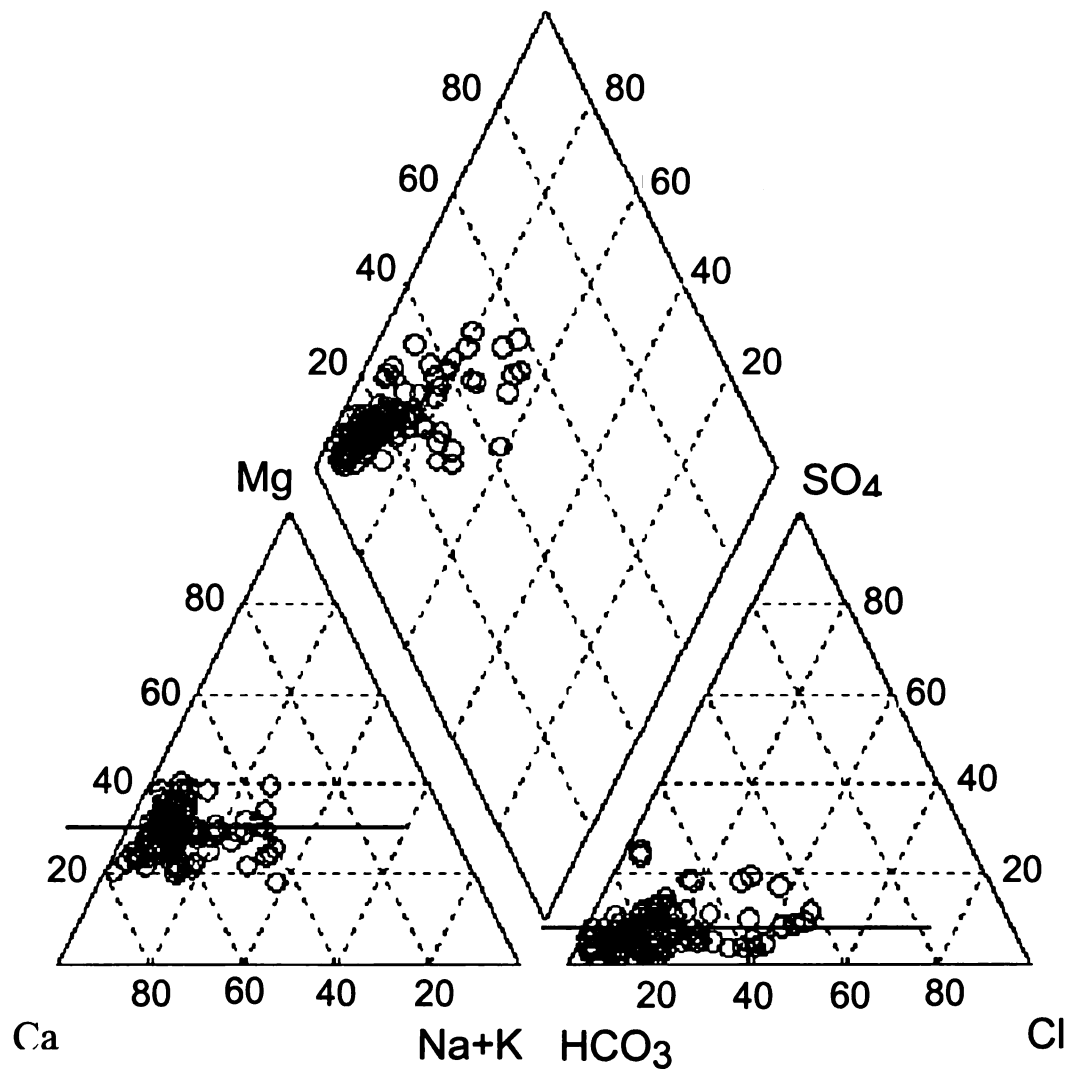


Figure 78. Piper diagram of lake water within the Muskegon River Watershed.

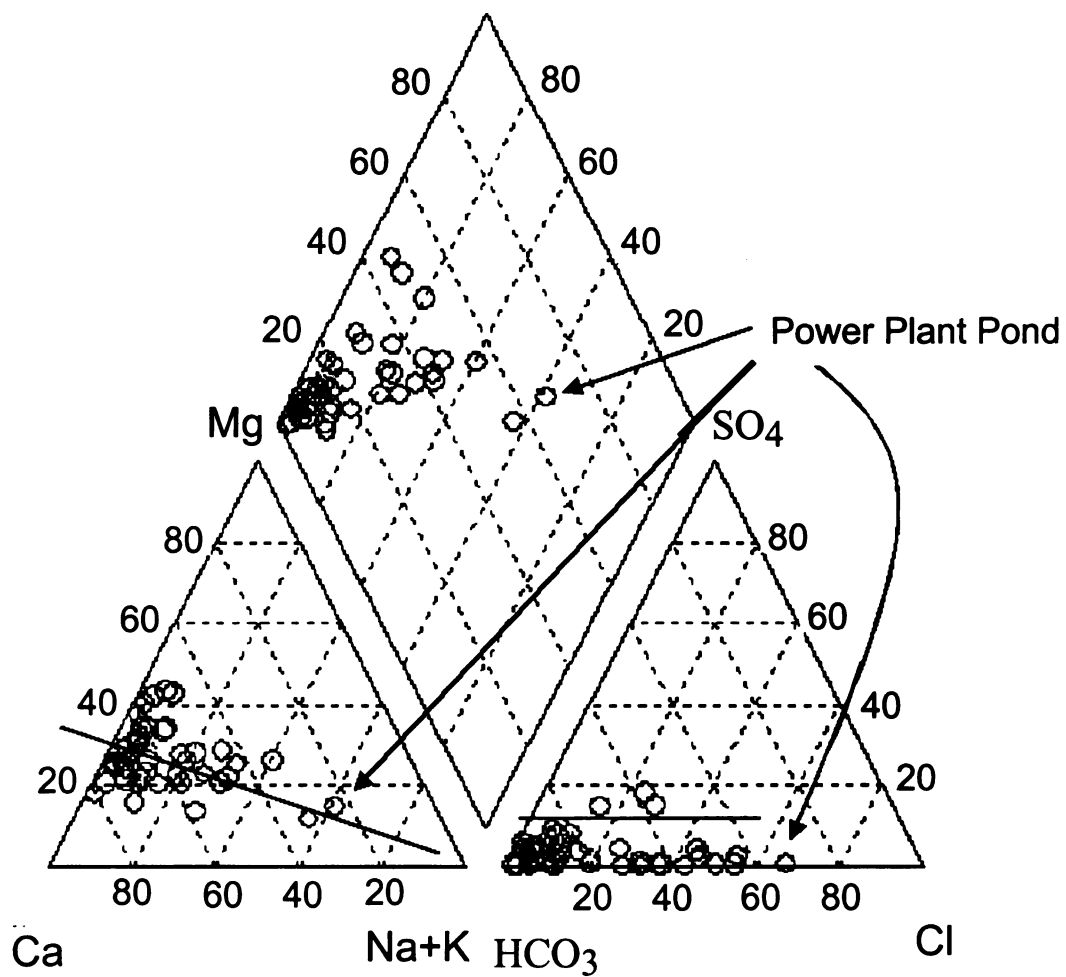


Figure 79. Piper diagram of wetland water within the Muskegon River Watershed.

Summary

The Piper diagrams for water in the Mississippian bedrock (Figure 72), Pennsylvanian bedrock (Figure 71), glacial drift (Figure 73), MRW drift (Figure 74), SBW drift (Figure 75), MRW streams (Figure 77), and MRW wetlands (Figure 79) show a similar trend in the cation triangle. The trend runs between the Ca dominant end of the cation triangle and the Na+K dominant end. Although the trend is similar between these different domains the placement of the points along this trend are different. The MRW Drift and MRW streams tend to plot much closer to the Ca dominant corner of the cation triangle while water in the Mississippian bedrock, Pennsylvanian bedrock, regional drift, and the SBW drift have more samples dispersed along the Ca/Na+K trend in the triangle. The MRW lakes show a single trend in the cation triangle that can be drawn horizontally across the triangle between 20 and 40 percent equivalents of Mg. The glacial drift (Figure 73), SBW drift (Figure 75), and the Pennsylvanian (Figure 71) bedrock water show two trends in the anion triangle. One trend runs between a HCO_3 dominant region and the Cl dominant region and the other runs from the HCO_3 dominant region and the SO_4 dominant region. The MRW streams also shows a second trend in the anion triangle but it is a different trend than any of the other anion trends. It runs between the HCO_3 corner toward the Cl- SO_4 side of the anion triangle, at a trajectory that if extended to the Cl- SO_4 side of the anion triangle would intersect it at approximately 50 percent Cl and SO_4 .

The Pennsylvanian (Figure 70), regional drift (Figure 72), and SBW drift (Figure 75) also have a trend in the anion triangle that runs between the HCO_3 corner of the anion triangle and the SO_4 corner of the anion triangle. The MRW stream cation trend that runs from the Ca dominant end of the triangle toward the Na+K end of the triangle runs through the samples that are downstream of the MCWMS. The MRW stream anion trend that can be projected toward equal equivalents of SO_4 and Cl also runs through the samples that are downstream of the MCWMS. If the MCWMS is a good representation of the treated sewage signal than if other hydrologic domains are influenced by treated sewage they should have similar trends in their respective Piper diagrams. Other surface waters and ground waters have a trend running from the Ca dominant corner of the cation triangle toward the Na+K dominant corner. The other waters do not have a similar trend in the anion triangle. This suggests that the other hydrologic domains are not influenced or not as influenced as streams are to treated sewage. The samples taken in the MRW, whether they are drift water or surface water, all show that the water in the MRW is for the most part Ca- HCO_3 facies. A Piper diagram of the drift water samples within the Saginaw Bay Watershed (Figure 75), the watershed that contains Bay County the county in which Long (1988) determined that the hydrologic characteristics were favorable for deep fluids to mix with near surface ground waters, shows a dramatic shift towards a higher percentage of Na+K. The water can be classified for the most part as Na+K-Cl facies water. The Saginaw Bay Watershed streams (Figure 76) appear to be shifted towards higher Na+K than the MRW samples. The Saginaw Bay Watershed ground water data (Figure 75)

have the same mixing trend for the cation triangle as the bedrock Piper diagrams have. The ground water feeding the stream water may be the result of saline waters in the bedrock upwelling and mixing with fresh water near the surface. The MRW surface waters and for the most part ground waters tend to be almost exclusively in the Ca-HCO₃ hydrochemical facies. The MRW ground water, MRW streams and MRW wetlands all have the same trend in the cation triangle, one that is dominantly in the Ca dominant corner of the triangle and is skewed toward the Na+K dominant corner of the triangle. The lakes (Figure 78) do not have the trend in the cation diagram that goes toward the Na+K corner of the Piper diagram. The lakes have a trend that runs horizontally through the cation triangle of their respective Piper diagrams. These trends show that the waters vary in Na+K and Ca but have a range of 20 to 40 percent equivalents for Mg on the cation triangle. The fact that the MRW streams, MRW Drift, and MRW wetlands have similar trends show evidence that supports the idea that they are all interconnected. The fact that the MRW lakes do not share the same trend is evidence that the processes occurring in the lakes may be significantly different than those in the wetlands, ground water, and streams. The Piper diagrams for the bedrock ground water (Mississippian and Pennsylvanian) show similar trends to the Piper diagrams for the MRW streams, MRW wetlands, and MRW Drift. The glacial drift waters in regions that are suspected to have saline waters (i.e., SBW drift) interfering in near surface waters have similar trends in their Piper diagrams. One difference between the MRW and the SBW ground waters is the amount of SO₄. The SBW ground waters appear to have a higher percentage equivalents of SO₄ than waters in the MRW. The bedrock aquifers, which represent the

regional bedrock, signal also have a higher percentage of sulfate than the waters in the MRW. This would suggest that processes occurring in the Drift ground water in the MRW and the SBW as well as the ground water in the bedrock are in fact different at least with respect to sulfate. The surface waters in the SBW and the MRW can only be compared to by cation diagram because the surface water data for the SBW does not have enough anion data to make a Piper diagram.

The fact that the $\text{Ca}/\text{Na}+\text{K}$ trend in the cation triangle and the HCO_3/Cl trend in the anion triangle in the MRW drift, MRW streams, and MRW wetlands are similar in direction as the bedrock water, and the SBW drift water (the SBW is a region suspected to have brine upwelling occurring within it) is consistent with the hypothesis that the excess Cl in the MRW is from saline waters upwelling from the bedrock layers below and mixing with the shallow drift aquifer in the MRW and eventually influencing the MRW surface waters. However, the samples that make up the $\text{Ca}/\text{Na}+\text{K}$ trend in the cation triangles of the piper diagrams of the MRW drift, MRW streams, and MRW wetlands, in general, plot much closer to the Ca end of the anion triangle than the SBW drift, SBW streams (trilinear diagram), Pennsylvanian bedrock water, and the Mississippian bedrock water. The HCO_3/Cl trend in the MRW drift, MRW streams, and MRW wetlands, in general, plot much closer to the HCO_3 end of anion triangle than the SBW drift, Pennsylvanian bedrock water, and the Mississippian bedrock water. This weakens the hypothesis that the excess Cl found in the surface waters is from brine upwelling since the region in which brine upwelling is suspected to occur although similar in direction of trends is

different in the extent to which the samples are found along the trend. Other sources of Cl to the watershed such as sewage and septic samples could also increase the concentration of Cl in a watershed. The stream samples taken downstream of the MCWDS are circled on the MRW streams Piper diagram. These samples show that they plot along the Ca/Na+K trend, however on the anion trend these samples do not plot along the HCO₃/Cl trend and plot on a separate trend due to an increase in equivalents SO₄ and Cl. Therefore these samples are distinguishable from the possibly brine influenced samples.

Processes such as Na and Cl dissolution from road salt may fit the piper diagrams of drift and surface waters better than the brine upwelling hypothesis. The bedrock aquifers that would contain the saline waters, the Pennsylvanian and the Mississippian, should look similar to the Piper diagrams of the MRW streams, MRW wetlands, and the MRW Drift. They are similar except in SO₄ concentration. The bedrock waters have samples that have much higher percentage equivalents of SO₄ than the MRW. The SBW drift, region expected to have brine upwelling occurring in the drift, have samples with a higher percentage SO₄ than the MRW drift as well. A source of Na and Cl to a watershed that does not contain SO₄ would be halite. This could give the HCO₃/Cl trends, with very little SO₄, trends that are found in the MRW drift, MRW streams, and MRW wetlands.

Chapter 6

GIS

Introduction

Halite dissolution, oil and gas exploration, road brining, natural brine upwelling, and or sewage/septic systems are possible sources of excess Cl to the MRW. Geographic Information Systems (GIS) was used to determine if any spatial correlation exists between Na/Cl (M) ratios of surface waters and possible sources of Cl such as oil and gas wells, road salt, and sewage/septic effluents. Surface geology can also have an effect on the concentration of Cl in a watershed.

The same Na/Cl (M) ratios used to give insight into the source of Cl in the watershed for the histograms in Chapter 4 were used in this Chapter as well. The selected sample locations, ones with Na/Cl (M) ratios within the specified range, as well as the sample locations that did not have the right specifications were kept. This was done in order to show where sample locations were relative to suspected sources and to give insight into what locations should have been selected and possibly why they were not. The selected sample locations are represented as green circles. Chloride concentrations of the samples selected are represented as vertical bars. The concentration of Cl in the sample is proportional to the length of the vertical bar. More than one bar may be present at a certain sample location because many sample locations were sampled more than once over the 3 sampling seasons that were used in the collection of the surface water data.

Oil and Gas Wells

Michigan has had a long history of oil and gas production. The first oil well was drilled in 1900, and as of 2001 almost 15,000 oil wells and 10,000 gas wells have been drilled in Michigan (IPAA, 2005). Brines are commonly waste products of oil and gas production. Since oil and gas production are present in the MRW, the relationship between oil and gas wells and excess Cl to the watershed needs to be explored. Oil wells have been used to explain the presence of saline waters in a near surface alluvium aquifer in Louisiana (Stoessell, 1997). The geochemistry of the oilfield brines was known and was compared to the geochemistry of saline waters in the shallow aquifer. Stoessell used mass ratios, one of those mass ratios being Na/Cl, to determine specifically which brine was entering into the near surface aquifer.

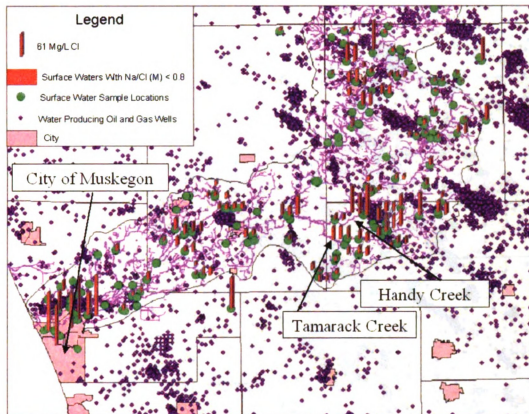
Table 2 shows the average Na/Cl molar ratios from formation waters within the Michigan Basin. Using GIS and a list of the oil and gas wells in Michigan taken from the MiGDL site (2005) it has been determined that the formations listed in Table 2 (Wilson, 1989) are used in oil and gas production in the Muskegon River watershed. It would be consistent with an alternative hypothesis, Cl in the watershed is from oil and gas production, if the surface waters draining regions with many oil and gas wells had Na/Cl (M) ratios consistent with formations used for oil and gas production in the MRW.

Figure 80 and Figure 81 are maps of the lower and upper portions of the MRW that show wells that may have produced brine either when they were drilled or during production. The amount of brine produced varies greatly from well to well. Figure 80 represents

surface water data from the lower portion of the watershed while Figure 81 represents that from the upper portion of the watershed.

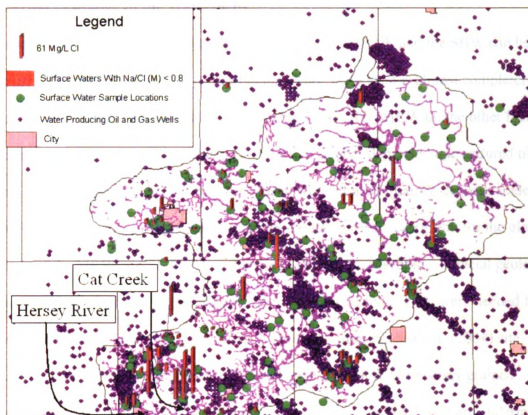
Surface water samples taken near and within Handy and Tamarack creeks, located in the southeastern most portion of the MRW (Figure 80), revealed that waters within these areas contain Na/Cl ratios consistent with a brine. These regions also have elevated Cl levels that can be seen on the map to be anomalously high as compared to regions surrounding it. As can be seen on the map (Figure 80) the region drained by these two creeks also contains a significant number of oil and gas wells. The Hersey River and Cat Creek both drain regions that have many oil and gas wells within them (Figure 81). Stream samples taken from the Hersey River and Cat Creek reveal samples that have Na/Cl (M) ratios consistent with that of a brine. The map (Figure 81) shows that the samples taken from these two streams have anomalously high levels of Cl as compared to surface water samples surrounding these two streams. Within the City of Muskegon, there are two stream locations that have a Na/Cl (M) ratio that is near that of brine. Even though this is within the city limits a few oil wells are still up stream of these streams and may have contributed to the Cl in the streams.

Road brining and brine upwelling are two additional possible sources of brine to the watershed. Oilfield brines are sometimes used as road brines and therefore distinguishing between them chemically is impossible. Another possible source of brine is upwelling from the Marshall formation.



● Surface Water Sample Locations

Figure 80. Map of the Lower portion of the Muskegon River Watershed. Locations of wells that may have produced brine were taken from the Department of Environmental Quality (2005) website. All surface water sample locations are represented as a green dot. Locations of samples with Na/Cl (M) ratios less than 0.8 are shown in brown. The concentration of Cl at the sample location is represented as the length of the brown column. Base Map from the Michigan Geographic Data Library (2005) website. Images in this thesis are presented in color.



● Surface Water Sample Locations

Figure 81. Map of the Upper portion of the Muskegon River Watershed. Locations of wells that may have produced brine were taken from the Department of Environmental Quality (2005) website. All surface water sample locations are represented as a green dot. Surface water samples with Na/Cl (M) ratios less than 0.8 are shown in brown. The concentration of Cl at the sample location is represented as the length of the brown column. Base Map from the Michigan Geographic Data Library (2005) website. Images in this thesis are presented in color

Quaternary Geology of the Watersheds

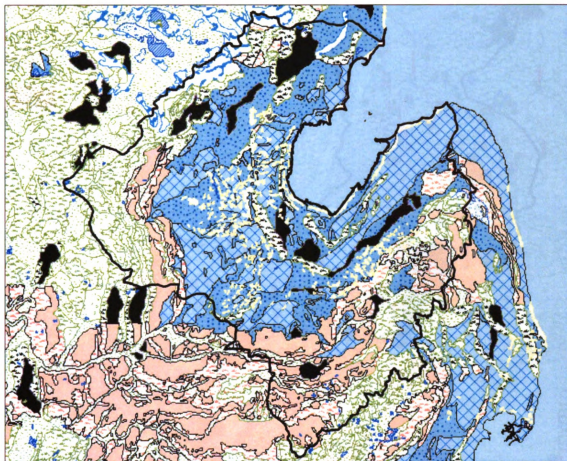
A general representation of the Quaternary geology of the MRW and the SBW can be seen in the first chapter (Figure 4). The Saginaw Bay Watershed is almost completely underlain by lacustrine deposits and basal lodgment tills. The MRW on the other hand is underlain by mainly glacial fluvial deposits and to a smaller degree coarse textured till. In general, finer grained deposits underlie the SBW while coarser-grained deposits underlie the MRW. Although the map (Figure 4) shows a good general description for the glacial geology of the MRW and SBW, it is not specific enough for this study. Glacial geology maps taken from the MiGDL (Michigan Geographic Data Library) site were needed for a more detailed map of these two watersheds. The maps from the MiGDL (2004) site shows that although the generalization is correct that the MRW has coarser grained deposits within it there are several different regions within the MRW that are underlain by fine-grained material. When trying to find a correlation between fine-grained sediments and sample locations with Na/Cl (M) ratios, within a watershed, with that of a brine, the more detailed map is needed.

Figure 82 shows the Saginaw Bay Watershed and the associated Quaternary geology. As can be seen from the map, the SBW is underlain by mostly fine-grained Quaternary deposits such as lacustrine clays, fine-textured glacial till, and end moraines of fine-textured till. On the extreme western edge and parts of the southern portion of the watershed significant glacial outwash sand and gravels and postglacial alluvium can be found as well as coarse textured endmoraines. Lacustrine sands and gravels can be found

between the fine-grained lacustrine clays and the course-grained glacial outwash sands and gravels.

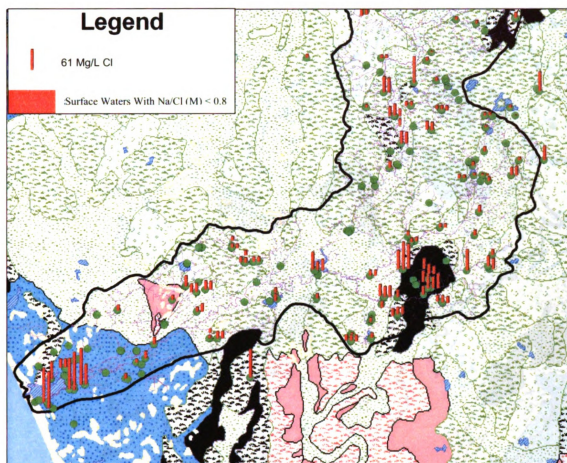
Figure 83 shows the Quaternary geology of the lower portion of the Muskegon River Watershed. It can be seen from the map that this area of the MRW is underlain primarily by course-textured glacial till and end moraines made up of course-grained glacial till. Lacustrine sands and gravels dominate the southwestern most portion of the watershed. Fine-grained glacial tills and end moraines of fine-grained till can be found sporadically throughout the watershed. With the exception of the southeastern portion of the watershed, the region drained by Handy and Tamarack creeks, there does not appear to be a correlation between fine-grained material and Na/Cl (M) ratios consistent with an oilfield brine.

Figure 84 shows the Quaternary geology of the upper portion of the Muskegon River Watershed. It can be seen from the map that this area of the MRW is mainly composed of end moraines of coarse-textured till and outwash sand and gravels. Ice contact sand and gravels as well as fine-grained glacial till and fine-grained end moraines are also present. Peat and muck are also present in this portion of the watershed. The map does not show any correlation between the presence of fine-grained glacial deposits and surface waters that have Na/Cl ratios similar to that of brine.



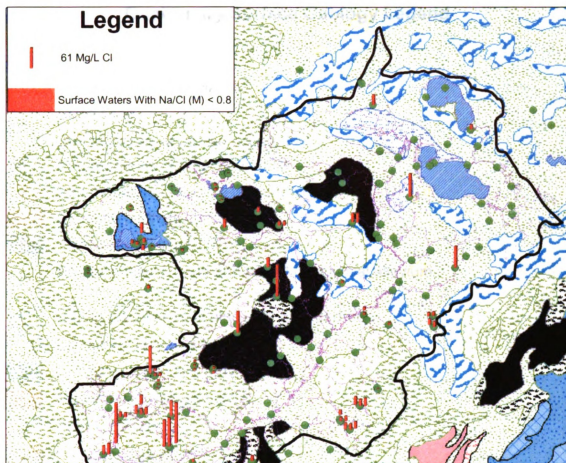
● Surface Water Sample Locations

Figure 82. Map of the Quaternary Geology (for quaternary geology legend see figure 85) of the Saginaw Bay Watershed. Base Map from the Michigan Geographic Data Library (2005) website. Images in this thesis are presented in color.



● Surface Water Sample Locations

Figure 83. Map of the Quaternary geology (for quaternary geology legend see Figure 85) of the lower half of the Muskegon River Watershed. All surface water sample locations are represented as a green dot. Surface water samples with Na/Cl (M) ratios less than 0.8 are shown in brown. The concentration of Cl at the sample location is represented as the length of the brown column. Base Map from the Michigan Geographic Data Library (2005) website. Images in this thesis are presented in color.



● Surface Water Sample Locations

Figure 84. Map of the Quaternary geology (for quaternary geology legend see figure 85) of the Upper portion of the Muskegon River Watershed. All surface water sample locations are represented as a green dot. Surface water samples with Na/Cl (M) ratios less than 0.8 are shown in brown. The concentration of Cl at the sample location is represented as the length of the brown column. Base Map from the Michigan Geographic Data Library (2005) website. Images in this thesis are presented in color.

Quaternary Surface Geology Legend

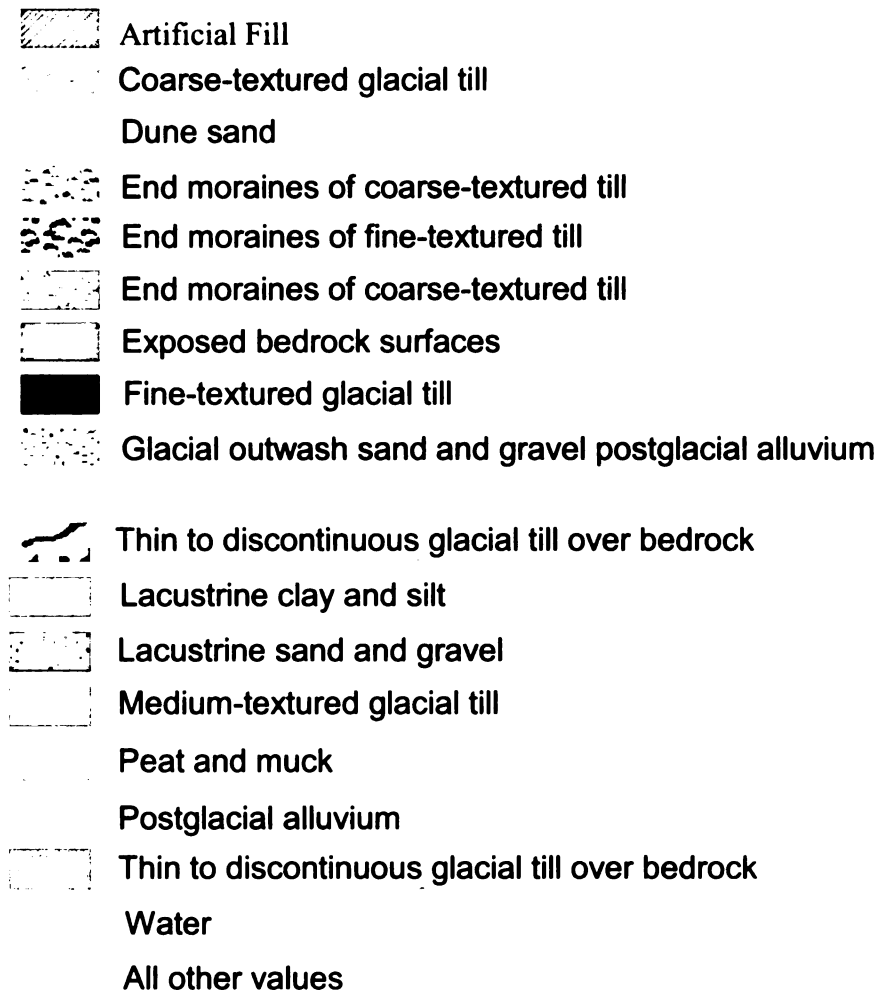


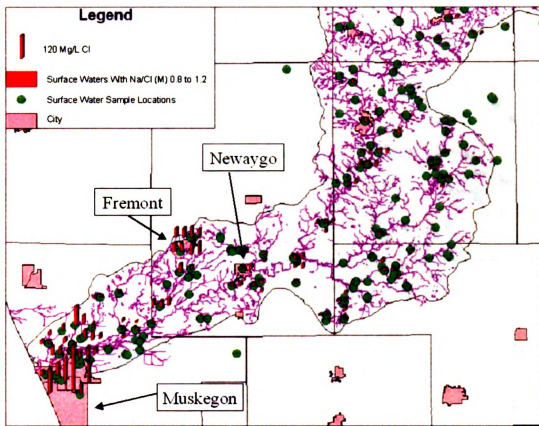
Figure 85. The legend shows the different colors and patterns used to show distinct types of quaternary surface geology in the Muskegon River Watershed. This legend is to be used with Figures 82-84. Images in this thesis are presented in color.

Road Salt

Lindeman (2002) observed a correlation between concentrations of Na (M) and Cl (M) in surface waters and urban land use. Road salt is applied to roads in winter to melt and prevent the formation of ice on roads. In regions that would have more roads it would be expected that the application would be higher by unit area. The areas that have more roads, such as cities, should not only have a Na/Cl (M) ratio similar to halite but should have a higher Cl concentration than surrounding surface waters with the same Na/Cl (M) ratio. The Na/Cl (M) ratio range that would be consistent with halite dissolution is 0.8 to 1.2; this is explained in Chapter 4.

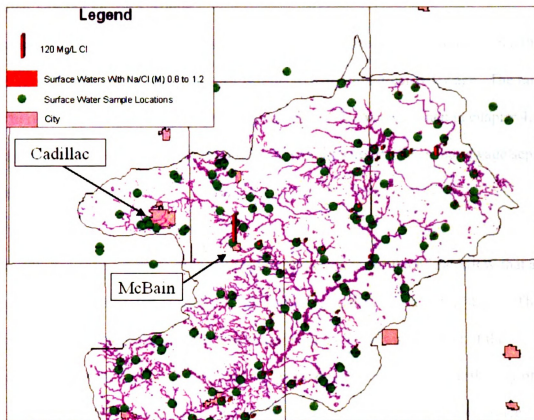
Figure 86 and Figure 87 show the locations of surface water samples and those sample locations that have a Na/Cl (M) ratio between 0.8 and 1.2. The maps show the locations of all surface water samples as yellow dots. The red boxes correspond to locations that have Na/Cl ratios between 0.8 and 1.2. The length of the box is proportional to the concentration of Cl in the sample. The two halite maps show that the samples with a Na/Cl (M) ratio consistent with road salt being the major contributor of Na and Cl are located near or within the cities of Muskegon, Fremont, and McBain. Although samples with comparatively low levels of Cl with Na/Cl (M) ratios consistent with the road salt are found throughout the watershed they are much less concentrated than those found in around the cities mentioned above. Cadillac (Figure 87), the largest city in the northern part of the watershed did not have many locations that have Na/Cl (M) values consistent with road salt. Those locations that did have comparatively low concentrations of Cl as compared to Cl concentrations found near Muskegon, Fremont, and McBain. This may

be due to the fact that samples in the streams were not taken near enough downstream of Cadillac and as a result had mixed with other sources such as septic or brine which had changed the ratio.



● Surface Water Sample Locations

Figure 86. Map of the lower portion of the Muskegon River Watershed. All surface water sample locations are represented as a green dot. Locations of surface water samples that have a Na/Cl molar ratio between 0.8 and 1.2 are represented with a brown bar. The concentration of Cl is represented by the length of the bar. Base Map from the Michigan Geographic Data Library (2005) website. Images in this thesis are presented in color.



● Surface Water Sample Locations

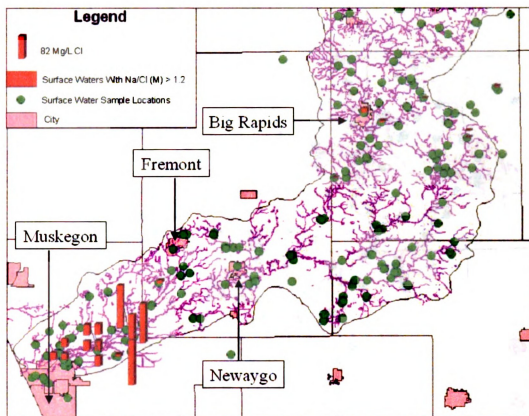
Figure 87. Map of the upper portion of the Muskegon River Watershed. All surface water sample locations are represented as a green dot. Locations of surface water samples that have a Na/Cl molar ratio between 0.8 and 1.2 are represented with a brown bar. The concentration of Cl is represented by the length of the bar. Base Map from the Michigan Geographic Data Library (2005) website. Images in this thesis are presented in color.

Treated Sewage Septic Systems

If excess Cl in the watershed is dominantly from septic/treated sewage systems then the water should have a Na/Cl (M) ratio that is reflective of septic/treated sewage. The range used to represent treated sewage/septic is greater than 1.2. As mentioned in chapter 4, it is suspected that the natural Na/Cl ratio should be in the same range as the sewage/septic systems.

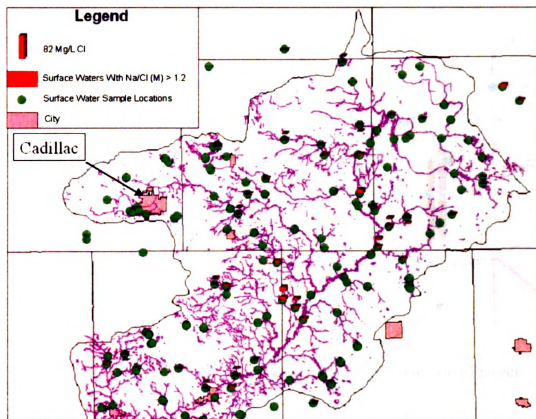
Figure 88 shows the locations of sample points in the lower portion of the MRW that are influenced by septic/treated sewage effluent according to the criteria of this thesis. The height of the columns represents the concentration of Cl in the water. Most of the samples with Na/Cl ratios consistent with the septic/treated sewage are near the city of Muskegon. The rest of the lower portion of the watershed has relatively few surface waters with this ratio of Na/Cl. The surface waters with Na/Cl ratios > 1.2 and the highest concentration Cl are found downstream of the MCWDS. Figure 90 is a close up of the area around the MCWMS and shows that samples downstream of this sewage treatment facility have similar Na/Cl ratios. Care must be taken when interpreting the results because samples from Mosquito Creek and Drain 31, those samples taken closest to the MCWMS, were used in determining the Na/Cl range for treated sewage/septic. However, samples further downstream in Mosquito creek and even samples downstream of the where Mosquito creek empties into the Muskegon River show similar Na/Cl ranges as those samples downstream of the MCWMS.

Figure 89 shows the locations of sample points in the upper portion of the MRW that have Na/Cl (M) ratios that would be consistent with the Na and Cl being from septic/treated sewage effluent. This map shows that there are a significant number of surface water samples that have the Na/Cl ratio consistent with treated sewage/septic but all have relatively low levels of Cl. Considering that the samples with the Na/Cl ratios consistent with treated sewage/septic are not found near cities and are of low concentrations the points are probably from either diluted septic or from natural processes such as plagioclase dissolution/atmospheric precipitation.



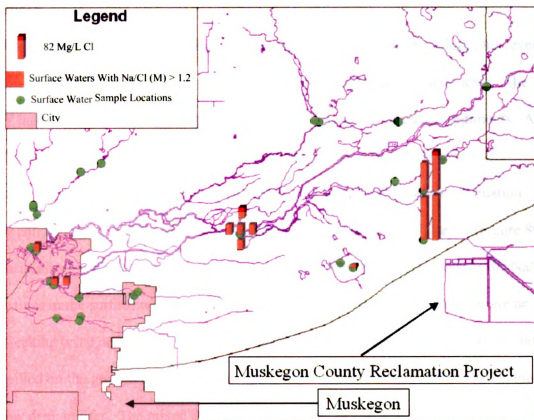
● Surface Water Sample Locations

Figure 88. Map of the lower portion of the Muskegon River Watershed. All surface water sample locations are represented as a green dot. Locations of surface samples that have a Na/Cl molar ratio greater than 1.2 are represented with a brown bar. The concentration of Cl is represented by the length of the bar. Base Map from the Michigan Geographic Data Library (2005) website. Images in this thesis are presented in color.



● Surface Water Sample Locations

Figure 89. Map of the upper portion of the Muskegon River Watershed. All surface water sample locations are represented as a green dot. Surface water samples that have a Na/Cl molar ratio greater than 1.2 are represented with a brown bar. The concentration of Cl is represented by the length of the bar. Base Map from the Michigan Geographic Data Library (2005) website. Images in this thesis are presented in color.



● Surface Water Sample Locations

Figure 90. Map of surface water samples near the city of Muskegon. All surface water sample locations are represented as a green dot. Surface water samples that have a Na/Cl molar ratio greater than 1.2 are represented with a brown bar. The concentration of Cl is represented by the length of the bar. Base Map from the Michigan Geographic Data Library (2005) website. Images in this thesis are presented in color.

Summary

The MRW and the SBW have distinctly different Quaternary surface geology; however, in some parts they both have fine-grained, i.e. less permeable, surface sediments. The MRW has tills and end moraines that are made up of fine-grained glacial sediments. A small section of fine-grained till in the end moraine occurs in the MRW where a significant number of surface water samples that have a Na/Cl (M) ratio of formation brines can be found. This section is drained by Tamarack and Handy Creeks (Figure 80). This area also has a large number of oil and gas wells. One possible reason for the Na/Cl (M) values in the surface water in this region could be that the oil and gas wells are or were leaking brine or, during production, brine was spilled on the ground. Once the brine has spilled on the ground it may seep into the ground and mix with fresher water in the shallow drift aquifer. The mixed brine/fresh water now in the aquifer may migrate down hydraulic gradient toward streams and other surface waters where it feeds these surface waters. The chemistry of the surface waters would then reflect this mixed brine fresh water legacy. Brines are also applied to roads as method of dust control and therefore could be the source for Na/Cl (M) values consistent with brine in the MRW. Another possibility is that the brine is the product of a natural upwelling. Only the extreme southwest corner of the watershed, just before the Muskegon River enters Lake Michigan, is suspected to have the right hydraulic conditions to have brines upwell into the overlying aquifer (Fleck and McDonald, 1978). Surface water samples above the southwestern most portion of the watershed contain high levels of Cl as well as a Na/Cl (M) ratio that would be consistent with brine upwelling. Whether it is natural upwelling, the result of oil and gas exploration, or industrial processes occurring within the City of

Muskegon, the presence of fine-grained sediments, by preventing the penetration of fresh meteoric water, can increase the salinity in the ground water. If the excess Cl were from upwelling from below, or from the input of septic tanks, fine-grained materials would decrease the dilution of the ground water. The ground water is what feeds the streams so the streams that are in an area with a subsurface source of Cl should have higher levels of Cl in them.

Maps showing the locations of surface water samples with Na/Cl (M) ratios similar to that of road salt are common throughout the watershed. However, surface water samples with Na/Cl (M) ratios consistent with dissolution of road salt have the highest Cl levels nearest to the cities of Muskegon, Fremont and McBain (Figure 86). This suggests that the effect of road salt on the concentration of Cl on the environment, although applied throughout the state on roads, affects urbanized watersheds the most. However, streams running through small towns such as McBain may also be significantly affected by the use of road salt. Cadillac, the largest town in the upper portion of the watershed, had surface waters within it that had Na/Cl (M) ratios consistent with the dissolution of halite, although it did not have Cl levels in the water that were significantly greater than the surrounding area. This maybe due to the fact that, stream sampling locations were too far downstream of Cadillac and may have been diluted by water draining less urbanized regions to show the full effect of the town. Some stream locations are located within the town but happened to be on the farthest upstream portion of the town and therefore may have not acquired enough ground water in town to show the urban effect.

There are few surface water locations in the lower portion of the MRW that have Na/Cl (M) ratios consistent with the treated sewage/septic systems. The highest concentrated samples are located just downstream of the MCWDS on Mosquito Creek as well as Drain 31. Samples at the mouth of Mosquito creek and downstream of the confluence of Mosquito creek and the Muskegon River show Na/Cl ratios consistent with treated sewage/septic. This suggests that the MCWDS has an effect on both Mosquito Creek as well as the Muskegon River. There are few samples in the rest of the lower portion of the MRW that have the Na/Cl ratio consistent with treated sewage/septic. The upper portion of the watershed has many samples that have the Na/Cl ratio that would be consistent with treated sewage/septic however, they are all much lower in concentration than the Cl concentrations found downstream of the MCWDS. Considering that most of these samples do not occur near cities, they are most likely from septic systems. Septic systems are used in rural settings, for the treatment and disposal of human waste. As it was mentioned earlier in this chapter, that although natural systems probably have similar Na/Cl ratios as those in treated sewage and septic, they should have much lower levels of both due to the low solubility of known Na bearing minerals in the drift and the lack of Cl bearing minerals in the drift.

Chapter 7

Summary and Conclusions

Summary

Geochemical modeling demonstrates that surface waters were more supersaturated with respect to calcite than the ground waters. Calcite was near equilibrium to undersaturated in the Mississippian bedrock unit (Figure 11), however the Pennsylvanian bedrock unit (Figure 12), glacial drift (Figure 13) and MRW drift (Figure 14) were near equilibrium. The streams (Figure 15) were the most supersaturated with respect to calcite of all of the waters tested. The lakes (Figure 16) and wetlands (Figure 17) had locations that were supersaturated, saturated, and near saturation with respect to calcite. The surface waters have several different processes that were controlling the saturation of calcite in water this is probably responsible for the wider range of saturation indices found in the surface waters as compared to the ground waters. The ground water has more dissolved CO_2 and as a result can dissolve up more calcite and still remain in equilibrium with this mineral. When the ground water enters into the surface waters it comes into equilibrium with an environment that has less dissolved CO_2 in it and as a result releases CO_2 to come into equilibrium with it. The loss of CO_2 in the water makes the solution temporarily supersaturated with respect to calcite, until it precipitates out of solution and causes the water to go back to equilibrium. Biological activity (photosynthesis) (Effler, 1984; Effler et al., 1981; Effler et al., 1982) and turbulence (Herman et al., 1987) may also decrease the concentration of CO_2 in the water. The presence of algae, something for calcite to

nucleate onto, can help start the precipitation of calcite (Kalff, 2002). While dissolved organic carbon, and soluble reactive phosphorous can prevent the precipitation of calcite (Kalff, 2002).

It was found that the Pennsylvanian (Figure 26) and the Mississippian (Figure 25) were the two most saturated, with respect to gypsum, of the hydrologic domains tested. The MRW streams (Figure 29) and the MRW drift (Figure 28) waters were very similar in their distribution of saturation indices. The MRW stream waters (Figure 29) show that areas downstream of the MCWDS are more saturated with respect to gypsum than any of the other waters tested. The streams are the most saturated with respect to gypsum of the surface waters while the wetlands (Figure 31) are the least saturated with respect to gypsum of all of the waters tested. The wetlands and lakes are the least saturated with respect to gypsum, possibly due to the presence of sulfate reducing bacteria, removing sulfate from the water decreasing the SI value for gypsum.

Quartz tended to be supersaturated in all of the ground waters tested (Figure 32, Figure 33, Figure 34, Figure 35). The streams (Figure 36) tended to be near-equilibrium to supersaturated with respect to quartz. Wetlands (Figure 38) and lakes (Figure 37) tended to be undersaturated with respect to quartz. Diatoms can remove silica from water thereby decreasing the saturation of quartz (Hurley et al., 1985).

The MRW drift waters and the MRW surface waters have similar Na/Cl (M) ratios when only samples with Cl concentrations greater than 10 mg/L are considered. When all

samples are considered the MRW drift contains a much higher percentage of Na/Cl (M) ratios greater than 1.2 when compared to the surface waters. This would suggest that the MRW drift is more influenced by treated sewage/septic and/or more likely plagioclase dissolution/atmospheric precipitation than the MRW surface waters. The surface waters tend to plot below 1.2 Na/Cl (M) which would be consistent with the Cl principally coming from oilfield brines and/or halite dissolution. It would also be consistent with the Cl coming from the Mississippian. Sodium/chloride (M) tables of water from the Mississippian bedrock tend to have Na/Cl (M) ratios below 0.8. The histograms of water within the Pennsylvanian bedrock show that the most dominant peaks lie within the range of the dissolution of halite. However the table showing the Na/Cl (M) ratios within the Pennsylvanian show that most samples have Na/Cl (M) ratios above 1.2 (M). Samples from the Pennsylvanian with Cl concentrations greater than 10 mg/L also show the same trend. The Pennsylvanian is not in direct contact with the drift in a region within the MRW where it has been established that the hydrologic conditions (in the Pennsylvanian bedrock) would allow for upwelling of waters in the bedrock aquifer into the drift aquifer. Therefore, the dissolution of halite, most likely as road salt, for Cl within the Na/Cl (M) range of 0.8 to 1.2 is a stronger argument than that for the Pennsylvanian being a source for Cl. The Mississippian bedrock has the right hydraulic conditions for upwelling at the mouth of the Muskegon River (Fleck and McDonald, 1978), however, oil and gas exploration occurs throughout the watershed as well. Water from the Mississippian bedrock as well as oilfield brines have Na/Cl (M) ratios below 0.8. Therefore, because both oilfield brines and Mississippian bedrock water plot within the same region on the Na/Cl (M) histogram as well as having evidence that both have

probable pathways into the surface waters, both are possible contributors to Cl in the watershed. However, the area in the MRW known to have the right conditions for brine upwelling to occur is very small. Oil and gas wells are spread throughout the watershed and therefore probably have a larger effect on the watershed as a whole.

All of the ground water logarithmic graphs (Figures 54-59) show a trend toward the seawater evaporation curve with increasing Na and Cl. This would appear to support the hypothesis that the Cl and Na in the water were from evaporated seawater; however, it would be difficult to determine from the logarithmic graphs the difference between the dissolution of halite (Figure 58) and the dilution of a brine. Brine upwelling is unlikely because the surface waters have less scatter than the drift found in the suspected upwelling regions (i.e., Saginaw Bay Drift). The scatter at low concentrations is apparent in the Pennsylvanian and Mississippian the underlying bedrock in both the Saginaw Bay Watershed and the Muskegon River Watershed. The low amount of scatter in the MRW surface waters could be derived from a brine if only the high concentration waters from bedrock formations below were interfering with the surface waters. If the high concentration waters from bedrock layers below were introduced into the MRW drift and surface waters the Na/Cl (M) values would show less scatter because the high concentration values in the Pennsylvanian and Marshall have less scatter at these concentrations. If this brine were then diluted the Na/Cl ratios would be the same as that in the original brine at high concentrations however the scatter at low concentrations would not be present. A pathway for only highly concentrated saline waters from bedrock to get into the aquifer is through road brining and oil and gas exploration.

The plots of Ca (M) vs. Mg (M) reveal that the bedrock drift ground water and the regional drift ground water in general have more dissolved Ca with respect to Mg than the surface waters and drift within the MRW. The MRW surface water and the MRW drift plot closer to the calcite/dolomite equilibrium line than the water in the bedrock aquifers.

The Piper diagrams reveal that there are two different trends present on the cation triangles. One trend runs at a constant range of percent equivalents of Mg (between 20 and 40%) and in general does not get any greater than 30 percent Na+K. This trend is the only one present in the MRW lakes (Figure 77) cation triangle. Another trend in the cation triangles runs at an angle from a Ca rich water to a Na+K rich water. This trend can be seen in the SBW watershed drift (Figure 75), glacial drift (Figure 73), MRW Drift (74), MRW Streams (Figure 77), Pennsylvanian (Figure 71), and Mississippian (Figure 72). The SBW streams ternary diagram (Figure 76) has both of the trends.

The anion triangles from the Pennsylvania (Figure 71), Mississippian (Figure 72), glacial drift (Figure 73), MRW Drift (Figure 74), SBW drift (Figure 75), MRW streams (Figure 77), MRW lakes (Figure 78), MRW wetlands (Figure 79) show a trend from the bicarbonate corner of the anion triangle towards the Cl end of the anion triangle. The anion triangle in the MRW streams (Figure 77) and the anion triangle for the MRW drift (Figure 74) show the same trend going from HCO₃ dominant water toward Cl dominant water. However, the MRW stream data have more samples that plot closer towards the Cl end of the triangle than the MRW drift does. The cation triangles from the MRW

streams (Figure 77), MRW Drift (Figure 74), Pennsylvanian (Figure 71), Mississippian (Figure 72), glacial drift (Figure 73), and the SBW streams (Figure 75) show a trend from the Ca corner of the cation triangle towards the Na+K end of the cation triangle. This trend may be the result of natural brine upwelling or possibly anthropogenic influences. The MRW streams (Figure 77) show a similar trend although with much less equivalents of Na+K and that runs into the points that are directly downstream of the (MCWDS) and therefore would suggest that these points are not from natural brine upwelling but from treated sewage possibly septic. However, the treated sewage samples plot on a line in the anion triangle that runs from the HCO_3 corner toward the Cl and SO_4 edge of the triangle. This trend shows the difference between the treated sewage samples and the samples from the Mississippian and Pennsylvanian, which have the same Ca to Na+K trend but do not share the same anion trend. The fact that these treated sewage samples plot on a separate trend than the other samples and that trend is different than the trends found in bedrock units that contain saline waters such as the Pennsylvanian and the Mississippian shows that treated sewage can be distinguished not within the cation triangle but within the anion triangle from these other sources of Cl to the watershed.

The Quaternary geology maps showing Na/Cl (M) ratios within the range of an oilfield brine or water from the Mississippian bedrock do not appear to show a strong correlation between fine grained surface material and Na/Cl (M) ratios within the range of an oilfield brine or water from the Mississippian bedrock. This is to be expected because only one location is known to have the right hydraulic conditions to have brines upwell and that

region (southwestern most portion of the watershed) does not have fine-grained surface deposits.

Surface water sample locations with Na/Cl ratios less than 0.8, within the range of naturally occurring brines (Figure 80 and Figure 81), appear to be located near oil and gas wells. Although, this spatial correlation does not establish that the cause for the Na/Cl ratios consistent with brines is from the spilling of brines from oil and gas production/exploration. Brines have other pathways to the surface water environment such as the application of brines to roads to prevent road dust. Another possibility is the upwelling of the Marshall formation into the overlying aquifer. However, only near the mouth of the Muskegon River is it known that the hydrologic conditions exist for upwelling to occur (Fleck and McDonald, 1978). The region near the mouth of the Muskegon River has several surface water samples that have Na/Cl ratios consistent with a brine source for Cl. This would support the hypothesis that the source for excess Cl, at least in the very southwestern portion of the watershed, is brine upwelling from saline waters below. However, the region is heavily urbanized and industrialized and the excess Cl may be the result of industrial processes or oil and gas production.

A map showing surface water sample locations with Na/Cl (M) ratios that were within the range of road salt (Figure 86 and Figure 87) showed that the waters with the highest levels of Cl tended to plot near the cities (i.e., Muskegon, and Fremont) in the lower portion of the watershed. Samples with relatively low levels of Cl with Na/Cl (M) ratios within the range of halite were found throughout the watershed. A stream running

through the town of McBain, appeared to have much higher Cl levels than any other stream in the upper portion of the watershed with a Na/Cl ratio consistent with halite dissolution. This would support the idea that dissolution of halite, probably from road salt, has a widespread effect on the levels of Cl in the upper portion of the watershed. When surface waters have Na/Cl (M) ratios similar to halite in the lower portion of the watershed the levels of the Cl tend to be much higher in general than that in the upper portion. This maybe due to other sources of Cl possibly anthropogenic sources besides watershed has larger cities and more roads and therefore more road salt application than the upper portion of the watershed.

Few surface water locations have Na/Cl (M) ratios within the range of septic/treated sewage effluents in the lower portion of the watershed (Figure 88). However, the samples found in the lower portion of the MRW with the Na/Cl (M) within the range of treated sewage/septic, in general, have higher concentrations of Cl than that found in the upper portion of the watershed. All of the high Cl samples are found down stream of the MCWDS.

Conclusions

The purpose of this thesis was to understand the source or sources for the Cl in surface waters (rivers, wetlands, lakes) of the Muskegon River Watershed. The hypothesis investigated was that the source for Cl in the surface waters of the MRW is the result of a natural process, the influence of upward migrating saline water. The alternative hypothesis was that the excesses in Cl are from road salt, sewage/septic systems, road

brining, natural atmospheric/water rock interactions, and/or oil and gas production and exploration. Geochemical modeling, ion ratios, ion vs. ion graphs as well as Geographical Information Systems were used to explore these hypotheses. The results are as follows:

- Na/Cl (M) ratios and graphs revealed that most surface waters in the MRW have Na/Cl (M) ratios consistent with the dissolution of halite and the dilution of a brine.
- GIS maps revealed that road salt was the most likely pathway for halite to the MRW surface waters. Activities associated with oil and gas exploration and road brine appear to be likely pathways for brines to enter into the surface waters.
- Although many surface waters have Na/Cl (M) ratios consistent with a brine, the hydrologic conditions needed for upwelling to occur are limited in the MRW. Therefore upwelling as a pathway for brine to surface waters is probably minor when compared to pathways such as road brining and activities associated with oil and gas exploration.

BIBLIOGRAPHY

AquaChem User's Manual, Aqueous Geochemical Data Analysis, Plotting, and Modeling (1998)

Badalamenti, L.S., 1992, The Geochemistry and Isotopic Chemistry of Saline Ground Water Derived from Near-Surface Deposits of the Saginaw Lowland, Michigan Basin, Thesis, Michigan State University, 126 pp

Boutt, D.F., Hyndman, D.W., Pijanowski, B.C., Long, D.T. 2001, Identifying Potential Land Use-Derived Solute Sources to Stream Baseflow Using Ground Water Models and GIS, *Ground Water*, Vol. 39: p 24-34

Carpenter, A.B., 1978, Origin and Chemical Evolution of Brines in Sedimentary Basins, Vol. 79: p 60-76

Case, L.C., 1945, Exceptional Silurian Brine Near Bay City, Michigan, *American Association of Petroleum Geologists*, Vol. 29: p 567-570

Dannemiller, G.T., Baltusis, M.A., 1990, Physical and chemical data for ground water in the Michigan basin, 1986-89: U.S. Geological Survey Open-File Report 90-368: 155 pp

Drever, J.I. 1997 *The Geochemistry of Natural Waters* 3rd edition, Prentice Hall, Upper Saddle River, NJ, 436 pp.

Effler, S.W., 1984 Carbonate Equilibria and the Distribution of Inorganic Carbon in Saginaw Bay, *J. Great Lakes Res.*, Vol. 10: p 3-14

Effler, S.W., Driscoll, C.T., 1985 Calcium Chemistry and Deposition in Ionically Enriched Onondaga Lake, New York, *Environmental Science and Technology*, Vol. 19: p 716-720

Effler, S.W., Field, S.D., Quirk, M., 1982, The seasonal cycle of inorganic carbon species in Cazenovia Lake, New York, 1977, *Freshwater Biology*, Vol. 12: p 139-147

Effler, S.W., Field, S.D., Wilcox, D.A. 1981 The Carbonate Chemistry of Green Lake, Jamesville, N.Y., *Journal of Freshwater Ecology* Vol. 1: p 141-153

Fleck, W.B., McDonald, M.G. (1978) Three-Dimensional Finite-Difference Model of Ground-Water System Underlying the Muskegon County Wastewater Disposal System Michigan, *Journal of Research U.S. Geological Survey*: p 307-318

GLIN, <http://www.great-lakes.net/lakes/ref/lakefact.html>, (accessed March 2005)

Hem, J.D., 1985, Study and Interpretation of the Chemical Characteristics of Natural Water, 3rd edition, U.S. Geological Survey Water-Supply Paper 2254: 263 pp

Herman, J.S. and Lorah, M.M., 1987, CO₂ Outgassing and Calcite Precipitation in Falling Spring Creek, Virginia, U.S.A., Chemical Geology, Vol. 62: p 251-262

Houghton, D. *Geological reports of Douglass Houghton, first state geologist of Michigan, 1837-1845*: The Michigan Historical Commission, 1928: 700 pp

Huling, E.E., Hollocher, T.C., 1972, Groundwater Contamination by Road Salt: Steady-State Concentrations in East Central Massachusetts, Science, Vol. 176: p 288-290

Hurley, J.P., Armstrong, D.E., Kenoyer, G.J., Bowser, C.J., 1985, Ground Water as a Silica Source for Diatom Production in a Precipitation-Dominated Lake, Science, Vol. 227: p 1576-1578.

IPAA (2005) Independent Petroleum Association of America
<http://www.ipaa.org/info/InYourState/default.asp?State=Michigan> (accessed, 2005)

Kalff, J. Limnology, Prentice Hall, 1993, 592 pp

Kolak, J.J., 2000, An Evaluation of Ground Water-Surface Water Interactions in Saginaw Bay, Lake Huron, with Implications for Trace Metal Cycling, Dissertation, Michigan State University, 391 pp

Langmuir, D., Aqueous Environmental Geochemistry, Prentice Hall, New Jersey, 600 pp

Lindeman, M.A., Saladin, N.P., Wayland, K.G., Long, D.T., Loughweed, V.L., Stevenson, R.J., Wiley, M., Hyndman, D.W., and Pijanowski, B.C., 2002, Influences of land use on the biogeochemistry of streams, G.S.A. Abstracts with Programs, Vol. 34: no.6, 177 pp

Long, D.T., Meissner, B.D., Wharer, M.A., Geochemistry of the Glaciofluvial Saginaw and Marshall Regional Aquifer Systems, Michigan, U.S. Geological Survey Professional Paper (Unpublished Work in Progress)

Long, D.T., Wilson, T.P., Takacs, M.J., and Rezabeck, D.H., 1988, Stable-isotope geochemistry of saline near-surface ground water: East-central Michigan basin, Geological Society of America Bulletin, Vol., 100: p 1568-1577

Long, D.T. (2005). Personal Communication

Lougheed, V. (2005) Personal Communication

Mariam, S., Mokma, D.L., 1995, Mineralogy of Two Sandy Spodosol Hydrosequences in Michigan, Soil Survey Horizons, Winter: p 121-132

Mariam, S., Mokma, D.L., 1996, Mineralogy of Two Fine-Loamy Hydrosequences in South-Central Michigan, Soil Survey Horizons, Summer: p 65-74

Mandle, R.J., Westjohn, D.B., 1989, Geohydrologic Framework and Ground-Water Flow in the Michigan Basin, American Water Resources Association, no. 13: p 83-109

Mason, F. M., Norton, S.A., Fernandez, I.J., Katz, L.E., 1999, Soil Processes and Chemical Transport Deconstruction of the Chemical Effects of Road Salt on Stream Water Chemistry, Journal of Environmental Quality, Vol. 28: p 82-91

Meissner, B.D., 1993, The Geochemistry and Source for Solutes in Ground Water from the Pennsylvanian Bedrock Sequence in the Michigan Basin, Thesis, Michigan State University, 115 pp

MiGDL, Michigan Geographic Data Library, <http://www.mcgi.state.mi.us/mgdl/>, accessed, 2005

Muller, G., Irion, G., and Forstner, U., 1972, Formation of Diagenesis of Inorganic Ca-Mg Carbonates in the Lacustrine Environment, Naturwissenschaften, Vol. 59: p 158-164

National Atmospheric Deposition Program, <http://nadp.sws.uiuc.edu/>, accessed 1/13/2004

Nelson, R. (2005) http://www.michigan.gov/deq/0,1607,%207-135-3311_4111_4231-97834--,00.html (accessed 2005)

Nordstrom, D.K., Plummer, L.N., Langmuir, D., Busenberg, E., May, H.M., Jones, B.F., Parkhurst, D.L., 1990, Revised chemical equilibrium data for major water-mineral reactions and their limitations: American Chemical Society Symposium Series, Vol. 416: p 398-413

Otsuki, A., and Wetzel, R.G. 1974 Calcium and total alkalinity budgets and calcium carbonate precipitation of a small hard-water lake, Arch. Hydrobiol., Vol. 73: p 14-30

Parkhurst, D.L. 1995 User's Guide to PHREEQC-A Computer Program for Speciation, Reaction-Path, Advective-Transport, and Inverse Geochemical Calculations. U.S. Geological Survey Water-Resources Investigations Report 95-4227

Piper, A.M., 1944, A Graphic Procedure in the Geochemical Interpretation of Water-Analyses, Transactions, American Geophysical Union, Vol. 25: p. 914-923

Plummer, L.N. Busenberg, E., 1982, The solubility of calcite, aragonite, and vaterite in CO₂ solutions between 0 and 90°C, and an evaluation of the aqueous model for the system CaCO₃-CO₂-H₂O: Geochimica et Cosmochimica Acta, Vol.: 47, p. 665-686

Robertson, W.D., Cherry, J.A., Sudicky, E.A., 1991, Ground-Water Contamination from Two Small Septic Systems on Sand Aquifers, *Ground Water*, Vol. 29, p. 82-92

Stoessell, R.K., 1997, Delineating the Chemical Composition of the Salinity Source for Saline Ground Waters: An Example from East-Central Concordia Parish, Louisiana, *Ground Water*, Vol. 35, p 409-417

Stout, N, <http://www.gvsu.edu/wri/isc/muskegon/studyarea.htm>, (accessed April 2005)

Strong, A.E., and Eadie, B.J. 1978 Satellite Observations of Calcium Carbonate Precipitations in the Great Lakes, *Limnology and Oceanography*, Vol. 23: p 877-887

Stumm, W.S., and Morgan, J.J., 1996, *Aquatic Chemistry*, 3rd ed. Wiley-Interscience, New York, 1022 pp

Wahrer, M.A., Long, D.T., Lee, R.W., 1996, Selected Geochemical Characteristics of Ground Water from the Glaciofluvial Aquifer in the Central Lower Peninsula of Michigan. U.S. Geological Survey Water-Resources Investigations Report 94-4017, Lansing, Michigan

Wahrer, M.A., 1993, The Geochemistry and Source of Solutes in Ground Water from the Glacial Drift Regional Aquifer, Michigan Basin, Thesis, Michigan State University, 111 pp

Westjohn, D.B., Weaver, T.L., 1998, Hydrogeologic Framework of the Michigan Basin Regional Aquifer System, U.S. Geological Survey Water-Resources Investigations Report 1418, Lansing, Michigan

Westjohn, D.B., Weaver, T.L., and Zacharias, K.F., 1994, Hydrology of Pleistocene Glacial Deposits and Jurassic "Red Beds" in the Central Lower Peninsula of Michigan, U.S. Geological Survey Water-Resources Investigations Report 93-4152, Lansing, Michigan

Wilson, T.P. (1989) Origin and Geochemical Evolution of the Michigan Basin Brine, Dissertation, Michigan State University, 106 pp

Wood, W.W., 1969, Geochemistry of Ground Water of the Saginaw Formation in the Upper Grand River Basin, Michigan, Ph.D. Thesis, 104 pp

MICHIGAN STATE UNIVERSITY LIBRARIES



3 1293 02736 6438